FULL PAPER

Amphiphilic Bistable Rotaxanes

Jan O. Jeppesen,*[a, b] **Kent A. Nielsen,**[a, b] **Julie Perkins,**[a] **Scott A. Vignon,**[a]
Alberto Di Fabio,[c] **Roberto Ballardini,**[c, d] **M. Teresa Gandolfi,***[c] **Margherita Venturi,***[c]
Vincenzo Balzani,[c] **Jan Becher,**[b] **and J. Fraser Stoddart***[a]

Abstract: Two molecular shuttles/switches—a slow one and a fast one—in the shape of amphiphilic, bistable [2]rotaxanes have been synthesized and characterized. Both [2]rotaxanes contain a hydrophobic, tetraarylmethane and a hydrophilic, dendritic stopper. They are comprised of two π-electron-rich stations—a monopyrrolotetrathiafulvalene unit and a 1,5-dioxynaphthalene moiety—which can act as recognition sites for the tetracationic cyclophane, cyclobis(paraquat-*p*-phenylene), to reside around. In addition, a model [2]rotaxane, incorporating only a monopyrrolotetrathiafulvalene unit in the rod section of the amphiphilic dumbbell

component and cyclobis(paraquat-*p*-phenylene) as the ring component, has been investigated. The dumbbell-shaped components were constructed using conventional synthetic methodologies to assemble 1) the hydrophobic, tetraaryl-methane stopper and 2) the hydrophilic, dendritic stopper. Next, 3) the hydrophobic stopper was fused to the 1,5-dioxynaphthalene moiety and/or the monopyrrolotetrathiafulvalene unit by appropriate alkylations, followed by 4) attachment of the hydrophilic stopper, once again by alkylation to give the dumbbell-shaped compounds. Finally, 5) the [2]rotaxanes were self-assembled by using the dumbbells as templates for the formation of the encircling cyclobis-(paraquat-*p*-phenylene) tetracations. The two [2]rotaxanes differ in their arrangement of the π-electron-rich units, one in which the SMe group of the monopyr-rolotetrathiafulvalene unit points toward the 1,5-dioxynaphthalene moiety ($2 \cdot 4 \mathrm{PF}_6$) and another in which it points away from the 1,5-dioxynaphthalene moiety ($3 \cdot 4 \mathrm{PF}_6$). This seemingly small difference in the orientation of the monopyrrolotetrathiafulvalene unit leads to profound changes in the physical properties of these rotaxanes. The bistable [2]rotaxanes were both isolated as brown solids. ¹H NMR and UV-visible spectroscopy, and electrochemical investigations, reveal the presence of both possible translational isomers at ambient temperature. As a consequence of the existence of both possible translational isomers in these bistable [2]rotaxanes, they exhibit a complex electrochemical behavior, which is further complicated by the presence of folded

conformations wherein the monopyrrolotetrathiafulvalene unit is involved in an "alongside" interaction with the tetracationic cyclophane. In the molecular shuttle/switch $2 \cdot 4 \mathrm{PF}_6$ a "knob", in the shape of the SMe group, is situated between the monopyrrolotetrathiafulvalene and the 1,5-dioxynaphthalene recognition sites, making it possible to isolate both translational isomers ($2 \cdot 4 \mathrm{PF}_6 \cdot$ GREEN and $2 \cdot 4 \mathrm{PF}_6 \cdot$ RED) and to investigate the kinetics of the shuttling of the cyclobis(paraquat-*p*-phenylene) tetracation between the two recognition sites. The shuttling processes, which are accompanied by clearly detectable color changes, can be followed by ¹H NMR and UV-visible spectroscopy, allowing the rate constants and energies of activation for the translation of the cyclobis(paraquat-*p*-phenylene) tetracations between the two recognition sites to be determined. In the molecular shuttle/switch $3 \cdot 4 \mathrm{PF}_6$, there is no "knob" situated between the 1,5-dioxynaphthalene and the monopyrrolotetrathiafulvalene recognition sites, resulting in a considerably faster shuttling of the cyclobis(paraquat-*p*-phenylene) tetracation between these two sites, making the separation of the two possible translational isomers of $3 \cdot 4 \mathrm{PF}_6$ impractical. However, the shuttling of the cyclobis(paraquat-*p*-phenylene) tetracation can be followed by dynamic ¹H NMR spectroscopy. At low temperatures, the major translational isomer is $3 \cdot 4 \mathrm{PF}_6 \cdot$ RED, while $3 \cdot 4 \mathrm{PF}_6 \cdot$ GREEN is the major isomer at higher temperature. In the bistable [2]rotaxanes shuttling of the cyclobis(paraquat-*p*-phenylene) tetracations can be driven by electrochemical oxidation of the monopyrrolotetrathiafulvalene unit. In complexes in which one of the two dumbbell stoppers is missing, electrochemical oxidation causes dethreading.

[a] Prof. J. F. Stoddart, Dr. J. O. Jeppesen,
K. A. Nielsen, Dr. J. Perkins, S. A. Vignon
Department of Chemistry and Biochemistry
University of California, Los Angeles
405 Hilgard Avenue, Los Angeles,
CA 90095-1569 (USA)
Fax: (+1)310-206-1843
E-mail: stoddart@chem.ucla.edu
joj@chem.sdu.dk

[b] Dr. J. O. Jeppesen, K. A. Nielsen,
Prof. J. Becher
Department of Chemistry
Odense University
(University of Southern Denmark)
Campusvej 55,
DK-5230, Odense M (Denmark)
Fax: (+45)66-15-87-80

[c] Prof. M. T. Gandolfi, Prof. M. Venturi,
A. Di Fabio, Dr. R. Ballardini,
Prof. V. Balzani
Dipartimento di Chimica "G. Ciamician"
Università di Bologna
Via Selmi 2, 40126 Bologna (Italy)
Fax: (+39)051-209-9456
E-mail: vbalzani@ciam.unibo.it

[d] Dr. R. Ballardini
ISOF-CNR Institute
Via Gobetti 101, 40129 Bologna (Italy)

Introduction

A [2]rotaxane[1] that contains two different recognition sites ("stations") in its dumbbell-shaped component can exist as two different translational isomers, whose populations reflect their relative free energies as determined primarily by the strength of the two different sets of noncovalent bonding interactions. In suitably designed [2]rotaxanes, the ring component resides preferentially (in ideal cases only) on one of the two recognition sites. In these systems, the properties of the preferential recognition site can be reversibly altered by external stimuli, such as light excitation, redox processes (either heterogeneous or homogeneous), and acid/base reactions. As a consequence, shuttling of the ring component between the two stations can occur.[2] Because of the extended molecular rearrangement involved in these shuttling processes, nondegenerate [2]rotaxanes are prime candidates for the construction of artificial molecular machines[3, 4, 5] and for the fabrication of molecular electronic devices.[6, 7, 8] A number of different protocols, based on self-assembly[9] have been developed[2, 10, 11] for the template-directed syntheses[12] of rotaxanes. The desirable features for the redox-controllable, amphiphilic [2]rotaxanes that have been employed[13] to fabricate single-molecule thick electrochemical junctions in electronic devices include 1) the siting of redox-active units along the rod section of the dumbbell component and 2) the presence of both hydrophobic and hydrophilic groups as stoppers at the ends of the dumbbell component.

In the context of such devices, the tetrathiafulvalene (TTF) unit—which has found widespread use in materials chemistry[14]—is an ideal redox-active unit in view of its excellent π-electron-donating properties. This led to its forming[15] a strong green 1:1 complex ($K_a = 8000\,\mathrm{M}^{-1}$ in MeCN)[2d] with the π-electron-accepting tetracationic cyclophane,[16] cyclobis-(paraquat-*p*-phenylene) (CBPQT[4+]), making it ideal for incorporation into redox-switchable [2]rotaxanes, along with a 1,5-dioxynaphthalene (DNP) moiety which also interacts, but somewhat more weakly[17] with CBPQT[4+], affording a red color in the process. Although a TTF unit and a DNP moiety have been incorporated[18] into the crown ether component of a redox-switchable [2]catenane—a compound which has already been employed in the fabrication of a solid-state electronically-reconfigurable switch[6]—no rotaxanes employing these two recognition sites for a CBPQT[4+] component had been described in the literature[19] prior to the publication of a preliminary communication[20] describing a small part of the research reported in this paper. In addition, rotaxanes incorporating TTF units in dumbbell components comprising two different stoppers had been unknown hitherto, most likely because of the lack of an appropriate TTF building block. Now that such a building block is available in the shape of the pyrrolo[3,4-*d*]tetrathiafulvalene unit,[21] we have designed amphiphilic bistable [2]rotaxanes in which the ring component is CBPQT[4+] and the dumbbell component—containing a monopyrrolo-TTF (MPTTF) unit and a DNP moiety within its rod section—is terminated by a hydrophilic dendritic stopper at one end and a hydrophobic tetraarylmethane stopper at the other end. Here, we describe the template-directed syntheses of three amphiphilic [2]rotaxanes (Figure 1), namely 1) a model compound **1** · 4PF$_6$ comprising only an MPTTF unit in the dumbbell-shaped component, 2) a
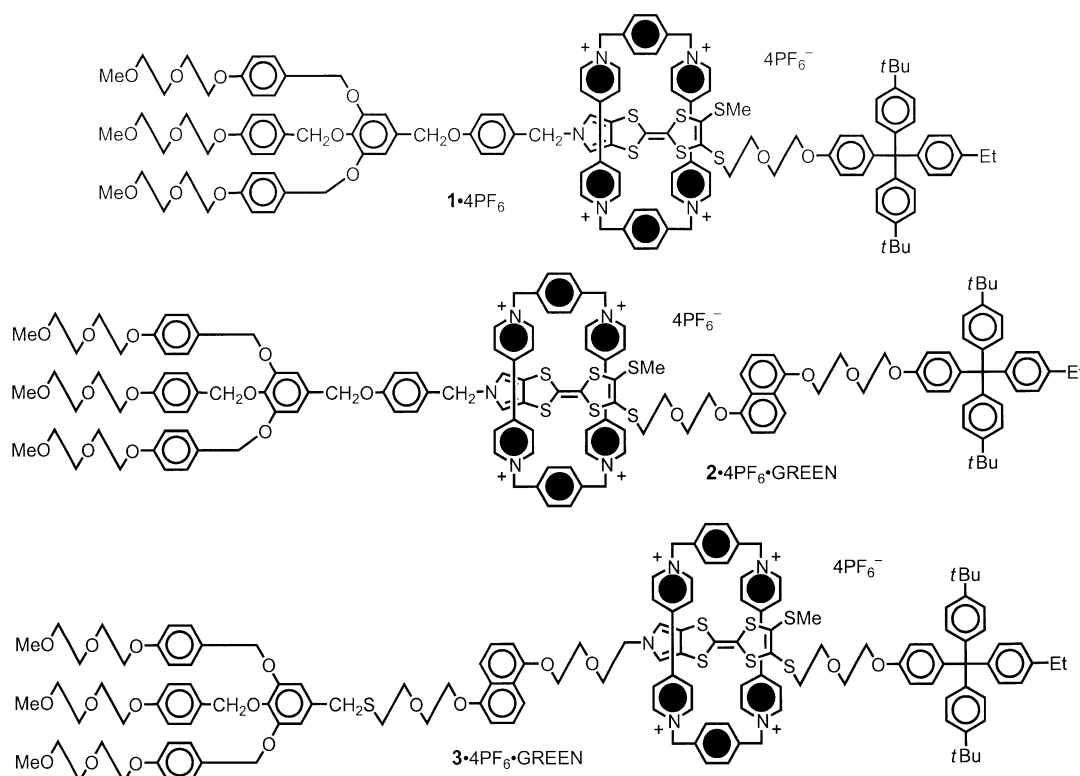
Figure 1. Molecular formulas of the single-station [2]rotaxane **1** · 4PF$_6$, the slow two-station [2]rotaxane **2** · 4PF$_6$, and the fast two-station [2]rotaxane **3** · 4PF$_6$ (only one translational isomer is shown in each case).

slow molecular shuttle/switch **2**·4PF$_6$ with a "knob" in the shape of an SMe group situated between the MPTTF and DNP recognition sites, hindering fast interconversion between the two translational isomers, and 3) a fast molecular shuttle/switch **3**·4PF$_6$ without a "knob" between the two recognition sites. Thereafter, we describe and discuss some mass spectrometric, photophysical, electrochemical, and ^{1}H NMR spectroscopic investigations of the [2]rotaxanes **1**·4PF$_6$, **2**·4PF$_6$, and **3**·4PF$_6$ and their corresponding dumbbell compounds, together with an extensive range of model compounds and complexes. Next the separation of the two possible translational isomers of the slow molecular shuttle/switch **2**·4PF$_6$ is described, and the kinetic and thermodynamic processes involved in their slow interconversion are discussed. Finally, it is shown that the relative populations of the two stable translational isomers of the fast molecular shuttle/switch **3**·4PF$_6$ in solution are heavily temperature dependent.

Results and Discussion

Design and synthetic strategy: Retrosynthetic analyses of the amphiphilic [2]rotaxanes **1**·4PF$_6$, **2**·4PF$_6$, and **3**·4PF$_6$ (Figure 1) reveal a range of possible disconnections. In the synthetic approaches that were eventually adopted, the dumbbell-shaped components were constructed by using conventional methodologies, followed by clipping of the tetracationic cyclophane CBPQT^{4+} employing the dumbbell-shaped components as templates. The syntheses (Scheme 1–6) of the amphiphilic dumbbells **7**, **17**, and **23**, require up to four different types of components: 1) a hydrophobic stopper, 2) a hydrophilic stopper, 3) an MPTTF unit, and 4) a DNP moiety. In order to minimize the number of synthetic steps, it was decided to prepare all the dumbbell-shaped components from common intermediates. For the hydrophobic stopper, a tetraarylmethane-based phenol **11** (Scheme 3),[13a, 22] which can be easily functionalized by using simple alkylation reactions, was chosen. For the hydrophilic stopper, dendrons **16** (Scheme 3) or **22** (Scheme 5),[13a, 22] which both contain glycol chains and can be functionalized by nucleophilic substitution reactions, were chosen. The DNP moiety was introduced as the monotosylate **10** (Scheme 3).[13a, 20] For the TTF unit, the asymmetric MPTTF building block **6** (Scheme 1),[21b, 22] which can be functionalized regioselectively by means of simple S- and N-alkylations in high yields, was chosen. With these components, the syntheses of the amphiphilic [2]rotaxanes **1**·4PF$_6$, **2**·4PF$_6$, and **3**·4PF$_6$ were achieved (Scheme 2–6) in a series of reactions involving relatively few steps.

Synthesis: The syntheses of the hydrophobic stopper **11**[13a, 22] and the hydrophilic stoppers **16** and **22**[13a, 22] have already been reported. Here, we describe improved syntheses of the MPTTF building block **6**[21b, 22] and the single-station [2]rotaxane **1**·4PF$_6$,[13a, 22] before outlining the syntheses of the slow molecular shuttle/switch **2**·4PF$_6$[20] and the fast molecular shuttle/switch **3**·4PF$_6$.[13b]

Our improved synthesis of the asymmetric MPTTF building block **6** was carried out as outlined in Scheme 1. Cross-coupling of 5-tosyl-(1,3)-dithiolo[4,5-c]pyrrole-2-one (**4**)[21] with two equivalents of 4-(2-cyanoethylthio)-5-methylthio-1,3-dithiole-2-thione (**5**)[23] in neat (EtO)$_3$P gave **6** (64%) in gram quantities after column chromatography.[24]
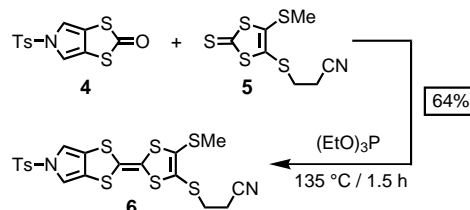
Scheme 1. Synthesis of the asymmetric MPTTF building block **6**.

We have previously reported[13a, 22] that the single-station [2]rotaxane **1**·4PF$_6$ can be self-assembled under ambient conditions by using the dumbbell-shaped component **7** as the template for the formation of the encircling CBPQT^{4+} tetracation from the dicationic precursor **8**·2PF$_6$[10] and the dibromide **9**. However, the yield was only 8% in this template-directed reaction.[25] By employing high-pressure conditions,[26] the supramolecular assistance to covalent synthesis (Scheme 2) was considerably enhanced, and the single-station [2]rotaxane **1**·4PF$_6$ was isolated in 21% yield from a mixture of the dumbbell **7**, **8**·2PF$_6$, and **9** subjected to a 10 kbar pressure in DMF at room temperature for three days.

The dumbbell **17**—the precursor to the slow molecular shuttle/switch **2**·4PF$_6$—was synthesized as shown in Scheme 3. Alkylation of the monotosylate **10**[13a, 20] with the
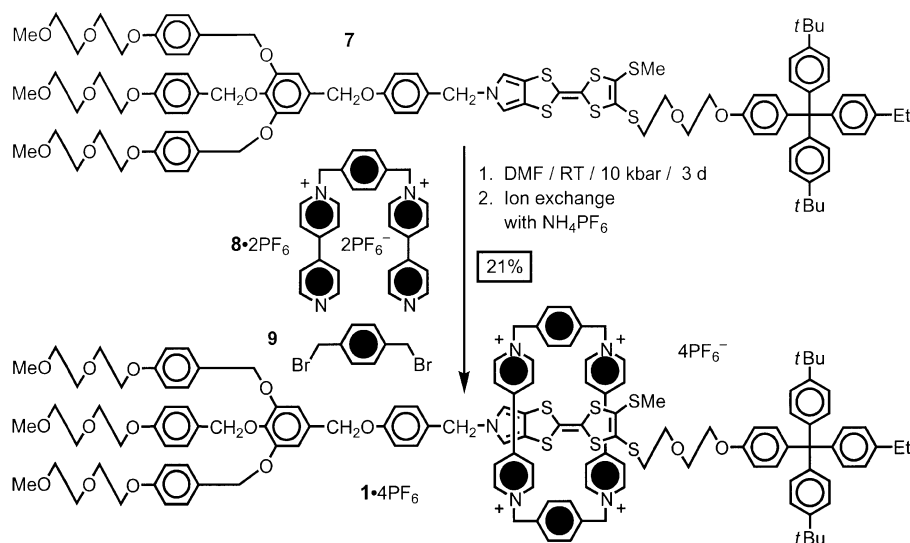
Scheme 2. Synthesis of the single-station [2]rotaxane **1**·4PF$_6$.
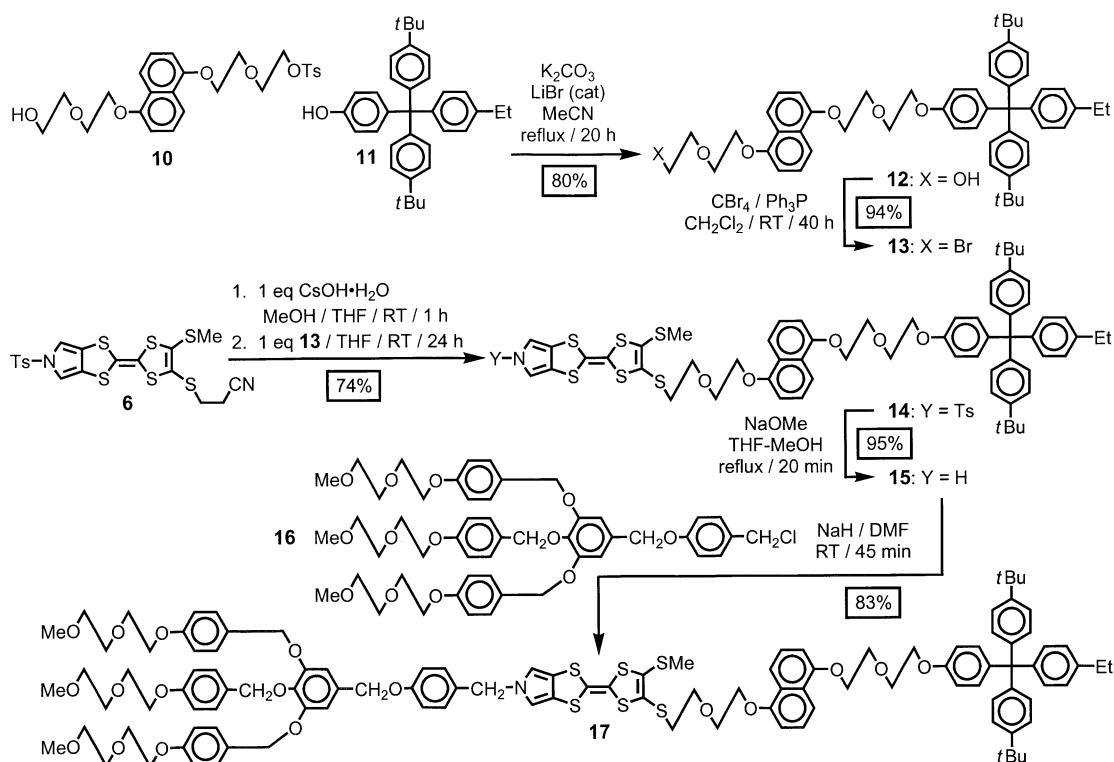
Scheme 3. Synthesis of the dumbbell compound **17**.

hydrophobic tetraarylmethane stopper **11**[13a, 22] in MeCN with LiBr as catalyst gave the alcohol **12** in 80% yield. Subsequent bromination of the free alcohol with CBr$_4$ and Ph$_3$P afforded the bromide **13** in good yield (94%). It could be coupled with the MPTTF building block **6**, following its in situ deprotection with one equivalent of CsOH·H$_2$O to give **14** in 74% yield. The tosyl protecting group on the MPTTF unit was removed

in excellent yield (95%) by using NaOMe in a THF/MeOH mixture. The resultant pyrrole nitrogen in **15** was alkylated with the chloride **16** carrying the hydrophilic stopper and, following purification by column chromatography, the dumbbell **17** was isolated in 83% yield. Formation of the [2]rotaxane **2**·4PF$_6$ was achieved (Scheme 4) in 23% yield[25] by using the dumbbell **17** as the template for the formation of
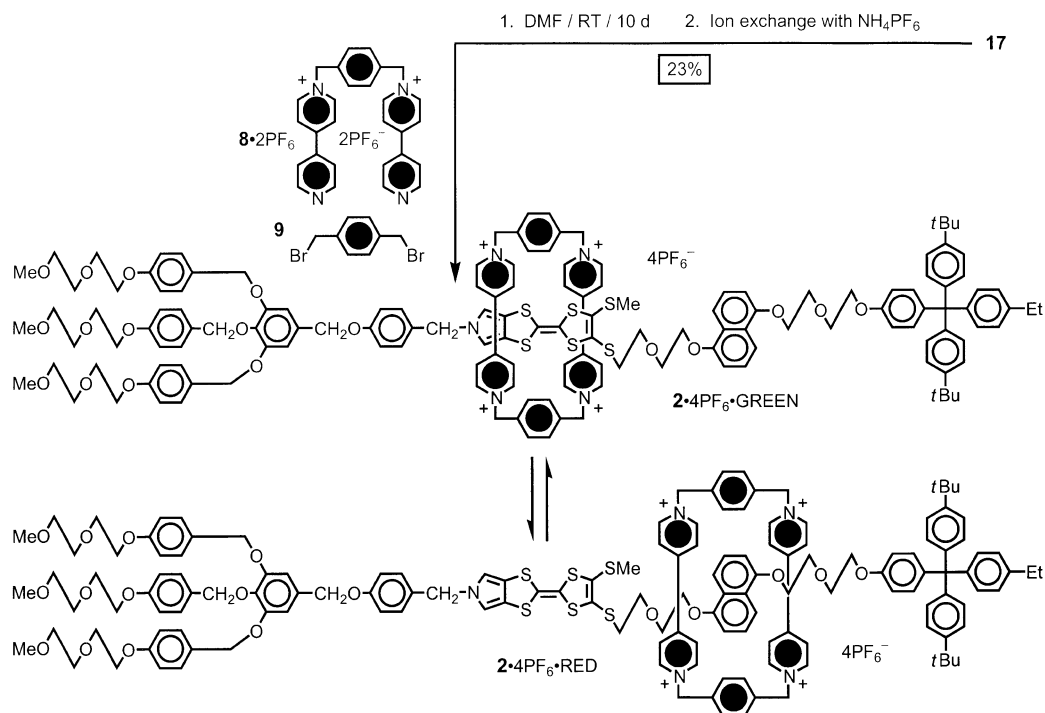
Scheme 4. Synthesis of the slow two-station [2]rotaxane **2**·4PF$_6$.
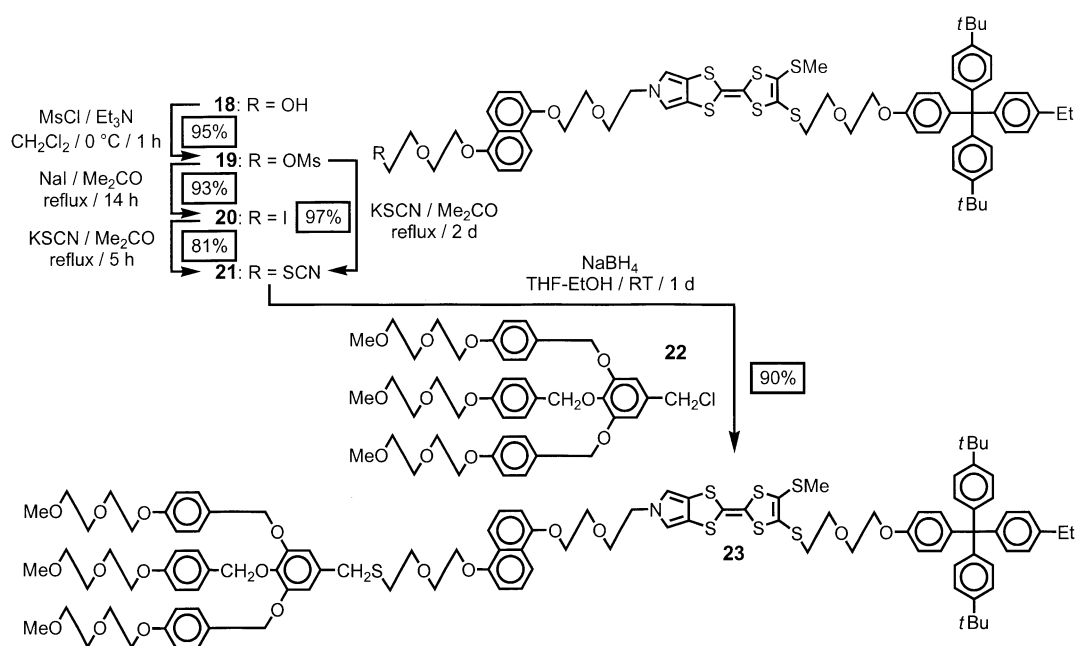
Scheme 5. Synthesis of the dumbbell compound **23**.

the encircling CBPQT[4+] tetracation from the dicationic precursor[10] **8**·2PF$_6$ and the dibromide **9**.

The preparation of the fast molecular shuttle/switch **3**·4PF$_6$ is outlined in Schemes 5 and 6. The synthesis of the semi-dumbbell-shaped compound **18** has been described previously.[13a] Direct reaction between the alcohol **18** and the chloride **16** in either THF or DMF containing NaH at 60 °C gave, in both cases, an inseparable mixture of unidentified products containing none of the desired dumbbell.[27] So, in order to

construct the dumbbell **23** (Scheme 5), the free hydroxyl function in compound **18** was initially converted to a mesyl group in 95 % yield (**18** → **19**), then to an iodide in 93 % yield (**19** → **20**), and finally to a thiocyanate group in 81 % yield (**20** → **21**). The thiocyanate **21** could also be obtained directly from the mesylate **19** in 97 % yield. The thiocyanate group was reduced in situ with NaBH$_4$, and the resulting thiolate[28] was subsequently coupled with the hydrophilic chloride[13a, 22] **22** in THF/EtOH to give the dumbbell **23** in 90 % yield. The
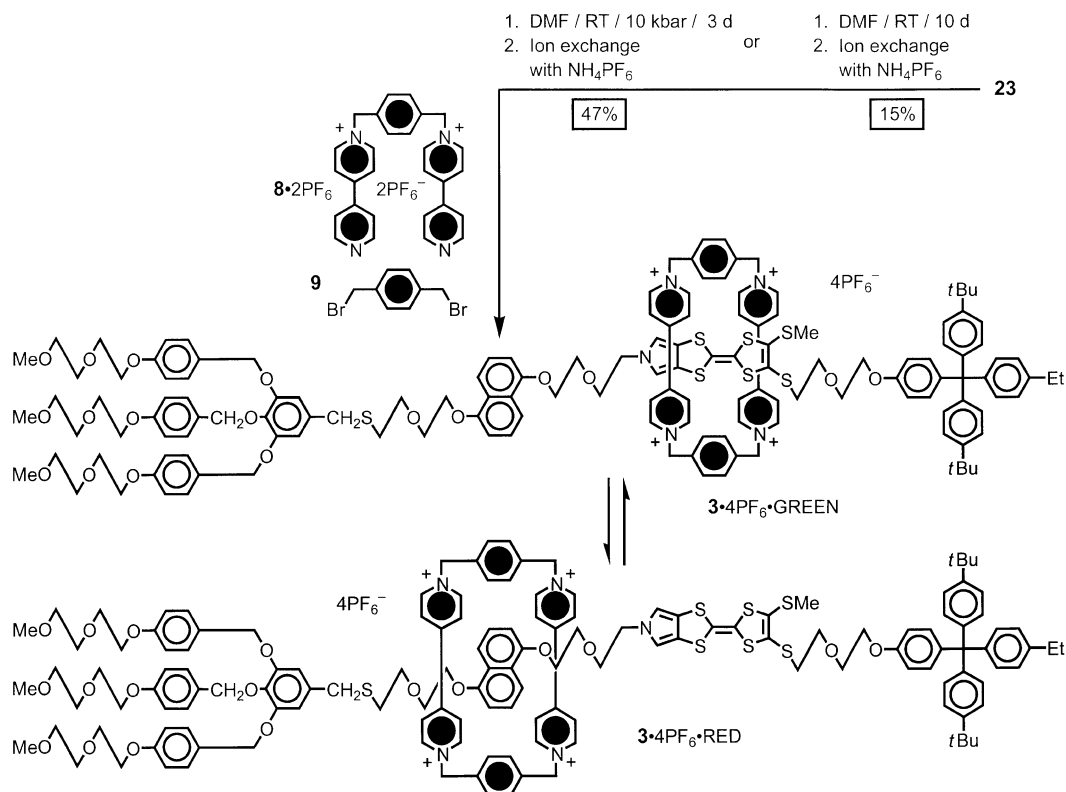
Scheme 6. Synthesis of the fast two-station [2]rotaxane **3**·4PF$_6$.

synthesis of the [2]rotaxane $3 \cdot 4\,PF_6$ was completed (Scheme 6) by the introduction of CBPQT[4+] using a clipping procedure. The dumbbell **23**, $8 \cdot 2\,PF_6$, and the dibromide **9**, were dissolved in anhydrous DMF. The reaction mixture was stirred at room temperature for ten days, and the pure [2]rotaxane $3 \cdot 4\,PF_6$ was isolated in 15 % yield, following column chromatography. In addition, it was possible to carry out the clipping procedure at high pressures in a reaction whereby the dumbbell **23**, $8 \cdot 2\,PF_6$, and the dibromide **9** were dissolved in anhydrous DMF in a teflon-tube and subjected to 10 kbar pressure at room temperature for three days. In this case, the pure [2]rotaxane $3 \cdot 4\,PF_6$ was isolated in 47 % yield, indicating the advantage of carrying out this type of reaction at ultra high pressures.

Mass spectrometric investigations: All the [2]rotaxanes reported in this paper were characterized (Table 1) by fast atom bombardment (FAB) mass spectrometry. The spectra obtained gave peaks corresponding to the $[M - PF_6]^+$, $[M - 2\,PF_6]^+$, and $[M - 3\,PF_6]^+$ ions, as well as some corresponding to the doubly positively charged ions $[M - 2\,PF_6]^{2+}$, $[M - 3\,PF_6]^{2+}$, and $[M - 4\,PF_6]^{2+}$. The FAB mass spectrum of the [2]rotaxane $2 \cdot 4\,PF_6$ is illustrated in Figure 2. Furthermore, the [2]rotaxane $3 \cdot 4\,PF_6$ was characterized by electrospray (ES) mass spectrometry. Its ES mass spectrum revealed peaks corresponding to the triply positively charged $[M - 3\,PF_6]^{3+}$ and quadruply positively charged $[M - 4\,PF_6]^{4+}$ ions. A comparison of the FAB mass spectra of the hydrophilic stopper **16** and the TTF derivatives **7** and **17** revealed the incipient radical cation character of the MPTTF unit. The FAB mass spectrum of the hydrophilic stopper **16** showed only peaks corresponding to fragmentations, and no molecular ion was detected. Attachment of an MPTTF unit to the hydrophilic stopper, as, for example, in **17** changed this situation entirely. The FAB mass spectrum of **17** showed a molecular ion as the major peak, and almost no fragmentation peaks were observed in the spectrum. This observation demonstrates a fundamental property of TTF, namely, that the TTF unit easily forms a radical cation.

Photophysical investigations: The photophysical properties have been studied in air-equil-
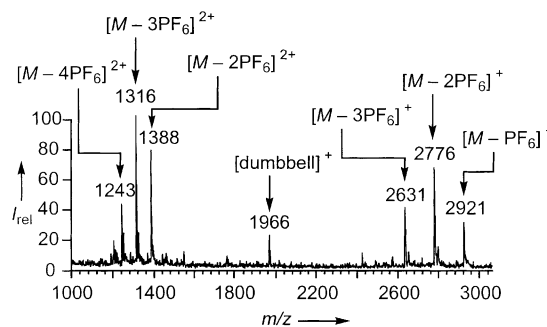
Figure 2. FAB-MS spectrum of the [2]rotaxane $2 \cdot 4\,PF_6$.

ibrated MeCN, Me_2CO, or Me_2SO solutions at room temperature. Four systems have been investigated (Schemes 2–8): 1) the semi-dumbbell components **18** and **24**; 2) the [2]pseudorotaxanes[29] **18** ⊂ CBPQT[4+] and **24** ⊂ CBPQT[4+]; 3) the dumbbell compounds **7**, **17**, and **23**; and 4) the [2]rotaxanes **1**[4+], **2**[4+], and **3**[4+]. We have also investigated the model compounds **25**,[21] **26**,[29d] **27**,[30] and **28**[13a] (Figure 3). These compounds and complexes contain several chromophoric units exhibiting strong absorption bands in the UV region. Some of these units—namely, the DNP and the oxybenzene ones—are also expected to show fluorescence.[11d, 31] In the case of the pseudorotaxanes and rotaxanes, broad and relatively weak charge-transfer (CT) bands[10, 18, 19f,k,p, 31a, 32] are also expected to appear in the visible spectral region. Such low-lying CT energy levels are usually responsible for the quenching of the fluorescent excited states of the DNP and oxybenzene units.[10, 18, 19p, 31a] There are also some structural differences that are important in comparing the photophysical properties of the systems under examination: 1) in all cases, except dumbbell **17**, the MPTTF unit is closer to the
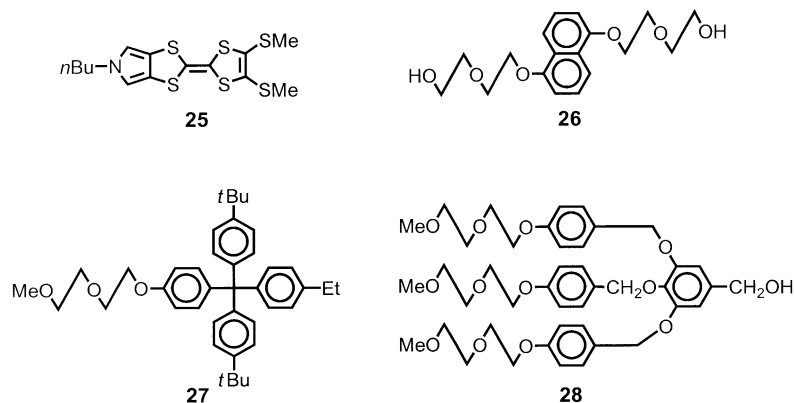
Figure 3. Molecular formulas of the model compounds of the π-electron donor stations (**25** and **26**) and the stoppers (**27** and **28**) of the dumbbell-shaped components of the [2]rotaxanes shown in Figure 1.

Table 1. FAB-MS data[a] for the [2]rotaxanes $1 \cdot 4\,PF_6$, $2 \cdot 4\,PF_6$, and $3 \cdot 4\,PF_6$.

[2]Rotaxane	M[b]	$[M - PF_6]^+$	$[M - 2\,PF_6]^+$	$[M - 3\,PF_6]^+$	$[M - 2\,PF_6]^{2+}$	$[M - 3\,PF_6]^{2+}$	$[M - 4\,PF_6]^{2+}$
$1 \cdot 4\,PF_6$	(2836)	2691	2546	2401	1273	1201	1128
$2 \cdot 4\,PF_6$	(3066)	2921	2776	2631	1388	1316	1243
$3 \cdot 4\,PF_6$	(3064)	2919	2774	2629	1387	1315	1242

[a] FAB spectra were obtained with a ZAB-SE mass spectrometer. The samples were dissolved in a small amount of 3-nitrobenzyl alcohol and the spectra were recorded in the positive-ion mode. [b] The peaks corresponding to the molecular ions were not observed. The molecular weights are shown in parentheses.

hydrophobic stopper than it is to the hydrophilic one; 2) dumbbells **17** and **23** differ from each other, not only because of the relative positions of the two π-electron-donating units on the rod section of the dumbbell, but also on account of there being a flexible *S*-containing diethyleneglycol chain adjacent to the hydrophilic stopper in **23**; and 3) an SMe "knob" on the MPTTF unit which slows down the shuttling of the tetracationic cyclophane component between this unit and the DNP one in the [2]rotaxane 2^{4+}, but not in the [2]rotaxane 3^{4+}, or in its related [2]pseudorotaxane $18 \subset CBPQT^{4+}$. As a result of these structural differences, difficulties are anticipated when comparing the properties derived from the CT interactions between the π-electron-donating units, contained in the semi-dumbbell and dumbbell components, and the π-electron-accepting tetracationic cyclophane. Nevertheless, interesting conclusions will likely be drawn by comparing the results obtained for "homogenous" couples, such as 1) the two [2]pseudorotaxanes $18 \subset CBPQT^{4+}$ and $24 \subset CBPQT^{4+}$, 2) the [2]pseudorotaxane $24 \subset CBPQT^{4+}$ and the [2]rotaxane 1^{4+}, 3) the [2]pseudorotaxane $18 \subset CBPQT^{4+}$ and the [2]rotaxane 3^{4+}, and 4) the three [2]rotaxanes 1^{4+}, 2^{4+}, and 3^{4+}.

Tetracationic cyclophane and model compounds: The absorption spectra of $CBPQT^{4+}$ and of the model compounds **25 – 28** are shown in Figure 4. None of these compounds displays absorption bands in the visible spectral region, apart from the MPTTF derivative **25**, which exhibits a weak tail. The DNP derivative **26** and the hydrophobic stopper fragment **27** reveal the expected fluorescence bands (Figure 4, inset), whereas the hydrophilic stopper fragment **28** does not show any emission, despite the fact that oxybenzene units are known to exhibit fluorescence. No emission is observed in the case of the MPTTF derivative **25**.
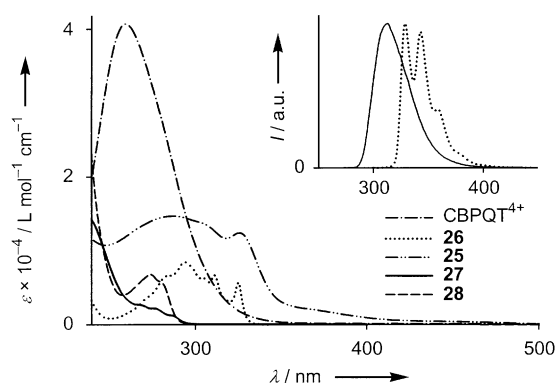
Figure 4. Absorption spectra of $CBPQT^{4+}$ and of the model compounds **25 – 28** recorded in MeCN at room temperature. The fluorescence spectra for the emitting species are shown in the inset.

Semi-dumbbells and their [2]pseudorotaxanes: The absorption spectra of the semi-dumbbell compounds **18** and **24** (Figure 5) are quite similar to the sum of the spectra of their model compounds (Figure 4). These results indicate that in the semi-dumbbell compounds **18** and **24** there are no significant interactions among their chromophoric units in the ground state. The characteristic fluorescence of the model compounds **26** and **27** (Figure 4, inset) is completely quenched in **18** and **24**. The most likely explanation for this quenching is the
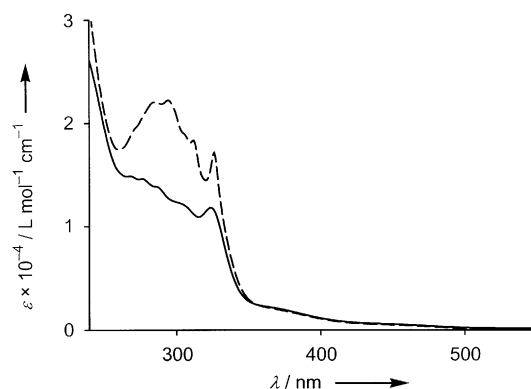
Figure 5. Absorption spectra of the semi-dumbbell compounds **18** (–––) and **24** (——) recorded in MeCN at room temperature.

occurrence of energy-transfer processes from the emitting excited states of the DNP moiety and the oxybenzene units in the tetraarylmethane groups to the lower energy excited states of the MPTTF unit.[18, 19p, 33]

Mixing equimolar amounts (8.3×10^{-4} M) of **24** and $CBPQT^{4+}$ in Me$_2$CO at 298 K leads to the formation of the [2]pseudorotaxane $24 \subset CBPQT^{4+}$ (Scheme 7),[34] as indicated by the immediate appearance of a green solution; this is
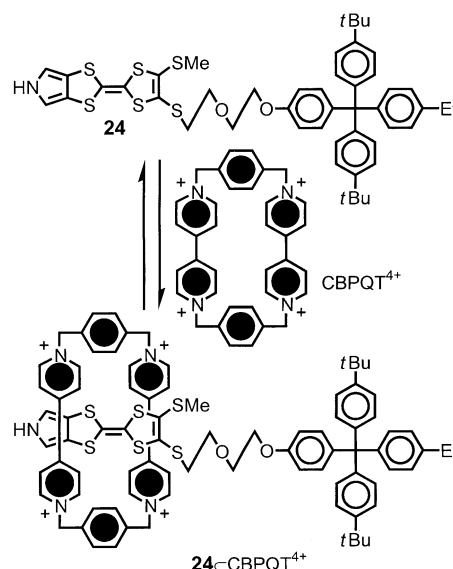
Scheme 7. Complexation of **24** by $CBPQT^{4+}$.

related to the presence of a broad CT absorption band centered on 805 nm.[35] This band is characteristic[15, 19p] of superstructures containing a TTF unit located inside $CBPQT^{4+}$. By using the CT band as a probe, a dilution experiment[15c, 35] was carried out and a binding constant (K_a) for the 1:1 complexation of $CBPQT^{4+}$ with the semi-dumbbell **24** was obtained. The K_a value of 1300 ± 200 M^{-1} ($\varepsilon = 1310$ L mol^{-1} cm^{-1}) in Me$_2$CO at 298 K corresponds to a free energy of complexation[36] ($-\Delta G^\circ$) of 4.2 kcal mol^{-1}.

Mixing equimolar amounts of **18** and the tetracationic cyclophane[16] $CBPQT^{4+}$ in Me$_2$CO leads to the formation of the bistable [2]pseudorotaxane $18 \subset CBPQT^{4+}$ (Scheme 8), as evidenced by the spontaneous formation of a brown solution.[13a] Since the [2]pseudorotaxane contains two donor units
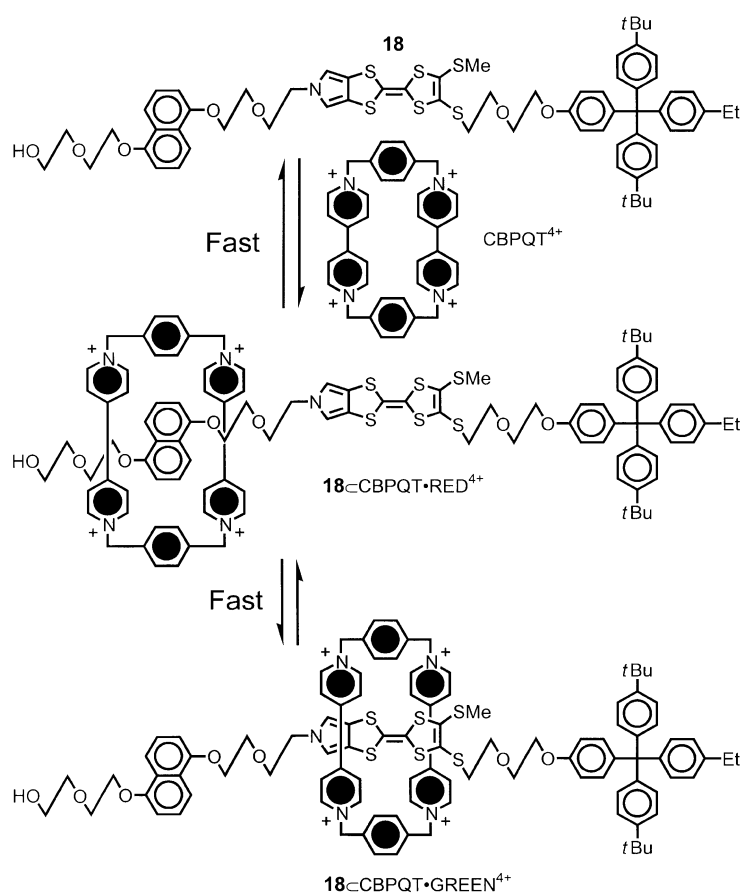
Scheme 8. Self-assembly of the two-station [2]pseudorotaxane **18** ⊂ CBPQT^{4+}.

(MPTTF and DNP), it can exist as a mixture of two translational isomers—one (**18** ⊂ CBPQT·GREEN^{4+}), in which the CBPQT^{4+} resides around the MPTTF unit, and the other (**18** ⊂ CBPQT·RED^{4+}), in which the CBPQT^{4+} resides around the DNP moiety. Indeed, a 1:1 mixture of CBPQT^{4+} and the semi-dumbbell **18** exhibits CT bands in Me$_2$CO centered around 745 nm (MPTTF/CBPQT^{4+}) and 545 nm (DNP/CBPQT^{4+}). These observations, taken together, indicate that the [2]pseudorotaxane **18** ⊂ CBPQT^{4+} is indeed a mixture of two translational isomers. The K_a and derived $-\Delta G°$ values[36] for the 1:1 complexation between CBPQT^{4+} and the semi-dumbbell **18** were obtained (Table 2) in Me$_2$CO at 298 K by UV-visible dilution experiments, by using both the MPTTF/CBPQT^{4+} and the DNP/CBPQT^{4+} CT

bands as probes.[15c, 35] The formation of **18** ⊂ CBPQT^{4+} and **24** ⊂ CBPQT^{4+} has also been followed by titrations of solutions of **18** or **24** with CBPQT^{4+} in MeCN (5.0 × 10^{-5} M) up to a value of seven for the [CBPQT^{4+}]/[**18**] and [CBPQT^{4+}]/[**24**] ratios. As previously observed for analogous systems,[18, 19f,p] formation of the [2]pseudorotaxanes is accompanied by a decrease of intensity in the UV region, and the appearance of weak and broad bands in the visible region. The titrations were carried out by monitoring the growth of the CT absorption bands at suitable wavelengths. Figure 6 illustrates the titration curves that have been fitted, assuming 1:1 complexation. Both the K_a values and the molar absorption coefficients (Table 2) at the selected wavelengths were taken as adjustable parameters, and a Newton–Raphson procedure was used[37] to minimize the squares of the residuals. After addition of seven equivalents of CBPQT^{4+}, 90 and 70% of the semi-dumbbell compounds **18** and **24**, respectively, were complexed. The $-\Delta G°$ values,[36] derived from the K_a values are also recorded in Table 2. Complexation is stronger in MeCN than in Me$_2$CO, a situation that has been observed previously for other donors.[15c, 38] After appropriate corrections, the absorption spectra of the two [2]pseudorotaxanes **18** ⊂ CBPQT^{4+} and **24** ⊂ CBPQT^{4+} in MeCN were obtained as shown in Figure 7. In the case of **24** ⊂ CBPQT^{4+}, the band with λ_{max} = 820 nm can be attributed to the CT interaction between the MPTTF unit[15, 19p] and CBPQT^{4+}. A comparison of the absorption spectrum of **24** ⊂ CBPQT^{4+} with the sum of the spectra of its separated components also shows a small increase in the absorption in the 350–450 nm region, which can be attributed to a CT interaction[11d, 31] between CBPQT^{4+} and the oxybenzene unit present in the hydrophobic stopper. Such an increase was also observed for **18** ⊂ CBPQT^{4+}. In the case of **18** ⊂ CBPQT^{4+}, the band with λ_{max} = 780 nm, assigned to the CT interaction between CBPQT^{4+} and the MPTTF unit, is accompanied by a broad absorption in the 450–650 nm region (Figure 7), which was assigned previously to a CT interaction between CBPQT^{4+} and the DNP moiety,[29d, 31a, 39] in

Table 2. Binding constants[35] (K_a) and free energy changes[36] ($-\Delta G°$) for the complexation of CBPQT^{4+} with the semi-dumbbell compounds **24** and **18** determined by UV-visible spectroscopy. Temperature: 298 K.

Com-pound	Solvent	λ_{max} [nm]	ε [L mol^{-1} cm^{-1}]	Data points	Correlation coefficient	K_a [M^{-1}][a]	$-\Delta G°$ [kcal mol^{-1}]
24[b]	Me$_2$CO	805	1310	15[c]	0.984	1 300[d,e]	4.2
24[d]	MeCN	820	1500	19	0.997	8 800[d,e]	5.4
18[b]	Me$_2$CO	545[e]	760	22[c]	0.917	25 000[d,e]	6.0
18[b]	Me$_2$CO	745	590	22[c]	0.959	25 000[d,e]	6.0
18[d]	MeCN	520[e]	1050	17	0.998	36 000[d,e]	6.2
18[d]	MeCN	780	920	17	0.999	26 000[d,e]	6.0

[a] Estimated error on K_a: ± 15%. [b] Determined from dilutions experiments. [c] Measurements were carried out from dilutions of two different stock solutions. [d] Determined from titration experiments. [e] Observed as a shoulder.
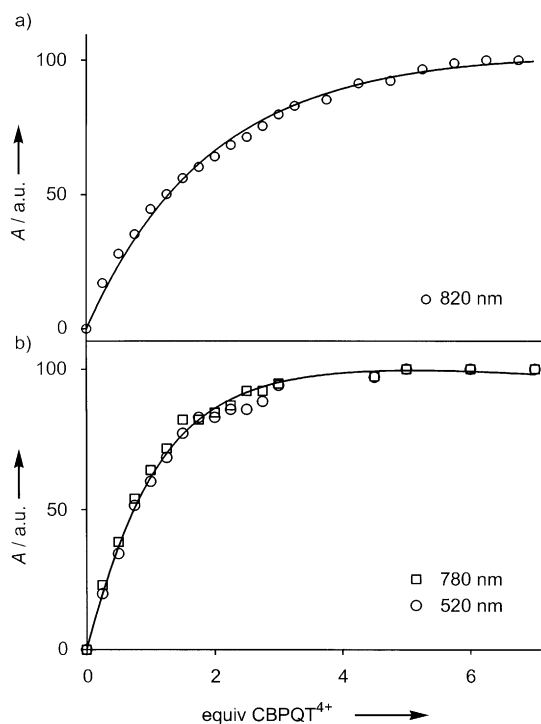
Figure 6. Titration curves for the formation of the [2]pseudorotaxanes a) $24 \subset CBPQT^{4+}$ and b) $18 \subset CBPQT^{4+}$ in MeCN at room temperature. For more details, see text.

agreement with the electrochemical findings (vide infra); this suggests that $18 \subset CBPQT^{4+}$ exists (Scheme 8) as a 1:1 mixture of the two translational isomers $18 \subset CBPQT \cdot GREEN^{4+}$ and $18 \subset CBPQT \cdot RED^{4+}$. A careful examination of the spectral region around 800 nm reveals that the MPTTF/CBPQT^{4+} CT bands in the two [2]pseudorotaxanes have different shapes, with their maxima displaced by 40 nm, an observation which is consistent with the existence in $18 \subset CBPQT \cdot RED^{4+}$ of folded conformations, wherein the MPTTF unit is involved in an "alongside" interaction with CBPQT^{4+}, as confirmed by the electrochemical results (vide infra). Although an in-depth analysis is made difficult because of the broad and overlapping nature of the two CT bands, information about the "alongside" MPTTF/CBPQT^{4+} CT
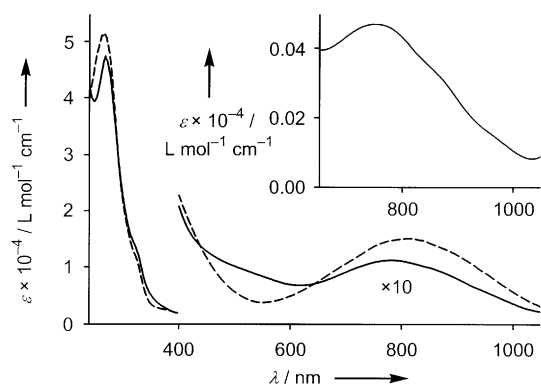
Figure 7. Absorption spectra of the [2]pseudorotaxanes $18 \subset CBPQT^{4+}$ (——) and $24 \subset CBPQT^{4+}$ (– – –) recorded in MeCN at room temperature. The contribution of the CT band of the "alongside" interacting MPTTF unit in $18 \subset CBPQT \cdot RED^{4+}$ is shown in the inset. For more details, see text.

interactions can be extracted from the spectroscopic data. If it is assumed that the CT interaction between the "inside" MPTTF and CBPQT^{4+} is identical in $18 \subset CBPQT^{4+}$ and $24 \subset CBPQT^{4+}$, then the contribution of the CT interaction between the "inside" MPTTF and CBPQT^{4+} will be 50% of the 820 nm band of $24 \subset CBPQT^{4+}$. When this contribution is subtracted from the experimental band then an absorption band with $\lambda_{max} = 780$ nm and $\varepsilon \sim 450$ Lmol^{-1}cm^{-1} appears (Figure 7, inset), which can be assigned to the "alongside" MPTTF/CBPQT^{4+} CT interactions. It is also worth noting that this ε value represents the "average" contribution to the CT interactions of all the possible conformers in which the MPTTF unit is "outside" the tetracationic cyclophane.

Dumbbells: The absorption spectra (Figure 8) of the dumbbell components **7**, **17**, and **23** are similar to the sums of the spectra of their model compounds (Figure 4), indicating that there are no significant electronic interactions among the
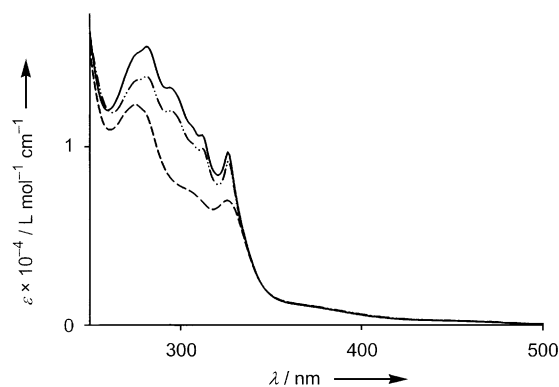
Figure 8. Absorption spectra of the dumbbell compounds **7** (– – –), **17** (——), and **23** (– ·· –) recorded in MeCN at room temperature.

chromophoric units in the ground state. Just as observed for the semi-dumbbell compounds **18** and **24**, the characteristic fluorescence of the model compounds **26** and **27** is completely quenched in the dumbbells. The most likely explanation for this quenching is the occurrence of an energy-transfer process from the emitting excited states of the DNP moiety and the oxybenzene units to the lower energy excited states of the MPTTF unit.[18, 19p, 33]

Single-station [2]rotaxane: The [2]rotaxane $\mathbf{1} \cdot 4PF_6$ was isolated as a green solid. A comparison of the absorption spectrum (Figure 9) of $\mathbf{1}^{4+}$ recorded in MeCN[40] with the sum of the spectra for CBPQT^{4+} and the dumbbell compound **7** reveals the expected decrease in the intensity in the UV region, and the appearance of weak and broad absorption bands in the 350–1100 nm region, typical of CT interactions.[10, 18, 19f,l,p] The band with $\lambda_{max} = 830$ nm ($\varepsilon = 1500$ Lmol^{-1}cm^{-1}) can be assigned to the interaction between the MPTTF unit and CBPQT^{4+} surrounding it. This band is similar to that exhibited by $24 \subset CBPQT^{4+}$ (Figure 9). The absorption in the 350–520 nm region could arise from CT interactions between the tetracationic cyclophane and oxybenzene units present in both stoppers, implying that folded
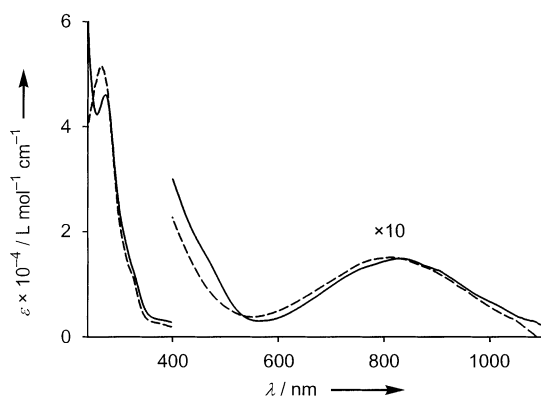
Figure 9. Comparison of the absorption spectra of the single-station [2]rotaxane $\mathbf{1}^{4+}$ (——) and the [2]pseudorotaxane $\mathbf{24} \subset$ CBPQT^{4+} (– – –) recorded in MeCN at room temperature.
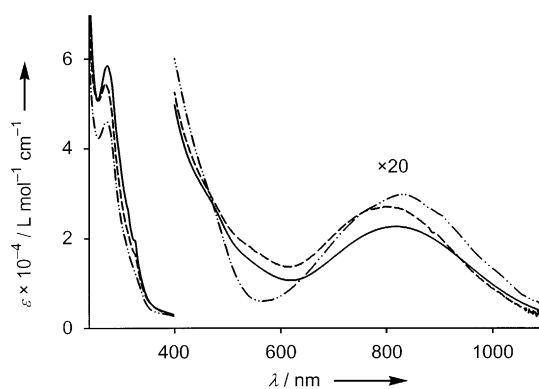
Figure 10. Comparison of the absorption spectra of the single-station [2]rotaxane $\mathbf{1}^{4+}$ (– · · –) and the two-station [2]rotaxanes $\mathbf{2}^{4+}$ (——) and $\mathbf{3}^{4+}$ (– – –) recorded in MeCN at room temperature.

conformations may be populated to some extent in solution.[11d, 31b,c]

Slow and fast two-station [2]rotaxanes: Both the [2]rotaxanes $\mathbf{2} \cdot 4\,\mathrm{PF}_6$ and $\mathbf{3} \cdot 4\,\mathrm{PF}_6$ were isolated as brown solids. They differ from the single-station [2]rotaxane $\mathbf{1}^{4+}$ because of the presence of a second π-electron-donating station, namely, a DNP moiety that, in $\mathbf{2}^{4+}$, is inserted between the MPTTF unit and the hydrophobic stopper, whereas in $\mathbf{3}^{4+}$ the DNP moiety is inserted between the MPTTF unit and the hydrophilic stopper. It should also be noted that in $\mathbf{2}^{4+}$ there is a bulky SMe group located "between" the two recognition sites. A comparison of the absorption spectra of $\mathbf{2}^{4+}$ and $\mathbf{3}^{4+}$ (Figure 10)[41] with the sums of the spectra for CBPQT^{4+} and the dumbbell compounds $\mathbf{17}$ and $\mathbf{23}$, respectively, shows the expected intensity decreases in the UV region and the appearance of very broad CT absorption bands across the 350–1100 nm spectral region. The two-station [2]rotaxane $\mathbf{3}^{4+}$ is expected to behave like the [2]pseudorotaxane $\mathbf{18} \subset$ CBPQT^{4+}. This is indeed the case, as it is evident from an inspection of the spectra shown in Figure 11. The spectra of both $\mathbf{3}^{4+}$ and $\mathbf{18} \subset$ CBPQT^{4+} exhibit a relatively large absorption in the 480–600 nm region, which is not observed for the [2]rotaxane $\mathbf{1}^{4+}$ (Figure 10) and the [2]pseudorotaxane $\mathbf{24} \subset$ CBPQT^{4+} (Figure 7). This absorption can clearly be assigned to the CT interaction[31a] between the DNP station and CBPQT^{4+}. According to electrochemical and ^{1}H NMR spectroscopic data (vide infra), approximately half of $\mathbf{3}^{4+}$ is present in MeCN at room temperature as the translational isomer in which CBPQT^{4+} encircles the DNP station.[42] The lower energy absorption band (600–1100 nm), which can be assigned to the CT interactions of the MPTTF encircled by CBPQT^{4+}, is similar to that observed for $\mathbf{18} \subset$ CBPQT^{4+} (Figure 11), although
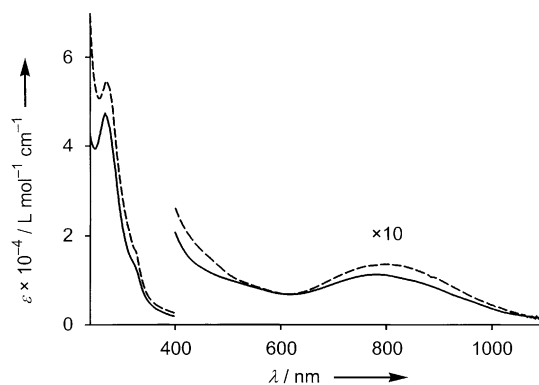
Figure 11. Comparison of the absorption spectra of the two-station [2]rotaxane $\mathbf{3}^{4+}$ (– – –) and the [2]pseudorotaxane $\mathbf{18} \subset$ CBPQT^{4+} (——) recorded in MeCN at room temperature.

it is displaced toward shorter wavelengths in comparison with the spectra of $\mathbf{1}^{4+}$ and $\mathbf{24} \subset$ CBPQT^{4+} (Table 3 and Figure 10). As in the case (vide supra) of $\mathbf{18} \subset$ CBPQT^{4+}, we believe that this shift arises from the contribution of "alongside" CT interactions between the MPTTF unit and CBPQT^{4+} in folded conformations. The lower energy absorption band of $\mathbf{2}^{4+}$ (Figure 10) is similar to those observed for $\mathbf{1}^{4+}$ and $\mathbf{24} \subset$ CBPQT^{4+} (Figure 9). This observation is consistent with the electrochemical and ^{1}H NMR spectroscopic results (vide infra), which show that, in the case of $\mathbf{2}^{4+}$, the predominant

Table 3. Photophysical data at 298 K for the [2]pseudorotaxanes $\mathbf{24} \subset$ CBPQT^{4+} and $\mathbf{18} \subset$ CBPQT^{4+} and for the [2]rotaxanes $\mathbf{1}^{4+}$, $\mathbf{2}^{4+}$, and $\mathbf{3}^{4+}$.

| Compound/Complex | Solvent | GREEN | | RED | |
		λ_{max} [nm]	ε [L mol^{-1} cm^{-1}]	λ[a] [nm]	ε [L mol^{-1} cm^{-1}]
$\mathbf{24} \subset$ CBPQT^{4+}	Me$_2$CO	805	1310	–	–
$\mathbf{24} \subset$ CBPQT^{4+}	MeCN	820	1500	–	–
$\mathbf{18} \subset$ CBPQT^{4+}	Me$_2$CO	745	590	545	760
$\mathbf{18} \subset$ CBPQT^{4+}	MeCN	780	920	520	1050
$\mathbf{1}^{4+}$	Me$_2$CO	810	1400	–	–
$\mathbf{1}^{4+}$	MeCN	830	1500	–	–
$\mathbf{2}^{4+}$	Me$_2$CO	805	860	540	760
$\mathbf{2}^{4+}$	MeCN	820	1100	520	880
$\mathbf{3}^{4+}$	Me$_2$CO	785	740	540	760
$\mathbf{3}^{4+}$	MeCN	800	1300	520	960
$\mathbf{3}^{4+}$	Me$_2$SO	765	1310	540	640

[a] Observed as a shoulder.

($\sim 75\%$) translational isomer is the one in which CBPQT^{4+} encircles the MPTTF unit.

Figure 12 shows the absorption spectra of the [2]rotaxane 3^{4+} recorded in MeCN, Me$_2$CO, and Me$_2$SO. In all of these solvents, a broad absorption band is observed in the region 600–1100 nm (Table 3); this can be assigned to the CT interactions of the MPTTF unit encircled by CBPQT^{4+}. In
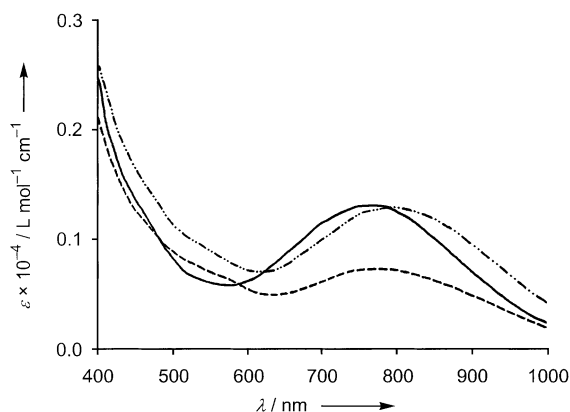
Figure 12. Absorption spectra (298 K) of an equilibrium mixture of the [2]rotaxanes $3 \cdot$ GREEN^{4+} and $3 \cdot$ RED^{4+} recorded in MeCN ($- \cdots -$), Me$_2$CO ($---$), and Me$_2$SO (——).

both MeCN and Me$_2$CO (brown solutions), a relatively large absorption in the 480–600 nm region is observed and can be assigned to a CT interaction between the DNP station and CBPQT^{4+}. However, in Me$_2$SO (dark green solution), only a tiny shoulder at 540 nm is observed, indicating that $3 \cdot$ GREEN^{4+} is the major translational isomer in this solvent, a conclusion that is in agreement with the ^{1}H NMR spectroscopic findings (vide infra). They suggest that 3^{4+} exists as a 1:1 mixture in MeCN, a 1:3 mixture in Me$_2$CO, and a 2:1 mixture in Me$_2$SO of the two translational isomers, $3 \cdot$ GREEN^{4+} and $3 \cdot$ RED^{4+}.

Electrochemical investigations: The electrochemical studies were carried out in argon-purged MeCN solutions at room temperature by using cyclic voltammetry (CV) and differential pulse voltammetry (DPV). Since the compounds and complexes that have been investigated contain numerous electro-active units, their electrochemical behavior is rather complex: for example, in the case of the [2]rotaxanes 2^{4+} and 3^{4+}, at least seven oxidation and four reduction processes were observed. We have mainly focussed our studies on the oxidation processes of the MPTTF and DNP electron-donating units contained in the semi-dumbbell and dumbbell compounds, and on the reduction processes of the CBPQT^{4+} electron-accepting cyclophane.

Semi-dumbbells, dumbbells, and tetracationic cyclophanes: The semi-dumbbells **18** and **24** and the dumbbells **7**, **17**, and **23** contain one (MPTTF) or two (MPTTF and DNP) electron-donating units[18, 19p, 31a] and either one or two stoppers, containing oxybenzene units, which are also expected to

exhibit some electron-donating power.[11d, 31b,c] The results obtained concerning the two stations are listed in Table 4, along with the data for the MPTTF **25** and DNP **26** model compounds (Figure 3). The semi-dumbbell **24** and the dumbbell **7** show two reversible, monoelectronic processes (Figure 13 and Table 4), assigned to the MPTTF unit and, at more positive potentials, irreversible oxidation processes associated with the stoppers. The observed processes take place at practically the same potentials as those recorded for the model compounds **25**, **27**, and **28** (MPTTF **25**: $+0.44$, $+0.74$ V; **27**: $+1.55$, $+1.76$ V; **28**: $+1.31$, $+1.63$, $+1.81$ V vs SCE), suggesting that there are no interactions among the electro-

Table 4. Electrochemical data[a] for the MPTTF and DNP model compounds **25** and **26**, the semi-dumbbell compounds **24** and **18**, the dumbbell compounds **7**, **17**, and **23**, the [2]psudorotaxanes $24 \subset$ CBPQT^{4+} and $18 \subset$ CBPQT^{4+}, and the [2]rotaxanes 1^{4+}, 2^{4+}, and 3^{4+}.

Compound/Complex	MPTTF[b] E_{ox} [V][c]		DNP[b] E_{ox} [V][d]
25	$+0.44$	$+0.74$	–
26	–	–	$+1.12$
24	$+0.44$	$+0.74$	–
18	$+0.41$	$+0.72$	$+1.24$
7	$+0.44$	$+0.74$	–
17	$+0.34$	$+0.70$	
23	$+0.39$	$+0.72$	
24 $\subset$ CBPQT^{4+}	$+0.47$	$+0.74$	–
18 $\subset$ CBPQT^{4+}	$+0.48$	$+0.74$[e]	$+1.24$
1^{4+}	$+0.77$	$+0.81$	–
2^{4+}	$+0.50$	$+0.74$[e]	
3^{4+}	$+0.54$	$+0.76$[e]	

[a] Argon-purged MeCN, room temperature, tetraethylammonium hexaflourophosphate (TEAPF$_6$) as supporting electrolyte, glassy carbon as working electrode, potential values in V versus SCE. [b] Units involved in the observed processes. [c] Reversible and monoelectronic processes, unless otherwise indicated. [d] Irreversible process. [e] Overlapping of processes. For more details, see text.
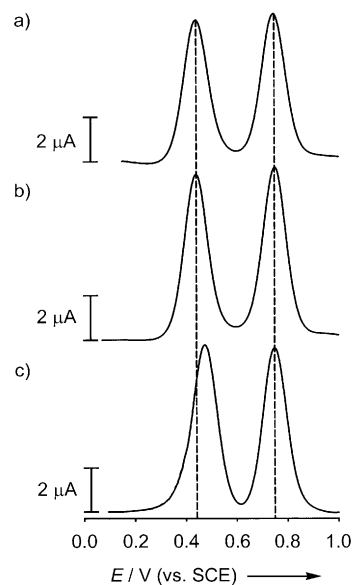
Figure 13. DPV peaks in MeCN solutions of a) the MPTTF model compound **25**, b) the semi-dumbbell compound **24**, and c) the [2]pseudo-rotaxane $24 \subset$ CBPQT^{4+}. The current intensity has been corrected to take into account differences in diffusion coefficients and concentrations.

active units. Comparison of the results obtained for the semi-dumbbell **18** and the dumbbells **17** and **23** (Figure 14 and Table 4) with those of the MPTTF model compound **25** shows that both the first and second oxidation processes associated with the MPTTF unit take place at a potential that is less
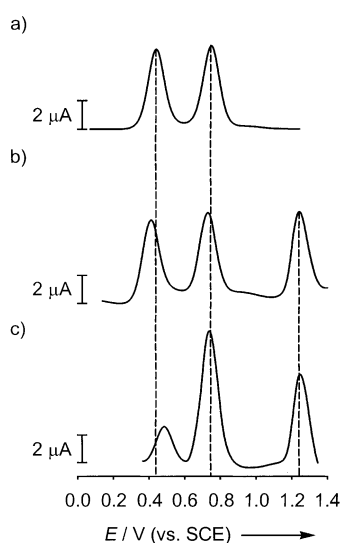
Figure 14. DPV peaks in MeCN solutions of a) the MPTTF model compound **25**, b) the semi-dumbbell compound **18**, and c) the [2]pseudo-rotaxane **18** ⊂ CBPQT^{4+}. The current intensity has been corrected to take into account differences in diffusion coefficients and concentrations.

positive than these observed for the model compound **25**. This behavior can be attributed to the presence of interactions arising between both the MPTTF$^{·+}$ and MPTTF^{2+} and the electron-donating units, for example, the DNP moiety, incorporated in the compounds.[18] Besides the MPTTF-based processes, the semi-dumbbell **18** and the dumbbells **17** and **23** show, at more positive potentials, irreversible processes that can be attributed to the oxidation of the DNP moiety as well as the oxybenzene units present in the two stoppers. For the dumbbells **17** and **23**, the first irreversible oxidation of the hydrophilic dendritic stopper takes place at a potential similar to that of the DNP moiety. The electron-accepting CBPQT^{4+} cyclophane shows the well-known reversible and bielectronic processes at −0.29 and −0.71 V versus SCE, which can be assigned to the simultaneous first and second reductions of the two bipyridinium units.[10]

[2]Pseudorotaxanes: The binding constants of CBPQT^{4+} with the semi-dumbbells **18** and **24** (33 000 and 8800 M^{-1} in MeCN for **18** ⊂ CBPQT^{4+} and **24** ⊂ CBPQT^{4+}, respectively) are not large enough to avoid the presence of substantial amounts of free species starting from equimolar concentrations of the two components. Therefore, the electrochemical characterization of the electron-donating and electron-accepting units in these [2]pseudorotaxanes has to be investigated in the presence of an excess of CBPQT^{4+} or semi-dumbbell components, respectively. In solutions of **18** (9.3×10^{-5} M) or **24** (1.5×10^{-4} M) in MeCN (in both cases, close to the solubility limit) and an excess (10 equivalents) of CBPQT^{4+}, the fractions of [2]pseudorotaxanes (96% for **18** ⊂ CBPQT^{4+} and 92% for

24 ⊂ CBPQT^{4+}) are very large compared with the small amount of uncomplexed semi-dumbbell compounds **18** and **24**. It has been possible, therefore, to study the oxidation of the electron-donating units engaged in these two [2]pseudo-rotaxanes. The low solubilities of the semi-dumbbell compounds **18** and **24**, however, have prevented us from performing electrochemical studies under conditions in which the complexed fraction of CBPQT^{4+} is large relative to the uncomplexed one.

Since the semi-dumbbell **24** contains only an MPTTF station for CBPQT^{4+} the [2]pseudorotaxane **24** ⊂ CBPQT^{4+} is the simplest system to have been examined. The results obtained for **24** and **24** ⊂ CBPQT^{4+} (Figure 13 and Table 4) show that, in the [2]pseudorotaxane, the first oxidation of the MPTTF unit is slightly shifted (30 mV) towards more positive potentials with respect to that of the semi-dumbbell **24**, while the second oxidation takes place at the same potential. These results can be explained[18, 19f] as follows: 1) in the [2]pseudo-rotaxane, the MPTTF unit is engaged in CT interactions with CBPQT^{4+}; and 2) after the first oxidation of the MPTTF unit, dethreading takes place as expected, because the CT inter-action is being destroyed and a Coulombic repulsion arises between the oxidized MPTTF unit and the tetracationic cyclophane.

In the [2]pseudorotaxane **18** ⊂ CBPQT^{4+}, there are two stations (one MPTTF and one DNP) on the semi-dumbbell component for CBPQT^{4+} to encircle. The simplest hypothesis is that CBPQT^{4+} encircles the MPTTF station, which accord-ing to its oxidation potential, is the better electron donor. If this is the case, the electrochemical behavior should be similar to that found in the [2]pseudorotaxane **24** ⊂ CBPQT^{4+}. At first sight, the observed potentials (+0.48 and +0.74 V vs. SCE, both in the range expected for MPTTF oxidation; Table 4) appear to be consistent with the above hypothesis. However, the CV shapes and current intensities, and the DPV peak areas for the two oxidation processes are different (Figure 14), indicating a more complex situation. The pres-ence of two discrete translational isomers of **18** ⊂ CBPQT^{4+} (Scheme 8) is also inconsistent with the results obtained, because there is no evidence for a noninteracting MPTTF station. These results suggest that the MPTTF station is always engaged in donor–acceptor interactions in at least two different ways. The simplest hypothesis that accounts for these results is that: 1) both the translational isomers are present and 2) in the isomer in which CBPQT^{4+} encircles the DNP moiety, the MPTTF unit is engaged in an "alongside" interaction with CBPQT^{4+} in a folded superstructure. We can thus assign the process at +0.48 V (shifted by 70 mV toward more positive potentials with respect to the same process in its semi-dumbbell **18**) to the first oxidation of the MPTTF unit interacting in an "alongside" manner with CBPQT^{4+}. The comparison with the current intensity of the CV wave and the area of the DPV peak at +0.48 V with those of **18** at +0.41 V (Figure 14) shows that approximately 50% of the MPTTF units are involved in "alongside" interactions. This situation implies that, in the [2]pseudorotaxane **18** ⊂ CBPQT^{4+}, there is also approximately 50% of the transla-tional isomer in which the MPTTF unit is located "inside" the electron-accepting cyclophane. It should be noted that the

potential for the first oxidation of the MPTTF unit in the translational isomer in which it is encircled by CBPQT^{4+} is closer to that observed for the [2]rotaxane $\mathbf{1}^{4+}$ (vide infra) than for the [2]pseudorotaxane $\mathbf{24} \subset$ CBPQT^{4+}. This shows that in the case of $\mathbf{24} \subset$ CBPQT^{4+} dethreading is faster than for $\mathbf{18} \subset$ CBPQT^{4+}, as might be expected. Therefore, in agreement with the behavior of the [2]rotaxane $\mathbf{1}^{4+}$, the first oxidation of the "inside" MPTTF unit has to be much more positively shifted than that of the "alongside" MPTTF unit, to the extent that it is expected to overlap with the second oxidation process. We can, therefore, assign the process observed at $+0.74$ V to both the first and second oxidation of the "inside" MPTTF unit, as well as to the second oxidation of the "alongside" MPTTF unit. This assignment is consistent with the current intensity of the CV wave and the area of the DPV peak of the process observed at $+0.74$ V, with respect to those of the process taking place at $+0.48$ V. The fact that the second oxidation of the MPTTF unit in $\mathbf{18} \subset$ CBPQT^{4+} takes place approximately at the same potential as that observed in the semi-dumbbell $\mathbf{18}$, regardless of its "alongside" and "inside" position, shows that, after the first oxidation of the MPTTF unit, CBPQT^{4+} leaves the MPTTF station. Since the potential for the oxidation of the DNP moiety is the same in $\mathbf{18} \subset$ CBPQT^{4+} as that found in the semi-dumbbell $\mathbf{18}$, we can conclude that after the second oxidation of the MPTTF unit the cyclophane is no longer engaged with the semi-dumbbell component. Whether dethreading had already occurred after the first MPTTF oxidation, as could be expected if the Coulombic repulsion between the monooxidized MPTTF unit and the tetracationic cyclophane overcomes the CT interaction of CBPQT^{4+} with the DNP moiety, cannot be said from the experimental results.

[2]Rotaxanes: Since the single-station [2]rotaxane $\mathbf{1}^{4+}$ contains, in its dumbbell component, only an MPTTF station for CBPQT^{4+}, it can be considered as a model for the electrochemical behavior of an MPTTF unit "inside" the CBPQT^{4+}. On going from the dumbbell $\mathbf{7}$ to the [2]rotaxane $\mathbf{1}^{4+}$, the two monoelectronic oxidation processes of the MPTTF unit, well separated in the dumbbell, occurs at two very close potentials, $+0.77$ and $+0.81$ V versus SCE (Figure 15 and Table 4). We assign the process at $+0.77$ V to the first oxidation of the MPTTF unit located "inside" the electron-accepting cyclophane. The shift of 330 mV toward more positive potential for the first oxidation process of the MPTTF unit in $\mathbf{1}^{4+}$ is easily explained on the basis of the electrostatic repulsion and the strong CT interaction with the two-electron-accepting bipyridinium units in CBPQT^{4+}. Since the electrochemical behavior of the [2]pseudorotaxanes $\mathbf{18} \subset$ CBPQT^{4+} and $\mathbf{24} \subset$ CBPQT^{4+} shows that CBPQT^{4+} leaves the MPTTF stations after their first oxidations, we can assign the process at $+0.81$ V to the second oxidation of an MPTTF unit that is no longer encircled by CBPQT^{4+}. The shift of 70 mV toward more positive potential for this process, compared to the same process in the dumbbell $\mathbf{7}$, can be accounted for by the presence of the two stoppers and the shortness of the dumbbell component, both features that force the tetracationic electron-accepting cyclophane to remain near to the dioxidized MPTTF unit.
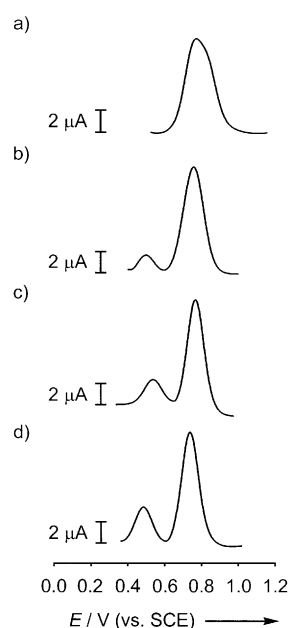
Figure 15. DPV peaks in MeCN solutions of a) the single-station [2]rotaxane $\mathbf{1}^{4+}$, b) the two-station [2]rotaxane $\mathbf{2}^{4+}$, c) the two-station [2]rotaxane $\mathbf{3}^{4+}$, and d) the [2]pseudorotaxane $\mathbf{18} \subset$ CBPQT^{4+}. The current intensity has been corrected to take into account differences in diffusion coefficients and concentrations.

A more complex situation arises in the case of the [2]rotaxanes $\mathbf{2}^{4+}$ and $\mathbf{3}^{4+}$, which can be expected to give two translational isomers (Schemes 4 and 6). In the potential range of MPTTF oxidation, two processes take place in both $\mathbf{2}^{4+}$ and $\mathbf{3}^{4+}$: at $+0.50$ and $+0.74$ V for $\mathbf{2}^{4+}$, and at $+0.54$ and $+0.76$ V versus SCE for $\mathbf{3}^{4+}$ (Figure 15 and Table 4). These two processes exhibit different CV current intensities and DPV peak areas. Following the manner in which we treated the [2]pseudorotaxane $\mathbf{18} \subset$ CBPQT^{4+} and taking the single-station [2]rotaxane $\mathbf{1}^{4+}$ as an appropriate reference for an MPTTF unit located "inside" CBPQT^{4+}, we can attribute the first process for $\mathbf{2}^{4+}$ and $\mathbf{3}^{4+}$ to the first oxidation of the MPTTF unit interacting "alongside" with CBPQT^{4+}. The comparison of the CV current intensity and the DPV peak area for this process in these two [2]rotaxanes and their corresponding dumbbells allows us to estimate that the percentage of the translational isomer with MPTTF interacting "alongside" is 20% for $\mathbf{2}^{4+}$ and 60% for $\mathbf{3}^{4+}$; as a consequence, the remaining 80% of $\mathbf{2}^{4+}$ and 40% of $\mathbf{3}^{4+}$ correspond to the translational isomer in which CBPQT^{4+} encircles the MPTTF unit. Therefore, we can attribute the process occurring at $+0.74$ V for $\mathbf{2}^{4+}$ and at $+0.76$ V for $\mathbf{3}^{4+}$ to the first and second oxidation processes of the "inside" MPTTF unit and to the second oxidation of the "alongside" MPTTF unit. These attributions are consistent with the CV current intensities and also with the DPV peak areas for the first and second oxidation processes observed in these two [2]rotaxanes. We have noticed that some of the results seem to indicate that the hydrophilic dendritic stopper plays an important role as far as the distribution of CBPQT^{4+} between the two stations is concerned. In the case of the [2]pseudorotaxane $\mathbf{18} \subset$ CBPQT^{4+}, which does not contain the hydro-

philic dendritic stopper, the two translational isomers are present in a 1:1 ratio, whereas, in case of the [2]rotaxane 3^{4+}, the station closer to the hydrophilic dendritic stopper (i.e., DNP) is preferred, as shown by the 3:2 ratio. The fact that the station closer (i.e., the MPTTF one) to the hydrophilic dendritic stopper is even more preferred (4:1 ratio) in the case of the [2]rotaxane 2^{4+} can be related to the different structures of the dumbbell components, including the presence of the SMe "knob" between the two electron-donating stations in 2^{4+}.

As far as the translational isomer with the MPTTF unit located "inside" CBPQT^{4+} is concerned, it is impossible to demonstrate the occurrence of the expected ring shuttling after oxidation of the MPTTF unit, since both oxidation processes for the free and encircled DNP moiety overlap with the irreversible oxidation processes of the oxybenzene units present in both of the stoppers. However, the fact that in the [2]rotaxanes 2^{4+} and 3^{4+} the second oxidation of the MPTTF unit, regardless of its "alongside" or "inside" location, is only slightly shifted (40 mV) toward more positive potentials compared (Table 4) with the same process in their corresponding dumbbells, seems to indicate that CBPQT^{4+} shuttling does take place. This shift, observed in the [2]rotaxanes, can be accounted for by 1) the presence of CBPQT^{4+}, which destroys the interactions of the oxidized MPTTF with the other electron-donating units believed to be present in the case of the dumbbell compounds 17 and 23; and 2) a Coulombic repulsion, which arises between the tetracationic cyclophane and the oxidized MPTTF unit.

For all the rotaxanes investigated, reduction processes involving the tetracationic cyclophane were also expected. In most of the pseudorotaxanes, rotaxanes, and catenanes, previously studied, the redox processes of the cyclophane were clean and very useful for interpreting the structures and the dynamic behavior of the systems.[2e,g, 10, 18, 19f, 31a] In the case of the present rotaxanes, however, although several reduction processes were observed, unfortunately all the reduction processes were irreversible and, in some cases, affected by adsorption phenomena. We suppose that such an unusual electrochemical behavior, which prevented us from obtaining useful pieces of information, is related to the extensive folding around CBPQT^{4+} of portions of the dumbbell components in these long and flexible compounds.

^{1}H NMR investigations: These were carried out in CD$_3$COCD$_3$, CD$_3$CN, or CD$_3$SOCD$_3$. Four systems were investigated (Schemes 2, 4, 6, and 8): 1) the single-station [2]rotaxane 1^{4+}, 2) the slow two-station [2]rotaxane 2^{4+}, 3) the [2]pseudorotaxane $18 \subset$ CBPQT^{4+}, and 4) the fast two-station [2]rotaxane 3^{4+}.

Single-station [2]rotaxane: A comparison of the ^{1}H NMR spectra (400 MHz, CD$_3$COCD$_3$, 298 K) of the dumbbell compound 7 and the [2]rotaxane 1^{4+} reveals significant chemical shift differences for the resonances associated with the protons located close to the MPTTF unit (Table 5), indicating that the tetracationic cyclophane encircles the MPTTF unit in the [2]rotaxane 1^{4+}.

Table 5. Selected ^{1}H NMR spectroscopic data[a] (δ and $\Delta\delta$ values) for the dumbbell compound 7 and the single-station [2]rotaxane 1^{4+} in CD$_3$COCD$_3$ at 298 K.

Compound	SCH_3	SCH_2CH$_2$O	SCH$_2$CH_2O	NCH_2Ar	Pyr-H[b]
7	2.39[c]	3.02[c]	3.72[c]	4.88[c]	6.71[c]
1^{4+}	2.64[c]	3.29[c]	3.95[c]	5.18[c]	6.44[c]
	+ 0.25[d]	+ 0.27[d]	+ 0.23[d]	+ 0.30[d]	− 0.27[d]

[a] ^{1}H NMR spectra were recorded at 400 MHz. [b] The resonances associated with the two pyrrole protons are nonequivalent and AB systems ($J = 2$ Hz) are observed in the spectra. The values reported correspond to the centroids of the AB systems. [c] δ values. [d] $\Delta\delta$ values in ppm.

Slow two-station [2]rotaxane: ^{1}H NMR spectroscopy indicated the presence of the two stable translational isomers present in the isolated product. The ^{1}H NMR spectrum (400 MHz) of 2^{4+} recorded at 298 K in CD$_3$COCD$_3$ showed two singlets at $\delta = 2.64$ and 2.47 ppm (Figure 16), which can be assigned to the protons in the SMe groups, attached to the MPTTF units in 2·GREEN^{4+} and 2·RED^{4+}, respectively. From the integrals of the two different SMe resonances, the ratio of the two translational isomers was estimated to be approximately 1:1.
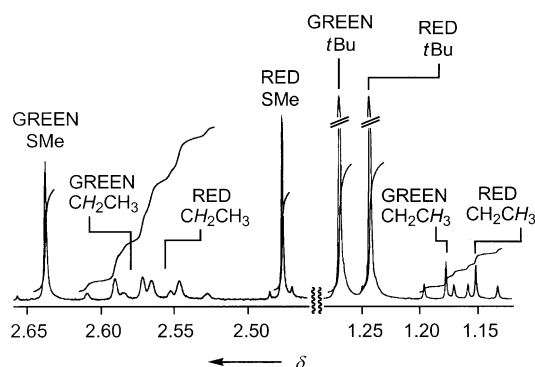
Figure 16. Partial ^{1}H NMR spectrum of an equilibrium mixture of the [2]rotaxanes 2·GREEN^{4+} and 2·RED^{4+} recorded at 400 MHz in CD$_3$COCD$_3$ at 298 K.

[2]Pseudorotaxane $18 \subset$ CBPQT^{4+}: The ^{1}H NMR spectrum (500 MHz) of an equilibrated 1:1 mixture of the semi-dumbbell 18 and CBPQT^{4+} recorded in CD$_3$COCD$_3$ at 300 K revealed broad signals, because of fast exchange between complexed (i.e., $18 \subset$ CBPQT^{4+}) and free species on the ^{1}H NMR timescale. The presence of both $18 \subset$ CBPQT· GREEN^{4+} and $18 \subset$ CBPQT·RED^{4+} in the complexed species is confirmed by the identification of singlets resonating at $\delta = 2.70$ and 2.34 ppm, which can be assigned to the SMe resonances, attached to the MPTTF unit in $18 \subset$ CBPQT· GREEN^{4+} and $18 \subset$ CBPQT·RED^{4+}, respectively. The ratio of the two co-conformations is roughly[43] estimated to be 3:1 in favor of $18 \subset$ CBPQT·RED^{4+}. Upon cooling the sample down to 245 K, all the signals sharpened and the ^{1}H NMR spectrum (500 MHz; Figure 17) revealed that $18 \subset$ CBPQT· RED^{4+} is almost exclusively present[44] in the CD$_3$COCD$_3$ solution at 245 K. The most diagnostic evidence, which indicates that CBPQT^{4+} encircles the DNP moiety, is the very high upfield shift of the resonances for the DNP-H-4/8 protons, which are observed as two doublets ($J = 8$ Hz) at $\delta = 2.59$ and 2.69 ppm. The δ values for the DNP-H-4/8 protons in

FULL PAPER

J. F. Stoddart, J. O. Jeppesen, M. T. Gandolfi, M. Venturi et al.
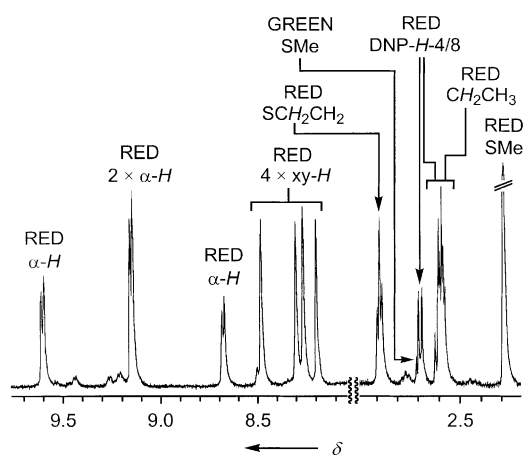
Figure 17. Partial ^{1}H NMR spectrum (500 MHz) of the 1:1 complexes formed between the semi-dumbbell compound **18** and CBPQT^{4+} recorded in CD$_3$COCD$_3$ at 245 K.

Figure 18. Partial ^{1}H NMR spectrum of an equilibrium mixture of the [2]rotaxanes **3**·GREEN^{4+} and **3**·RED^{4+}, recorded at 500 MHz in CD$_3$CN at 300 K.

18 ⊂ CBPQT·RED^{4+} and the same protons in the semi-dumbbell compound **18** are shifted upfield by 5.21 and 5.14 ppm, respectively. They are of a similar magnitude to those previously reported.[45] Moreover, one intense SMe singlet (Figure 17) resonating at $\delta = 2.29$ ppm is observed. The limited amount of **18** ⊂ CBPQT·GREEN^{4+} present in the CD$_3$COCD$_3$ solution at 245 K is indicated by a very small singlet at $\delta = 2.71$ ppm arising from the SMe protons in **18** ⊂ CBPQT·GREEN^{4+}.

Fast two-station [2]rotaxane: The ^{1}H NMR spectrum (500 MHz) of the [2]rotaxane **3**$^{4+}$ recorded in CD$_3$CN at 300 K (Figure 18) showed two triplets ($J = 8$ Hz) at $\delta = 5.79$ and 5.91 ppm and two doublets ($J = 8$ Hz) at $\delta = 6.12$ and 6.24 ppm; these can be assigned to the DNP-H-3/7 and the DNP-H-2/6 protons, respectively, in **3**·RED^{4+}. The presence of **3**·GREEN^{4+} in the isolated mixture is confirmed by the appearance of an AB system ($J = 2$ Hz) at $\delta = 6.30$ and 6.32 ppm (Figure 18), which can be assigned to the two chemically nonequivalent pyrrole protons in **3**·GREEN^{4+}. Furthermore, two singlets at $\delta = 2.27$ and 2.61 ppm are observed, which can be assigned to the SMe resonances attached to the TTF unit in **3**·RED^{4+} and **3**·GREEN^{4+}, respectively. Finally, four singlets are observed in the region $\delta = 4.6$–5.0 ppm (Figure 18), in the form of an ^{1}H NMR spectroscopic signature; this results from the two different sets of ArCH_2O protons in the hydrophilic dendritic stopper of **3**·RED^{4+} ($\delta = 4.71$ and 4.86 ppm) and **3**·GREEN^{4+} ($\delta = 4.79$ and

4.89 ppm). From the integrals of the signals for the DNP H-2/6 protons in **3**·RED^{4+} and the two pyrrole protons in **3**·GREEN^{4+}, the ratio of the two translational isomers was estimated to be approximately 1:1 at 300 K in CD$_3$CN.

The ^{1}H NMR spectrum (500 MHz) of the [2]rotaxane **3**$^{4+}$ in CD$_3$COCD$_3$ at 300 K revealed that the ratio of **3**·RED^{4+} and **3**·GREEN^{4+} in this solvent is 3:1 in favor of **3**·RED^{4+}. On cooling this sample down to 245 K, the color of the solution changed to red, and the ^{1}H NMR spectrum revealed that **3**·RED^{4+} is almost exclusively present in the CD$_3$COCD$_3$ solution at 245 K (Figure 19). The most diagnostic signals, indicating that CBPQT^{4+} encircles the DNP moiety, are the very high upfield shifted ones for the DNP-H-4/8 protons, which are observed as two doublets ($J = 8$ Hz) at $\delta = 2.44$ and
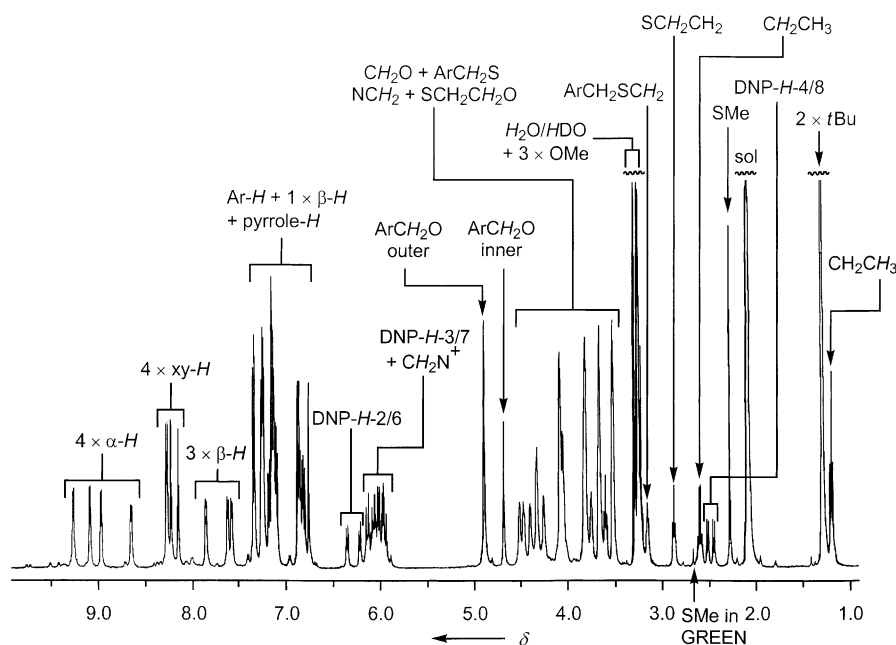
Figure 19. Full ^{1}H NMR spectrum (500 MHz) of the fast two-station [2]rotaxane **3**$^{4+}$ recorded in CD$_3$COCD$_3$ at 245 K.

2.51 ppm. The values of $\Delta\delta$ for the DNP-H-4/8 protons in $3 \cdot 4PF_6 \cdot RED$ and the same protons in the dumbbell compound **23** are -5.35 and -5.36 ppm, respectively. They are of similar magnitudes to those previously reported.[45] Moreover, only one intense SMe singlet, resonating at $\delta = 2.27$ ppm, is observed. The limited amount of $3 \cdot GREEN^{4+}$ present in CD_3COCD_3 at 245 K is, for example, evidenced by a very small singlet at $\delta = 2.67$ ppm arising from the SMe protons in $3 \cdot GREEN^{4+}$.

The ^1H NMR spectrum (500 MHz, CD_3SOCD_3) recorded on the [2]rotaxane 3^{4+} at 300 K indicated that $3 \cdot GREEN^{4+}$ is the major translational isomer in CD_3SOCD_3. Although, all resonances are broad at this temperature, most likely on account of slow site-exchange processes in this solvent, the presence of $3 \cdot GREEN^{4+}$ as the major isomer is evident. The ^1H NMR spectrum revealed a broad singlet at $\delta = 6.49$ ppm, which can be assigned to the two pyrrole protons in $3 \cdot GREEN^{4+}$. The presence of $3 \cdot RED^{4+}$ in this solvent can be identified from the presence of a broad multiplet at $\delta = 6.05 - 6.20$ ppm, which can be assigned to the DNP-H-2/6 protons in $3 \cdot RED^{4+}$. From the integrals of the two pyrrole protons in $3 \cdot GREEN^{4+}$ and the DNP-H-2/6 protons in $3 \cdot RED^{4+}$, the ratio of the two translational isomers was estimated to be approximately[46] 2:1 in favor of $3 \cdot GREEN^{4+}$ at 300 K in CD_3SOCD_3. Upon heating (400 K) of this sample, all the signals sharpen and the existence of $3 \cdot GREEN^{4+}$ as the only translational isomer at 400 K is easily discerned from the ^1H NMR spectrum (500 MHz). For example, only one SMe singlet (Figure 20) resonating at $\delta = 2.68$ ppm is observed. Moreover, a singlet resonating at $\delta = 6.35$ ppm and integrating for two protons, is also evident, and can be assigned to the two pyrrole protons in $3 \cdot GREEN^{4+}$. Finally, no signals are observed in the region $\delta = 6.0 - 6.3$ ppm that would result from the DNP-H-2/6 protons being located inside the cyclophane, supporting the conclusion that the MPTTF unit of the dumbbell-shaped component is encircled exclusively by $CBPQT^{4+}$ at 400 K in CD_3SOCD_3.

Dynamic investigations: These were carried out in CD_3COCD_3, CD_3CN, or CD_3SOCD_3. Three systems were investigated: 1) the single-station [2]rotaxane 1^{4+}, 2) the slow two-station [2]rotaxane 2^{4+}, and 3) the fast two-station [2]rotaxane 3^{4+}.

Single-station [2]rotaxane: The resonances associated with the α- and β-bipyridinium protons on the cyclophane component $CBPQT^{4+}$ in the single-station [2]rotaxane 1^{4+} are observed to undergo coalescence with increasing temperature. This is most clearly seen with the α-bipyridinium protons (Figure 21b), which exist as two sets of signals at low temperature and coalesce into one set of signals at high temperature (presumably each of these sets consists of multiple overlapping signals). The process by which these protons are interconverted is termed pyridinium rotation (Figure 21a, process I), and involves rotation of one of the pyridinium units about its axis of substitution. The barrier[47] ($\Delta G^{\pm}$) for this process to occur was determined[48] (Table 6) and observed to be 15.3 kcal mol^{-1} at 260 K.[49] This can be compared to values obtained for the same process in a series of [2]catenanes,[50] for which the barriers were observed to range from $16 - 17$ kcal mol^{-1}. The lower barrier in the present case can be attributed to the much less constricted nature of the tetracationic cyclophane in the [2]rotaxane relative to the [2]catenanes.

In addition to rotation of the pyridinium units, evidence for rotation of the p-xylyl units (Figure 21a, process II) of the $CBPQT^{4+}$ component can also be seen in the ^1H NMR spectra. At low temperatures it is possible to observe two sets of signals again (Figure 21c), which coalesce into one signal at higher temperatures. The $\Delta G^{\pm}$ value for this process can be similarly determined, and was found to be 11.7 kcal mol^{-1} at 193 K. Once again, a comparison can be made with the data obtained for the p-xylyl rotation in the [2]catenanes (a range of values from $11 - 13$ kcal mol^{-1}). In this case the value for the [2]rotaxane is nearly the same as that for the [2]catenanes, suggesting that the environment of the p-xylyl units is similar in both cases.

Slow two-station [2]rotaxane: Thin-layer chromatography (TLC) of the [2]rotaxane $2 \cdot 4PF_6$ showed green and red spots with similar intensities, indicating the existence of two isolable translational isomers, one in which $CBPQT^{4+}$ encircles the MPTTF unit (i.e., $2 \cdot GREEN^{4+}$) and another in
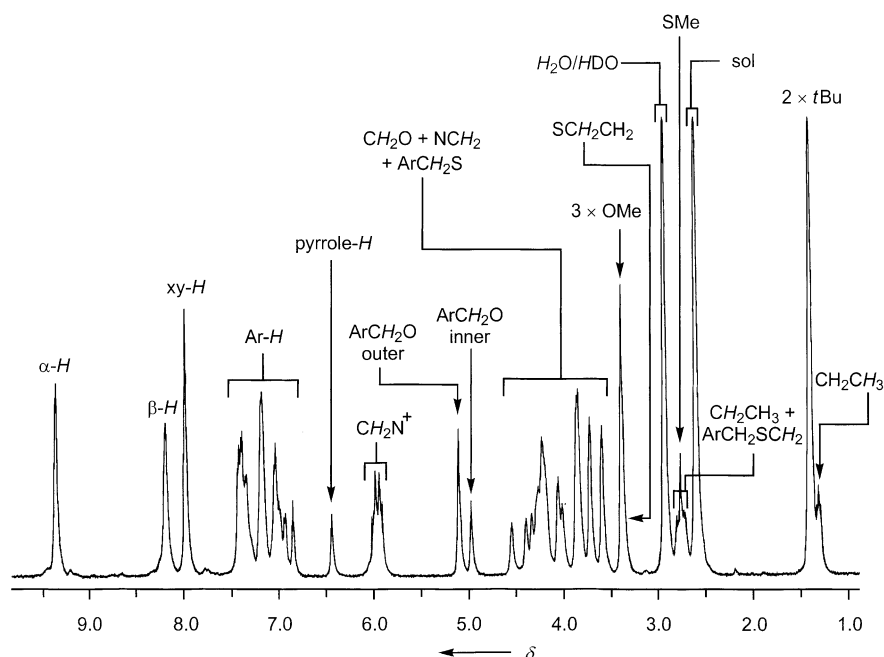
Figure 20. Full ^1H NMR spectrum (500 MHz) of the fast two-station [2]rotaxane 3^{4+} recorded in CD_3SOCD_3 at 400 K.
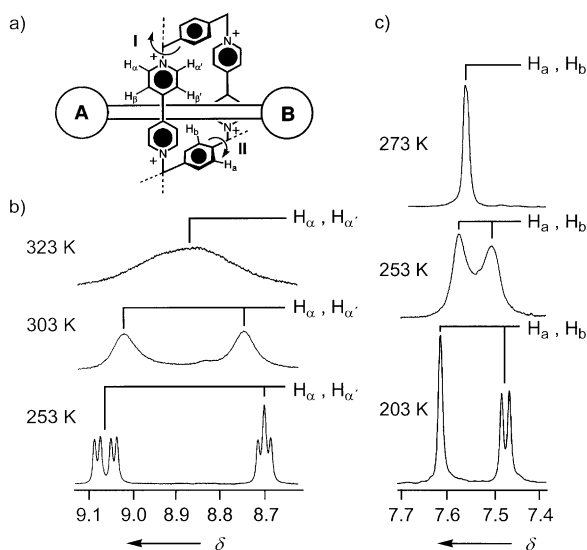
Figure 21. a) A schematic representation of the pyridinium unit rotation process (**I**) occurring in the bipyridinium units present in the tetracationic cyclophane component of the single-station [2]rotaxane **1**⁴⁺ and the *p*-xylyl unit rotation process (**II**) occurring in the tetracationic cyclophane component of **1**⁴⁺. Rotation of the pyridinium units around the axis of the bipyridinium units brings about the exchange of H$_\alpha$ with H$_{\alpha'}$ and H$_\beta$ with H$_{\beta'}$. Rotation of the *p*-xylyl units around their substituted axis causes exchange between H$_a$ and H$_b$. Partial variable temperature ¹H NMR spectra (500 MHz) of a CD₃COCD₃ solution of the single-station [2]rotaxane **1**⁴⁺ of b) the α-bipyridinium region and c) the *p*-xylyl region.

which CBPQT⁴⁺ encircles the DNP moiety (i.e., **2·RED**⁴⁺). By employing preparative thin-layer chromatography (PTLC), it was possible to separate the red and green translational isomers, that is, **2·RED**⁴⁺ and **2·GREEN**⁴⁺.[35] ¹H NMR and UV-visible spectroscopy clearly suggest that CBPQT⁴⁺ encircles the DNP moiety in the [2]rotaxane **2·RED**⁴⁺. After isolation of **2·RED**⁴⁺, a ¹H NMR spectrum (500 MHz) was recorded (Figures 22 and 23a) at 225 K in CD₃COCD₃. As expected, it shows only one signal for the SMe protons, as a singlet resonating (Figure 23a) at δ = 2.49 ppm. The resonances for the protons attached to the DNP moiety are shifted significantly to higher field relative to the resonances for the same protons in the dumbbell compound **17**. For example, the DNP-*H*-2/6 protons resonate as two doublets (J = 8 Hz) at δ = 6.33 and 6.29 ppm and one of the DNP-*H*-3/7 protons resonates as a triplet (J = 8 Hz) at δ = 6.14 ppm (Figure 22). The signal for the other DNP-*H*-3/7 proton is obscured by the multiplet for the ⁺NC*H*₂ protons. These chemical shifts values are similar to those reported previously for a DNP moiety being encircled by CBPQT⁴⁺.[45, 51] On account of the asymmetry in the dumbbell

component, four doublets (J = 6–7 Hz) for both the α- and β-bipyridinium protons and four singlets for the protons on the *p*-xylyl units are observed in the ¹H NMR spectrum of the [2]rotaxane **2·RED**⁴⁺ at 225 K (Figure 22). The UV-visible spectrum of **2·RED**⁴⁺ reveals a CT absorption band in the form of a shoulder at 540 nm (Figure 24). It results from the DNP moiety being located inside CBPQT⁴⁺.[29d, 39] Furthermore, no absorption band is observed in the region 750–850 nm for a CT interaction that would result from the MPTTF unit being located inside the cyclophane[15] and so support the conclusion that the DNP moiety in the dumbbell component is encircled exclusively by CBPQT⁴⁺. Leaving the red solution of **2·RED**⁴⁺ to stand for 24 h at room temperature results in a return to the "original" spectrum (Figure 24), as a consequence of the shuttling of CBPQT⁴⁺ from the DNP recognition site in **2·RED**⁴⁺ to the MPTTF recognition site. The kinetics of the shuttling of CBPQT⁴⁺ from the DNP recognition site in **2·RED**⁴⁺ to the MPTTF recognition site were investigated by using ¹H NMR spectros-

Figure 22. Partial ¹H NMR spectrum of the isolated [2]rotaxane **2·RED**⁴⁺ recorded at 500 MHz in CD₃COCD₃ at 225 K.

Table 6. *p*-Xylyl and bipyridinium rotation kinetic data and thermodynamic data for the single-station [2]rotaxane **1**⁴⁺ in CD₃COCD₃.

Process	T [K][a]	k_{ex} [s⁻¹][b]	$\Delta G^{\neq}$ [kcal mol⁻¹][c]
p-xylyl	193	0.23	11.7
rotation	203	0.65	11.9
bipyridinium	260	0.83	15.3
rotation	273	2.65	15.4

[a] Calibrated using neat MeOH sample, see: ref. [49]. [b] Measured using spin saturation transfer method, see ref. [48]. [c] ± 0.1 kcal mol⁻¹.

Figure 23. Partial ¹H NMR spectra (500 MHz) of the isolated [2]rotaxane **2·RED**⁴⁺, recorded in CD₃COCD₃ at a) 225 K/0 h, b) 300 K/1 h, c) 300 K/3 h, d) 300 K/5 h, e) 300 K/8 h, and f) 300 K/21 h. The singlet at δ = 2.49 ppm corresponds to the SMe resonance when CBPQT⁴⁺ encircles the DNP moiety and the singlet at δ = 2.65 ppm corresponds to the SMe resonance when CBPQT⁴⁺ encircles the MPTTF unit.
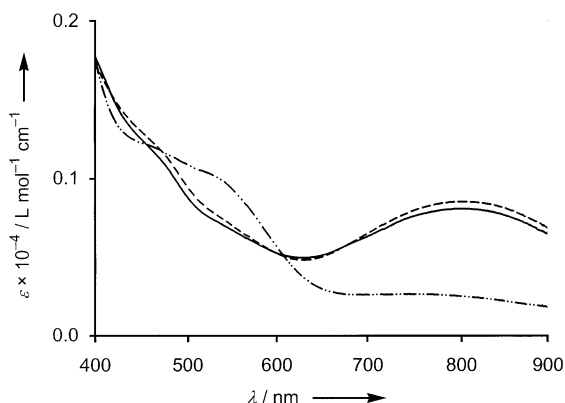
Figure 24. Absorption spectra recorded at 298 K in a Me_2CO solution of an equilibrium mixture of the [2]rotaxanes $\mathbf{2}\cdot GREEN^{4+}$ and $\mathbf{2}\cdot RED^{4+}$ (——) and of the [2]rotaxane $\mathbf{2}\cdot RED^{4+}$ ($-\cdot\cdot-$) immediately after its isolation. Allowing the red solution of $\mathbf{2}\cdot RED^{4+}$ to stand for 24 h at room temperature regenerates the "original" spectrum (– – –).

copy. After isolation of $\mathbf{2}\cdot RED^{4+}$ and recording of an ¹H NMR spectrum (500 MHz) at 225 K in CD_3COCD_3 (Figure 23a), the sample was heated to 300 K and the shuttling of $CBPQT^{4+}$ from the DNP recognition site in $\mathbf{2}\cdot RED^{4+}$ to the MPTTF recognition site was followed by using the SMe resonances as probes (Figure 23b–f). After 21 h at 300 K, equilibration is complete and the 1:1 mixture of $\mathbf{2}\cdot RED^{4+}$ and $\mathbf{2}\cdot GREEN^{4+}$ is re-established (Figure 23f). As a consequence of these spectroscopic variations, the color of the solution changes from red to brown. By employing a first-order kinetic treatment,[52, 53] a rate constant ($k = 2 \times 10^{-5}\,s^{-1}$) for the slippage of $CBPQT^{4+}$ over the SMe group, in the direction from $\mathbf{2}\cdot RED^{4+}$ to $\mathbf{2}\cdot GREEN^{4+}$, was obtained. The free energy of activation[47] ($\Delta G^{\ddagger}$) for this isomerization is 24 kcal mol⁻¹. Despite the fact that $\mathbf{2}\cdot GREEN^{4+}$ is less polar than $\mathbf{2}\cdot RED^{4+}$, it was only possible to extract an extremely small amount of $\mathbf{2}\cdot GREEN^{4+}$ from the silica on the PTLC plate. The UV-visible spectrum[35] recorded in Me_2CO at 298 K of this fraction shows, as expected, only a broad CT absorption band centered on 800 nm. Although it was not possible to isolate sufficient amounts of $\mathbf{2}\cdot GREEN^{4+}$ after PTLC to follow its interconversion into $\mathbf{2}\cdot RED^{4+}$ by ¹H NMR spectroscopy, it turned out to be possible to shift the equilibrium between the two translational isomers from 1:1 to 9:1 in favor of $\mathbf{2}\cdot GREEN^{4+}$ by heating a CD_3SOCD_3 solution of the brown 1:1 mixture to 425 K. Figure 25a–e shows the partial ¹H NMR spectra (500 MHz) of $\mathbf{2}^{4+}$ recorded in CD_3SOCD_3 at 310, 350, 365, 395, and 425 K. The AB system centered on $\delta = 6.21$ ppm (at 395 K) corresponds to the two pyrrole protons on the MPTTF unit in $\mathbf{2}\cdot GREEN^{4+}$, whereas the doublet centered on $\delta = 6.27$ ppm at 395 K can be assigned to the two DNP-H-2/6 protons in $\mathbf{2}\cdot RED^{4+}$. It is evident from Figure 25a–e that the relative populations of the two translational isomers shift upon heating. Additionally, the signals arising from the protons on $CBPQT^{4+}$ are simplified as a result of fast exchange of all the relevant sites in the cyclophane component $CBPQT^{4+}$. The ¹H NMR spectrum (500 MHz) of $\mathbf{2}^{4+}$,[35] recorded in CD_3SOCD_3 at 410 K

revealed that the ratio between the two translational isomers is approximately 6:1 in favor of $\mathbf{2}\cdot GREEN^{4+}$. The α- and β-bipyridinium protons in $\mathbf{2}\cdot GREEN^{4+}$ appear as two sharp doublets ($J = 6$ Hz) and the p-xylyl protons appear as one sharp singlet. The $^+NCH_2$ protons in $\mathbf{2}\cdot GREEN^{4+}$ are observed as an AB system ($J = 13$ Hz), which is a direct consequence of the asymmetry present in the dumbbell component and the interlocked nature of $\mathbf{2}^{4+}$. This asymmetry means that the pairs of $^+NCH_2$ protons in $CBPQT^{4+}$ cannot become equivalent under any circumstances, that is, they are inherently heterotopic. Upon heating to 425 K, the color of the solution changed from brown to green. The solution was subsequently quenched at 273 K (ice-bath) and the conversion of $\mathbf{2}\cdot GREEN^{4+}$ to $\mathbf{2}\cdot RED^{4+}$ was followed at 300 K, using the signals for the protons on the MPTTF unit in $\mathbf{2}\cdot GREEN^{4+}$ and the DNP-H-2/6 protons in $\mathbf{2}\cdot RED^{4+}$ as probes. On this occasion, a first-order rate constant of $3 \times 10^{-4}\,s^{-1}$ was obtained for the slippage of $CBPQT^{4+}$ over the SMe group, in the direction from $\mathbf{2}\cdot GREEN^{4+}$ to $\mathbf{2}\cdot RED^{4+}$. The associated $\Delta G^{\ddagger}$ value for this isomerization is 22 kcal mol⁻¹. Thus, the barrier for the shuttling of $CBPQT^{4+}$ over the SMe group[54] in CD_3SOCD_3 is 2 kcal mol⁻¹ less than that recorded in CD_3COCD_3. This observation is probably a direct consequence of the decrease in all intramolecular noncovalent bonding interactions, when CD_3SOCD_3 is the solvent.

Figure 26 shows the absorption spectra of the isolated 1:1 mixture of the slow two-station [2]rotaxane $\mathbf{2}^{4+}$ recorded in MeCN at 298 K. The spectrum changes with time, such that the absorption bands for the MPTTF/$CBPQT^{4+}$ CT interaction (centered around 820 nm) increased in intensity and the DNP/$CBPQT^{4+}$ CT interaction (centered around 520 nm) decreased in intensity; this clearly indicates that shuttling of $CBPQT^{4+}$ from the DNP recognition site in $\mathbf{2}\cdot RED^{4+}$ to the
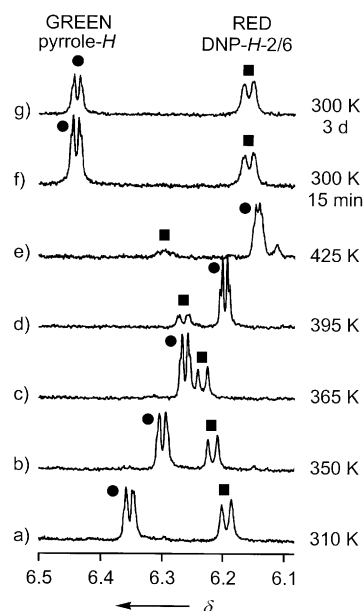
Figure 25. Partial variable temperature ¹H NMR spectra of an equilibrium mixture of the [2]rotaxanes $\mathbf{2}\cdot GREEN^{4+}$ and $\mathbf{2}\cdot RED^{4+}$ recorded at 500 MHz in CD_3SOCD_3 at a) 310 K, b) 350 K, c) 365 K, d) 395 K, and e) 425 K. Spectra f) and g) were recorded at 300 K 15 min and 3 h, respectively, after the sample had been heated to 425 K and quenched.
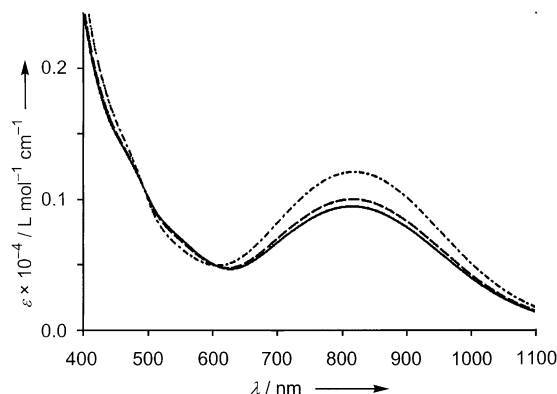
Figure 26. Absorption spectra recorded at 298 K on a MeCN solution (4.1×10^{-4} M) of the slow two-station [2]rotaxane 2^{4+} immediately after its preparation (——), after 1 h (– – –), and after 20 h (– · –).

Figure 27. a) Partial variable temperature (VT) ^{1}H NMR spectra of an equilibrium mixture of the [2]rotaxanes $3 \cdot GREEN^{4+}$ and $3 \cdot RED^{4+}$ recorded at 500 MHz in CD$_3$CN. b) Temperature controlled variation in the population of two translational isomers $3 \cdot RED^{4+}$ and $3 \cdot GREEN^{4+}$ in CD$_3$CN.

MPTTF recognition site occurs. After 20 h, the system had reached equilibrium and no perceptible changes were observed in UV-visible spectra recorded subsequently. The ^{1}H NMR spectrum (500 MHz, 300 K), recorded on a solution of the isolated slow two-station [2]rotaxane 2^{4+} in CD$_3$CN, showed immediately, after its preparation, that the ratio[55] between $2 \cdot GREEN^{4+}$ and $2 \cdot RED^{4+}$ was approximately 1:1, whereas the ^{1}H NMR spectrum (500 MHz, 300 K) recorded on an equilibrated (after 48 h) solution of the two [2]rotaxanes $2 \cdot GREEN^{4+}$ and $2 \cdot RED^{4+}$ in CD$_3$CN revealed that the ratio[55] was 3:1 in favor of $2 \cdot GREEN^{4+}$.

Fast two-station [2]rotaxane: Since the ^{1}H NMR investigations of the [2]rotaxane 3^{4+} show that shuttling of CBPQT^{4+} is temperature dependent, variable-temperature (VT) ^{1}H NMR spectroscopy was carried out in CD$_3$CN, since this solvent allows spectra to be recorded over the widest temperature range. The VT ^{1}H NMR experiment (500 MHz) shows (Figure 27a) that $3 \cdot RED^{4+}$ is the major translational isomer at low temperature (red solution), whereas $3 \cdot GREEN^{4+}$ is the major isomer at higher temperature (green solution). This observation was supported by a temperature controlled UV-visible experiment. At 298 K in MeCN, absorption bands for both the MPTTF/CBPQT^{4+} CT interaction (centered around 800 nm) and the DNP/CBPQT^{4+} CT interaction (centered around 520 nm) were clearly evident (Figures 10 and 12). On increasing the temperature, the CT band centered around 800 nm increased in intensity and that around 520 nm decreased in intensity. The reverse was true on decreasing the temperature. From integration of the signals for the DNP-*H*-2/6 protons in $3 \cdot RED^{4+}$, and for the two pyrrole protons in $3 \cdot GREEN^{4+}$, and also for the ArC*H*$_2$O protons in $3 \cdot RED^{4+}$ and $3 \cdot GREEN^{4+}$, the temperature-dependent variations (Figure 27b) in the population of the two translational isomers were obtained. In order to study the kinetics of the shuttling of CBPQT^{4+} between the two recognition sites, a sample of 3^{4+} in CD$_3$CN was heated to 350 K and an ^{1}H NMR spectrum was recorded, revealing the presence of $3 \cdot GREEN^{4+}$ as the major isomer, approximately 8:1 in favor of $3 \cdot GREEN^{4+}$. Next, the solution was cooled down to 300 K, followed by an immediate recording of an ^{1}H NMR spectrum, an experiment which showed that the 1:1 mixture of $3 \cdot RED^{4+}$ and $3 \cdot GREEN^{4+}$
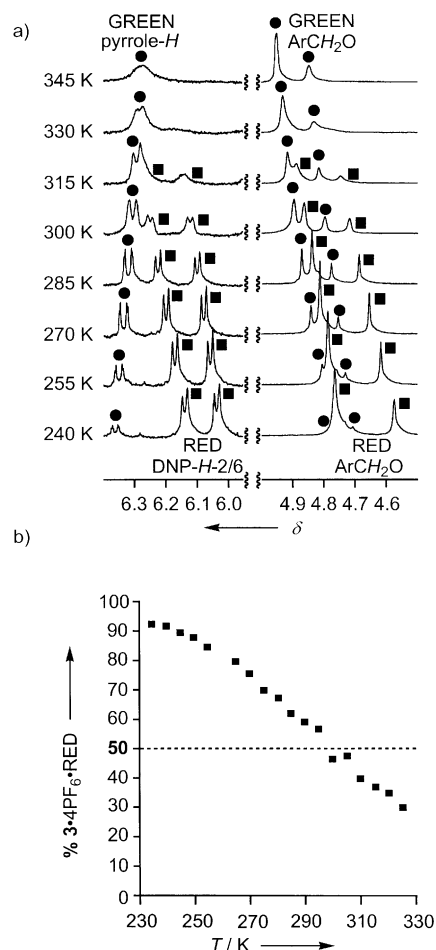
was re-established after less than five minutes. Thus, the shuttling of CBPQT^{4+} between the two recognition sites in 3^{4+} is a much faster process than the shuttling of CBPQT^{4+} in the slow bistable [2]rotaxane 2^{4+}. All attempts to separate the two translational isomers of the fast [2]rotaxane 3^{4+} by employing PTLC failed on account of the fast shuttling of CBPQT^{4+} between the two recognition sites in 3^{4+}.

Conclusion

In conclusion, the syntheses and characterizations of two amphiphilic bistable [2]rotaxanes, with two different recognition sites—an MPTTF unit and a DNP moiety—for CBPQT^{4+} have been reported. In both cases, the [2]rotaxanes were isolated as mixtures of the two possible translational isomers. Based on the redox properties of the dumbbell compounds **17** and **23**, one could have expected a strong preference for CBPQT^{4+} to reside around the MPTTF station in the [2]rotaxanes 2^{4+} and 3^{4+}. The results obtained, however, confirm[10, 15c, 18, 19l,p, 31a, 56] that the interaction of CBPQT^{4+}

with electron-donating units also depends on other factors, such as extension of $\pi - \pi$ stacking and the formation of hydrogen bonds. The electrochemical and photophysical studies show that the [2]pseudorotaxane $18 \subset \text{CBPQT}^{4+}$ and the [2]rotaxanes 2^{4+} and 3^{4+}—all containing both an MPTTF and a DNP station for encircling CBPQT^{4+}—exhibit a complicated behavior that cannot be explained by the presence of two simple translational isomers. The results obtained suggest that—owing to the length and flexibility of $18 \subset \text{CBPQT}^{4+}$, 2^{4+}, and 3^{4+}—in the translational isomer in which CBPQT^{4+} encircles the DNP moiety, the MPTTF unit is engaged "alongside" with CBPQT^{4+} in a folded structure in order to maximize the CT interactions. The relative orientation of the MPTTF unit and the DNP moiety with respect to the hydrophilic dendritic stopper also seems to affect the localization of CBPQT^{4+} on the (semi)dumbbell component, most likely because of CT and C–H···O hydrogen-bonding interactions between the hydrophilic stopper and CBPQT^{4+}. The steric hindrance exhibited from the SMe group situated between the two recognition sites in the slow molecular shuttle/switch 2^{4+} made it possible to isolate the translational isomers $2 \cdot \text{RED}^{4+}$ and $2 \cdot \text{GREEN}^{4+}$ and to study the kinetics of the shuttling of the tetracationic cyclophane between the two recognition sites. The processes, which are accompanied by clearly detectable color changes, can be followed by ^1H NMR and UV-visible spectroscopy; this allows us to determine the rate constants and the associated energies of activation for both the shuttling of CBPQT^{4+} from the DNP recognition site in $2 \cdot \text{RED}^{4+}$ to the MPTTF recognition site in $2 \cdot \text{GREEN}^{4+}$, as well as the shuttling of CBPQT^{4+} from the MPTTF recognition site in $2 \cdot \text{GREEN}^{4+}$ to the DNP recognition site in $2 \cdot \text{RED}^{4+}$. In the fast molecular shuttle/switch 3^{4+}, the steric hindrance between the two recognition sites is decreased by the insertion of a planar pyrrole moiety, instead of a bulky SMe group as in 2^{4+}, between the DNP and MPTTF recognition sites. This interchange results in considerably faster shuttling of CBPQT^{4+} between the two recognition sites, rendering the separation of $3 \cdot \text{RED}^{4+}$ and $3 \cdot \text{GREEN}^{4+}$ impossible. The shuttling of CBPQT^{4+} in 3^{4+} is highly temperature dependent and has been followed by variable temperature ^1H NMR spectroscopy. At low temperature (235 K), the major isomer is $3 \cdot \text{RED}^{4+}$, whereas at higher temperature (330 K) the major isomer is $3 \cdot \text{GREEN}^{4+}$. In the bistable [2]rotaxanes 2^{4+} and 3^{4+} shuttling of the macrocyclic ring component CBPQT^{4+} can be driven by electrochemical oxidation of the MPTTF unit. In the [2]pseudorotaxanes $18 \subset \text{CBPQT}^{4+}$ and $24 \subset \text{CBPQT}^{4+}$, in which one of the stoppers on the dumbbell component is absent, electrochemical oxidation causes dethreading.

Experimental Section

General methods: Chemicals were purchased from Aldrich and were used as received, unless indicated otherwise. The compounds 5-tosyl-(1,3)-dithiolo[4,5-c]pyrrole-2-one (**4**)[21] (Scheme 1), 4-(2-cyanoethylthio)-5-methylthio-1,3-dithiole-2-thione (**5**)[23] (Scheme 1), the dumbbell compound **7**,[13a] 1,1′′-[1,4-phenylenebis(methylene)]bis(4,4′-bipyridin-1-ium) bis(hexafluorophosphate) (**8**·2PF$_6$)[10] (Schemes 2, 4 and 6), 2-[2-[5-[2-(2-hydroxyethoxy)ethoxy]naphthalene-1-yloxy}ethoxy]ethane tosylate (**10**)[13a]

(Scheme 3), 4-[bis(4-*tert*-butylphenyl)(4-ethylphenyl)methyl]phenol (**11**)[13a] (Scheme 3), compound **16**[13a] (Scheme 3), the semi-dumbbell compound **18**[13a] (Scheme 5), compound **22**[13a] (Scheme 5), the semi-dumbbell compound **24**[13a] (Scheme 7), and cyclobis(paraquat-*p*-phenylene) tetrakis-(hexafluorophosphate) (CBPQT·4PF$_6$)[16] (Schemes 7 and 8) were all prepared according to literature procedures. Solvents were dried according to literature procedures.[57] All reactions were carried out under an anhydrous argon or nitrogen atmosphere. High-pressure experiments were carried out in a teflon tube on a Psika high-pressure apparatus. Thin-layer chromatography (TLC) was carried out by using aluminium sheets pre-coated with silica gel 60F (Merck 5554). The plates were inspected under UV light and, if required, developed in I$_2$ vapor. Column chromatography was carried out by using silica gel 60F (Merck 9385, 0.040 – 0.063 mm), while preparative thin-layer chromatography (PTLC) was performed on UNIPLATE silica gel PTLC plates. Melting points were determined on an Electrothermal 9100 apparatus or a Büchi melting point apparatus and are uncorrected. ^1H and ^{13}C spectra were recorded (at room temperature except where stated otherwise) on either a Bruker AC200 (200 and 50 MHz, respectively), Bruker ARX400 (400 and 100 MHz, respectively), Bruker ARX500 or Bruker AMX500 (500 and 125 MHz, respectively) spectrometers, with residual solvent as the internal standard. All chemical shifts are quoted on a δ scale, and all coupling constants (J) are expressed in Hertz (Hz). Electron impact ionization mass spectrometry (EIMS) was performed on a AUTO-SPEC instrument. Fast atom bombardment (FAB) mass spectra were obtained using a ZAB-SE mass spectrometer, equipped with krypton primary atom beam, utilizing a 3-nitrobenzyl alcohol matrix, while electrospray mass spectrometry (ESMS) was performed on a Finnigan MAT TSQ 700 triple quadrupole mass spectrometer, whereby the rotaxanes were electrosprayed from MeCN solutions. Infrared (IR) spectra were recorded on a Perkin – Elmer 580 spectrophotometer. Micro-analyses were performed by Quantitative Technologies, Inc.

2-[4-(2-Cyanoethylthio)-5-methylthio-1,3-dithiole-2-yliden]-5-tosyl-(1,3)-dithiolo[4,5-c]pyrrole (6): Ketone **4** (1.48 g, 4.75 mmol) and thione **5** (1.26 g, 4.75 mmol) were suspended in distilled (EtO)$_3$P (35 mL) and heated to 135 °C (during heating the two solids dissolved leaving a red solution and after 10 – 15 min a yellow orange precipitate was formed). Two additional portions of **5** (each, 0.63 g, 2.37 mmol) were added after 15 and 30 min, respectively. The red reaction mixture was stirred for another hour at 135 °C, and cooled to room temperature; addition of MeOH (80 mL) yielded an orange solid, which was filtered and washed with MeOH (3 × 50 mL). The yellow solid was suspended in boiling CH$_2$Cl$_2$ (70 mL), and the hot mixture was filtered, whereupon the filter was washed with boiling CH$_2$Cl$_2$ (30 mL). The combined organic-phase filtrate was concentrated in vacuo, and the resulting yellow solid was resuspended in CH$_2$Cl$_2$ (50 mL) and subjected to column chromatography (SiO$_2$, CH$_2$Cl$_2$). (Before the column was eluted a yellow solid exclusively containing the symmetric bis(pyrrolo)TTF was removed carefully.) The yellow band ($R_f = 0.4$) was collected, and the solvent evaporated to give a yellow solid, which was dissolved in CH$_2$Cl$_2$/MeOH (1:1 v/v, 400 mL) and concentrated to approximately half of its volume to precipitate the product. The yellow crystals were collected by filtration, washed with MeOH (2 × 50 mL) and dried in vacuo to give compound **6** (1.60 g, 64%) as yellow needles. M.p. 192.5 – 193 °C (lit.[21b] 186.5 – 187 °C); ^1H NMR (CD$_3$SOCD$_3$, 200 MHz): $\delta = 2.39$ (s, 3H), 2.50 (s, 3H), 2.83 (t, $J = 6.6$ Hz, 2H), 3.10 (t, $J = 6.6$ Hz, 2H), 7.41 (s, 2H), 7.46 (d, $J = 8.4$ Hz, 2H), 7.83 ppm (d, $J = 8.4$ Hz, 2H); ^{13}C NMR (CD$_3$SOCD$_3$, 50 MHz): $\delta = 18.4$, 18.7, 21.3, 31.0, 112.4, 113.0, 118.1, 119.1, 120.9, 126.2, 127.0, 130.6, 132.7, 134.6, 146.1 ppm (2 signals are missing/overlapping); MS (FAB): m/z (%): 528 (100) $[M]^+$; elemental analysis calcd (%) for C$_{19}$H$_{16}$N$_2$O$_2$S$_7$ (528.8): C 43.15, H 3.05, N 5.30; found: C 42.83, H 3.02, N 5.07.

Single-station [2]rotaxane 1·4PF$_6$: A solution of the dumbbell **7** (0.41 g, 0.24 mmol), **8**·2PF$_6$ (0.50 g, 0.71 mmol), and the dibromide **9** (0.19 g, 0.72 mmol) in anhydrous DMF (10 mL) was transferred to a teflon-tube and subjected to 10 kbar of pressure at room temperature for 3 d. The green suspension was directly subjected to column chromatography (SiO$_2$), and unreacted dumbbell was eluted with Me$_2$CO, whereupon the eluent was changed to Me$_2$CO/NH$_4$PF$_6$ (1.0 g NH$_4$PF$_6$ in 100 mL Me$_2$CO) and the green band was collected. Most of the solvent was removed in vacuo ($T < 30$ °C) followed by addition of H$_2$O (80 mL). The resulting precipitate was collected by filtration, washed with Et$_2$O (50 mL) and dried affording **1**·4PF$_6$ (0.14 g, 21%) as a green solid. M.p. 135 °C (decomp); ^1H NMR

(400 MHz, CD$_3$COCD$_3$): $\delta = 1.19$ (t, $J = 7.6$ Hz, 3H), 1.28 (s, 18H), 2.60 (q, $J = 7.6$ Hz, 2H), 2.64 (s, 3H), 3.28 (s, 6H), 3.29 (s, 3H), 3.29 (t, $J = 6.4$ Hz, 2H), 3.47–3.50 (m, 6H), 3.61–3.65 (m, 6H), 3.77–3.81 (m, 6H), 3.95 (t, $J = 6.4$ Hz, 2H), 3.98–4.01 (m, 2H), 4.08–4.14 (m, 6H), 4.23–4.25 (m, 2H), 4.69 (s, 2H), 4.80 (s, 4H), 4.97 (s, 2H), 5.18 (s, 2H), 5.98–6.08 (m, 8H), 6.43 and 6.45 (AB q, $J = 2.1$ Hz, 2H), 6.78 (s, 2H), 6.83–6.85 (m, 4H), 6.94 (d, $J = 8.7$ Hz, 4H), 7.07–7.12 (m, 10H), 7.18 (d, $J = 8.6$ Hz, 2H), 7.26–7.31 (m, 10H), 7.38 (br s, 4H), 7.69 (d, $J = 8.7$ Hz, 2H), 7.94–8.06 (m, 8H), 8.45 (br s, 4H), 9.16 (br s, 4H), 9.48 ppm (br s, 4H); MS (FAB): m/z (%): 2691 (4) $[M - PF_6]^+$, 2546 (14) $[M - 2PF_6]^+$, 2401 (16) $[M - 3PF_6]^+$, 1738 (7), 1273 (15) $[M - 2PF_6]^{2+}$, 1200.5 (35) $[M - 3PF_6]^{2+}$, 1128 (20) $[M - 4PF_6]^{2+}$; UV/Vis (Me$_2$CO, 298 K): λ_{max} (ε) = 810 nm (1400 L mol^{-1} cm^{-1}); UV/Vis (Me$_2$CN, 298 K): λ_{max} (ε) = 830 nm (1500 L mol^{-1} cm^{-1}); elemental analysis calcd (%) for C$_{134}$H$_{145}$F$_{24}$N$_5$O$_{15}$P$_4$S$_6$ · 2 H$_2$O (2837.9): C 56.00, H 5.23, N 2.44; found: C 56.07, H 5.06, N 2.28.

Compound 12: A solution of the monotosylate **10** (2.45 g, 4.99 mmol) and **11** (2.38 g, 4.99 mmol) in anhydrous MeCN (50 mL) containing K$_2$CO$_3$ (6.9 g, 50 mmol), LiBr (0.2 g, catalytic amount), and [18]crown-6 ($\sim$50 mg, catalytic amount) was heated under reflux for 20 h. After cooling down to room temperature, the reaction mixture was filtered and the residue washed with MeCN (50 mL). The combined organic-phase filtrate was concentrated in vacuo, and the brown oily residue was dissolved in CH$_2$Cl$_2$ (150 mL), washed with H$_2$O (2 × 100 mL), and dried (MgSO$_4$). After removal of the solvent the residue was purified by column chromatography (SiO$_2$, CH$_2$Cl$_2$/MeOH 49:1). The colorless band ($R_f = 0.2$) was collected, and the solvent evaporated to give a colorless oil, which was redissolved in CH$_2$Cl$_2$ (20 mL) and concentrated providing compound **12** (3.20 g, 80 %) as a white foam. ^{1}H NMR (CDCl$_3$, 200 MHz): $\delta = 1.26$ (t, $J = 7.6$ Hz, 3H), 1.33 (s, 18H), 2.19 (s, 1H), 2.65 (q, $J = 7.6$ Hz, 2H), 3.71–3.82 (m, 4H), 3.97–4.10 (m, 6H), 4.14–4.19 (m, 2H), 4.27–4.35 (m, 4H), 6.80–6.88 (m, 4H), 7.06–7.15 (m, 10H), 7.24–7.42 (m, 6H), 7.90 (d, $J = 8.5$ Hz, 1H), 7.92 ppm (d, $J = 8.4$ Hz, 1H); ^{13}C NMR (CDCl$_3$, 50 MHz): $\delta = 15.4$, 28.3, 31.5, 34.4, 61.9, 63.2, 67.4, 68.0, 68.1, 69.8, 70.0, 70.1, 72.7, 105.9 (2 signals overlapping), 113.3, 114.6, 114.9, 124.2, 125.2, 125.3, 126.7, 126.8, 126.9, 130.8, 131.1, 132.3, 139.9, 141.4, 144.3, 144.7, 148.4, 154.3, 154.4, 156.6 ppm; MS (FAB): m/z (%): 794 (63) $[M]^+$, 689 (15), 661 (29), 383 (100); elemental analysis calcd (%) for C$_{53}$H$_{62}$O$_6$ (795.1): C 80.07, H 7.86; found: C 79.85, H 7.88.

Compound 13: Ph$_3$P (0.70 g, 2.67 mmol) was added portionwise to a solution of the alcohol **12** (1.75 g, 2.20 mmol) and CBr$_4$ (0.88 g, 2.65 mmol) in anhydrous CH$_2$Cl$_2$ (15 mL) at room temperature. The reaction mixture was stirred for 16 h, whereupon additional CBr$_4$ (0.88 g, 2.65 mmol), followed by Ph$_3$P (0.70 g, 2.67 mmol) was added and the reaction mixture was stirred for another 24 h. After concentration, the residue was purified by column chromatography (SiO$_2$, CH$_2$Cl$_2$/hexane 2:1). The colorless band ($R_f = 0.3$) was collected and the solvent evaporated, affording a colorless oil, which was repeatedly dissolved in CH$_2$Cl$_2$ (3 × 50 mL) and concentrated to provide compound **13** (1.77 g, 94 %) as a white foam. ^{1}H NMR (CDCl$_3$, 200 MHz): $\delta = 1.26$ (t, $J = 7.6$ Hz, 3H), 1.33 (s, 18H), 2.65 (q, $J = 7.6$ Hz, 2H), 3.54 (t, $J = 6.2$ Hz, 2H), 3.94–4.10 (m, 8H), 4.14–4.19 (m, 2H), 4.28–4.36 (m, 4H), 6.80–6.89 (m, 4H), 7.06–7.15 (m, 10H), 7.24–7.42 (m, 6H), 7.90 (d, $J = 8.4$ Hz, 1H), 7.91 ppm (d, $J = 8.4$ Hz, 1H); ^{13}C NMR (CDCl$_3$, 50 MHz): $\delta = 15.4$, 28.3, 30.5, 31.5, 34.4, 63.2 (C(Ar)$_4$), 67.4, 68.0, 69.8, 70.0, 70.2, 71.6 (6 out of 7 CH$_2$O signals, one overlapping), 105.8 (2 signals overlapping), 113.3, 114.7, 114.9, 124.2, 125.2, 125.3, 126.7, 126.8 (2 signals overlapping), 130.8, 131.1, 132.3, 139.9, 141.4, 144.3, 144.7, 148.3, 154.3, 154.4, 156.6 ppm; MS (FAB): m/z (%): 858 (30) $[M+2]^+$, 856 (27) $[M]^+$, 753 (8), 751 (8), 725 (15), 723 (14), 383 (100); elemental analysis calcd (%) for C$_{53}$H$_{61}$BrO$_5$ (858.0): C 74.20, H 7.17; found: C 74.36, H 7.20.

Compound 14: A solution of **6** (0.27 g, 0.51 mmol) in anhydrous THF (35 mL) was degassed (Ar, 10 min) before a solution of CsOH · H$_2$O (0.090 g, 0.54 mmol) in anhydrous MeOH (3.5 mL) was added dropwise by syringe over a period of 1 h at room temperature. The mixture was stirred for 15 min, whereupon a solution of the bromide **13** (0.46 g, 0.54 mmol) in anhydrous THF (5 mL) was added in one portion and the reaction mixture was stirred for 24 h at room temperature. The solvent was evaporated, and the resulting yellow residue was dissolved in CH$_2$Cl$_2$ (100 mL), washed with brine (100 mL), H$_2$O (2 × 100 mL), and dried (MgSO$_4$). Removal of the solvent gave a yellowish orange foam, which was purified by column chromatography (SiO$_2$, CH$_2$Cl$_2$/hexane 4:1). The broad yellow band ($R_f = 0.3$) was collected and concentrated affording a yellow foam, which was repeatedly dissolved in CH$_2$Cl$_2$ (2 × 20 mL) and concentrated to give

compound **14** (0.47 g, 74 %) as a yellow foam. ^{1}H NMR (CD$_3$COCD$_3$, 200 MHz): $\delta = 1.19$ (t, $J = 7.6$ Hz, 3H), 1.28 (s, 18H), 2.37 (s, 3H), 2.39 (s, 3H), 2.60 (q, $J = 7.6$ Hz, 2H), 3.07 (t, $J = 6.3$ Hz, 2H), 3.83 (t, $J = 6.3$ Hz, 2H), 3.94–4.06 (m, 6H), 4.14–4.19 (m, 2H), 4.26–4.34 (m, 4H), 6.84 (d, $J = 8.9$ Hz, 2H), 6.88–6.96 (m, 2H), 7.05–7.13 (m, 10H), 7.22–7.43 (m, 10H), 7.79–7.85 ppm (m, 4H); MS (FAB): m/z (%): 1252 (100) $[M]^+$; elemental analysis calcd (%) for C$_{69}$H$_{73}$NO$_7$S$_7$ (1252.8): C 66.15, H 5.87, N 1.12; found: C 66.34, H 6.02, N 1.05.

Compound 15: Compound **14** (0.42 g, 0.34 mmol) was dissolved in anhydrous THF/MeOH (1:1 v/v, 50 mL) and degassed (Ar, 10 min) before NaOMe (25 % solution in MeOH, 1.1 mL, 0.27 g, 5.0 mmol) was added in one portion. The yellow solution was heated under reflux for 20 min before being cooled to room temperature, whereupon the solvent was evaporated. The yellow residue was dissolved in CH$_2$Cl$_2$ (100 mL), washed with H$_2$O (3 × 100 mL), and dried (MgSO$_4$). Concentration gave a yellow foam, which was subjected to column chromatography (SiO$_2$, CH$_2$Cl$_2$). The yellow band ($R_f = 0.5$) was collected and concentrated to provide compound **15** (0.35 g, 95 %) as a yellow foam. ^{1}H NMR (CD$_3$COCD$_3$, 200 MHz): $\delta = 1.20$ (t, $J = 7.6$ Hz, 3H), 1.29 (s, 18H), 2.42 (s, 3H), 2.60 (q, $J = 7.6$ Hz, 2H), 3.09 (t, $J = 6.4$ Hz, 2H), 3.85 (t, $J = 6.4$ Hz, 2H), 3.93–4.05 (m, 6H), 4.14–4.19 (m, 2H), 4.28–4.32 (m, 4H), 6.79 (s, 2H), 6.84 (d, $J = 9.0$ Hz, 2H), 6.93 (d, $J = 7.7$ Hz, 1H), 6.95 (d, $J = 7.7$ Hz, 1H), 7.05–7.13 (m, 10H), 7.24–7.39 (m, 6H), 7.82 (d, $J = 8.3$ Hz, 1H), 7.85 (d, $J = 8.4$ Hz, 1H), 10.35 ppm (br s, 1H); MS (FAB): m/z (%): 1098 (100) $[M]^+$; elemental analysis calcd (%) for C$_{62}$H$_{67}$NO$_5$S$_6$ (1098.6): C 67.78, H 6.15, N 1.27; found: C 67.81, H 6.15, N 1.24.

Dumbbell 17: Compound **15** (0.23 g, 0.21 mmol) and the chloride **16** (0.21 g, 0.23 mmol) were dissolved in anhydrous DMF (10 mL) and degassed (Ar, 10 min) before NaH (0.021 g of a 60 % suspension in mineral oil, 0.53 mmol) was added. The reaction mixture was stirred for 45 min at room temperature, causing the initially yellow solution to become more orange. H$_2$O (40 mL) was added (dropwise until no more gas evolution was observed), followed by addition of brine (40 mL). The yellow precipitate was filtered and dried. The crude product was purified by column chromatography (SiO$_2$, CH$_2$Cl$_2$/EtOAc 2:1). The yellow band ($R_f = 0.4$) was collected and the solvent evaporated affording a yellow oil, which was repeatedly dissolved in CH$_2$Cl$_2$ (3 × 20 mL) and concentrated, providing compound **17** (0.34 g, 83 %) as a yellow foam. ^{1}H NMR (CD$_3$COCD$_3$, 400 MHz): $\delta = 1.17$ (t, $J = 7.6$ Hz, 3H), 1.26 (s, 18H), 2.38 (s, 3H), 2.57 (q, $J = 7.6$ Hz, 2H), 3.05 (t, $J = 6.4$ Hz, 2H), 3.26 (s, 9H), 3.45–3.48 (m, 6H), 3.60–3.63 (m, 6H), 3.74–3.79 (m, 6H), 3.81 (t, $J = 6.4$ Hz, 2H), 3.90–4.00 (m, 6H), 4.05–4.13 (m, 8H), 4.24–4.27 (m, 4H), 4.88 (s, 2H), 4.96 (s, 2H), 5.00 (s, 6H), 6.72 and 6.75 (AB q, $J = 2.1$ Hz, 2H), 6.79 (d, $J = 8.8$ Hz, 2H), 6.80 (d, $J = 9.1$ Hz, 2H), 6.83 (s, 2H), 6.88–6.93 (m, 8H), 7.03–7.12 (m, 10H), 7.15 (d, $J = 8.7$ Hz, 2H), 7.22–7.33 (m, 8H), 7.36 (d, $J = 8.8$ Hz, 4H), 7.80 (d, $J = 8.5$ Hz, 1H), 7.82 ppm (d, $J = 8.5$ Hz, 1H); MS (FAB): m/z (%): 1966 (100) $[M]^+$, 1757 (21), 1548 (13), 1203 (20); elemental analysis calcd (%) for C$_{112}$H$_{127}$NO$_{18}$S$_6$ (1967.6): C 68.37, H 6.51, N 0.71; found: C 68.17, H 6.49, N 0.66.

Slow two-station [2]rotaxane 2·4PF$_6$: A solution of **17** (0.28 g, 0.14 mmol), **8**·2PF$_6$ (0.30 g, 0.42 mmol) and **9** (0.11 g, 0.42 mmol) in anhydrous DMF (10 mL) was stirred for 10 d at room temperature (after approximately 1 d the color changed to dark green and a white precipitate was formed). The green suspension was directly subjected to column chromatography (SiO$_2$), and unreacted **17** was eluted with Me$_2$CO, whereupon the eluent was changed to Me$_2$CO/NH$_4$PF$_6$ (1.0 g NH$_4$PF$_6$ in 100 mL Me$_2$CO) and the brown band containing **2·4PF$_6$** was collected. Most of the solvent was removed under vacuum ($T < 30\,^\circ$C) followed by addition of H$_2$O (50 mL). The resulting precipitate was collected by filtration, washed with Et$_2$O (20 mL) and dried, affording **2·4PF$_6$** (0.10 g, 23 %) as a brown solid. M.p. 150°C (decomp). The data given below are for the 1:1 mixture of the two translational isomers. MS (FAB): m/z (%): 2921 (4) $[M - PF_6]^+$, 2776 (9) $[M - 2PF_6]^+$, 2631 (6) $[M - 3PF_6]^+$, 1966 (3), 1388 (10) $[M - 2PF_6]^{2+}$, 1315.5 (13) $[M - 3PF_6]^{2+}$, 1243 (6) $[M - 4PF_6]^{2+}$; UV/Vis (Me$_2$CO, 298 K): λ_{max} (ε) = 540 (760), 805 nm (860 L mol^{-1} cm^{-1}); elemental analysis calcd (%) for C$_{148}$H$_{159}$F$_{24}$N$_5$O$_{18}$P$_4$S$_6$ · 2 H$_2$O (3068.1): C 57.26, H 5.29, N 2.26; found: C 56.86, H 5.19, N 2.11.

Separation of the translational isomers of 2·4PF$_6$: The two translational isomers were separated by using preparative thin-layer chromatography (PTLC), which was performed at room temperature with Me$_2$CO/NH$_4$PF$_6$ (1.0 g NH$_4$PF$_6$ in 100 mL Me$_2$CO) as eluent. Immediately after elution, the

red band ($R_f = 0.45$) containing $2 \cdot 4\,PF_6 \cdot RED$ was extracted into Me$_2$CO. The solvent was removed in vacuo ($T < 10\,°C$) and the red residue dissolved in CD$_3$COCD$_3$, giving a red solution, which was cooled to $-78\,°C$ in a Me$_2$CO/dry ice bath for storage.

Data for $2 \cdot 4\,PF_6 \cdot RED$: ^{1}H NMR (CD$_3$COCD$_3$, 500 MHz, 225 K): $\delta = 1.10$ (t, $J = 7.6$ Hz, 3H), 1.18 (s, 18H), 2.49 (s, 3H), 2.50 – 2.60 (m, 4H), 3.20 (s, 3H), 3.23 (s, 6H), 3.72 – 3.76 (m, 8H), 4.00 – 4.05 (m, 8H), 4.12 – 4.16 (m, 2H), 4.26 – 4.31 (m, 2H), 4.34 – 4.45 (m, 10H), 4.78 (s, 2H), 4.87 (s, 2H), 4.95 (s, 4H), 5.00 (s, 2H), 5.91 – 6.05 (m, 9H), 6.14 (t, $J = 8.2$ Hz, 1H), 6.29 (d, $J = 8.2$ Hz, 1H), 6.33 (d, $J = 8.2$ Hz, 1H), 6.76 – 6.80 (m, 6H), 6.86 – 6.94 (m, 8H), 7.01 – 7.06 (m, 10H), 7.22 – 7.28 (m, 8H), 7.38 (d, $J = 8.4$ Hz, 4H), 7.54 (d, $J = 5.8$ Hz, 2H), 7.59 (d, $J = 5.8$ Hz, 2H), 7.70 (d, $J = 6.3$ Hz, 2H), 7.72 (d, $J = 6.6$ Hz, 2H), 8.06 (s, 2H), 8.16 (s, 2H), 8.29 (s, 2H), 8.36 (s, 2H), 9.07 (d, $J = 6.6$ Hz, 2H), 9.09 (d, $J = 6.9$ Hz, 2H), 9.19 (d, $J = 6.4$ Hz, 2H), 9.34 ppm (d, $J = 6.5$ Hz, 2H); the signals from $5 \times CH_2O$ (10H) are obscured under the intense H$_2$O signal, which appears at 3.26 – 3.69; UV/Vis (CD$_3$COCD$_3$, 298 K): $\lambda_{max} = 540$ nm.

Although $2 \cdot 4\,PF_6 \cdot GREEN$ appears to be less polar than $2 \cdot 4\,PF_6 \cdot RED$, it was only possible to extract an extremely small amount of $2 \cdot 4\,PF_6 \cdot GREEN$ ($R_f = 0.5$) from the silica on the PTLC plate. The UV/Vis spectrum recorded in CD$_3$COCD$_3$ at 298 K of this fraction shows, as expected, only a broad CT absorption band centered on 800 nm. As a consequence of the extremely limited amount of $2 \cdot 4\,PF_6 \cdot GREEN$, isolated from the PTLC experiment it was not possible to record an ^{1}H NMR spectrum. Alternatively, it was possible to shift the equilibrium of the two translational isomers from 1:1 to 9:1 in favor of $2 \cdot 4\,PF_6 \cdot GREEN$ by heating a CD$_3$SOCD$_3$ solution of the brown 1:1 mixture to 425 K. The data given below are for the major isomer at 410 K.

Data for $2 \cdot 4\,PF_6 \cdot GREEN$: ^{1}H NMR (CD$_3$SOCD$_3$, 500 MHz, 410 K): $\delta = 1.23$ (t, $J = 7.6$ Hz, 3H), 1.31 (s, 18H), 2.62 (q, $J = 7.6$ Hz, 2H), 2.68 (s, 3H), 3.30 (s, 9H), 3.33 (s, $J = 6.2$ Hz, 2H), 3.49 – 3.54 (m, 6H), 3.62 – 3.66 (m, 6H), 3.77 – 3.83 (m, 6H), 3.89 – 3.92 (m, 2H), 3.90 – 4.00 (m, 2H), 4.06 (t, $J = 6.2$ Hz, 2H), 4.11 – 4.23 (m, 10H), 4.32 – 4.36 (m, 2H), 4.45 – 4.47 (m, 2H), 4.90 (s, 2H), 5.05 (s, 6H), 5.11 (s, 2H), 5.86 and 5.90 (AB q, $J = 13.1$ Hz, 8H), 6.16 and 6.17 (AB q, $J = 2.0$ Hz, 2H), 6.83 – 6.89 (m, 6H), 6.95 – 6.99 (m, 6H), 7.03 – 7.11 (m, 12H), 7.20 – 7.41 (m, 14H), 7.83 (d, $J = 8.0$ Hz, 2H), 7.87 (s, 8H), 8.08 (d, $J = 6.3$ Hz, 8H), 9.29 ppm (d, $J = 6.3$ Hz, 8H); UV/Vis (CD$_3$COCD$_3$, 298 K): $\lambda_{max} = 800$ nm.

[2]Pseudorotaxane $18 \subset CBPQT \cdot 4\,PF_6$: Dissolving a 1:1 mixture of the semi-dumbbell compound **18** and CBPQT $\cdot 4\,PF_6$ in CD$_3$COCD$_3$ at 298 K produced a brown solution ($c = 2.12 \times 10^{-3}$ M), and a ^{1}H NMR spectrum (500 MHz) was recorded at 300 K. The signals were extremely broad, because the exchange between the complexed and free species occurs rapidly on the ^{1}H NMR timescale. Upon cooling the sample down to 245 K, all the signals sharpened, and the ^{1}H NMR spectrum (500 MHz) revealed (Figure 17) that $18 \subset CBPQT \cdot RED^{4+}$ is almost exclusively present in the CD$_3$COCD$_3$ solution at 245 K. The data given below are for $18 \subset CBPQT \cdot RED^{4+}$ in CD$_3$COCD$_3$ at 245 K. ^{1}H NMR (CD$_3$COCD$_3$, 500 MHz, 245 K): $\delta = 1.19$ (t, $J = 7.6$ Hz, 3H), 1.29 (s, 18H), 2.29 (s, 3H), 2.59 (d, $J = 8.0$ Hz, 1H), 2.60 (q, $J = 7.6$ Hz, 2H), 2.69 (d, $J = 8.0$ Hz, 1H), 2.89 (t, $J = 6.2$ Hz, 2H), 3.65 (t, $J = 6.2$ Hz, 2H), 3.78 – 3.92, 4.02 – 4.10, and 4.30 – 4.58 (m, 20H), 5.10 (unresolved t, 1H), 5.95 – 6.05 (m, 2H), 6.15 – 6.25 (m, 8H), 6.29 (d, $J = 8.0$ Hz, 1H), 6.47 (d, $J = 8.0$ Hz, 1H), 6.86 (d, $J = 8.9$ Hz, 2H), 7.05 – 7.35 (m, 18H), 7.75 (d, $J = 6.6$ Hz, 2H), 7.87 (d, $J = 6.6$ Hz, 2H), 7.89 (d, $J = 6.6$ Hz, 2H), 8.20 (s, 2H), 8.27 (s, 2H), 8.31 (s, 2H), 8.49 (s, 2H), 8.69 (d, $J = 6.6$ Hz, 2H), 9.16 (d, $J = 6.6$ Hz, 4H), 9.62 ppm (d, $J = 6.6$ Hz, 2H).

Compound 19: MsCl (0.05 mL, 0.078 g, 0.68 mmol) was added dropwise to an ice-cooled solution of the alcohol **18** (0.50 g, 0.42 mol) and Et$_3$N (0.21 mL, 0.15 g, 1.48 mmol) in anhydrous CH$_2$Cl$_2$ (40 mL). The yellow reaction mixture was stirred for 1 h at 0 °C, whereupon the ice-bath was removed. The reaction mixture was diluted with CH$_2$Cl$_2$ (50 mL), washed with H$_2$O (3 × 50 mL), and dried (MgSO$_4$). Concentration in vacuo gave a yellow oil, which was subjected to column chromatography (SiO$_2$: CH$_2$Cl$_2$/MeOH 99:1). The yellow band ($R_f = 0.4$) was collected and concentrated to give compound **19** (0.50 g, 95 %) as a yellow foam. ^{1}H NMR (CD$_3$COCD$_3$, 500 MHz): $\delta = 1.22$ (t, $J = 7.6$ Hz, 3H), 1.31 (s, 18H), 2.45 (s, 3H), 2.62 (q, $J = 7.6$ Hz, 2H), 3.08 (t, $J = 6.4$ Hz, 2H), 3.10 (s, 3H), 3.78 (t, $J = 6.4$ Hz, 2H), 3.82 – 3.84 (m, 2H), 3.87 – 3.89 (m, 2H), 3.93 – 3.95 (m, 4H), 4.04 – 4.06 (m, 2H), 4.11 – 4.13 (m, 4H), 4.29 – 4.31 (m, 2H), 4.35 – 4.37 (m, 2H), 4.43 – 4.45 (m, 2H), 6.77 and 6.78 (AB q, $J = 2.0$ Hz, 2H), 6.84 (d, $J = 8.6$ Hz, 2H),

6.95 (d, $J = 8.0$ Hz, 1H), 7.00 (d, $J = 8.0$ Hz, 1H), 7.07 – 7.15 (m, 10H), 7.32 (d, $J = 8.6$ Hz, 4H), 7.36 (t, $J = 8.0$ Hz, 1H), 7.43 (t, $J = 8.0$ Hz, 1H), 7.83 (d, $J = 8.0$ Hz, 1H), 7.86 ppm (d, $J = 8.0$ Hz, 1H); MS (FAB): m/z (%): 1263 (100) $[M]^+$; elemental analysis calcd (%) for C$_{67}$H$_{77}$NO$_9$S$_7$ (1264.8): C 63.62, H 6.14, N 1.11; found: C 63.55, H 5.85, N 1.24.

Compound 20: Compound **19** (0.50 g, 0.40 mmol) was dissolved in anhydrous Me$_2$CO (50 mL), and NaI (0.59 g, 3.94 mmol) was added in one portion. The reaction mixture was heated under reflux for 14 h, before being cooled to room temperature and the solvent removed in vacuo. The yellow residue was dissolved in CH$_2$Cl$_2$ (100 mL), washed with H$_2$O (2 × 70 mL), and dried (MgSO$_4$). Concentration in vacuo gave a yellow foam, which was purified by column chromatography (SiO$_2$: CH$_2$Cl$_2$). The yellow band ($R_f = 0.6$) was collected and concentrated to provide compound **20** (0.48 g, 93 %) as a yellow foam. ^{1}H NMR (CD$_3$COCD$_3$, 500 MHz): $\delta = 1.21$ (t, $J = 7.6$ Hz, 3H), 1.31 (s, 18H), 2.43 (s, 3H), 2.60 (q, $J = 7.6$ Hz, 2H), 3.06 (t, $J = 6.4$ Hz, 2H), 3.39 (t, $J = 6.2$ Hz, 2H), 3.75 (t, $J = 6.4$ Hz, 2H), 3.79 – 3.81 (m, 2H), 3.83 – 3.85 (m, 2H), 3.89 (t, $J = 6.2$ Hz, 2H), 3.90 – 3.93 (m, 2H), 4.00 – 4.02 (m, 2H), 4.08 – 4.10 (m, 4H), 4.26 – 4.28 (m, 2H), 4.32 – 4.33 (m, 2H), 6.75 and 6.77 (AB q, $J = 2.1$ Hz, 2H), 6.81 (d, $J = 8.8$ Hz, 2H), 6.92 (d, $J = 8.0$ Hz, 1H), 6.98 (d, $J = 8.0$ Hz, 1H), 7.09 – 7.16 (m, 10H), 7.32 (d, $J = 8.5$ Hz, 4H), 7.36 (t, $J = 8.0$ Hz, 1H), 7.42 (t, $J = 8.0$ Hz, 1H), 7.83 (d, $J = 8.0$ Hz, 1H), 7.89 ppm (d, $J = 8.0$ Hz, 1H); MS (FAB): m/z (%): 1295 (100) $[M]^+$; elemental analysis calcd (%) for C$_{66}$H$_{74}$INO$_6$S$_6$ (1296.6): C 61.14, H 5.75, N 1.08; found: C 61.28, H 5.46, N 0.99.

Compound 21

Method A: Compound **20** (0.48 g, 0.37 mmol) was dissolved in anhydrous Me$_2$CO (40 mL), and KSCN (0.36 g, 3.70 mmol) was added in one portion. The reaction mixture was heated under reflux for 5 h. After being cooled to room temperature, the solvent was removed in vacuo. The yellow residue was dissolved in CH$_2$Cl$_2$ (100 mL), washed with H$_2$O (2 × 100 mL), and dried (MgSO$_4$). Concentration in vacuo gave a yellow foam, which was subjected to column chromatography (SiO$_2$, CH$_2$Cl$_2$/hexane 9:1). The yellow band ($R_f = 0.3$) was collected and concentrated to a yellow oil, which was repeatedly redissolved in CH$_2$Cl$_2$ (2 × 20 mL) and concentrated to give compound **21** (0.37 g, 81 %) as a yellow foam.

Method B: Compound **19** (0.54 g, 0.43 mmol) was dissolved in anhydrous Me$_2$CO (50 mL), and KSCN (1.24 g, 12.8 mmol) was added in one portion. The yellow reaction mixture was heated under reflux for 1 d, whereupon additional KSCN (0.83 g, 8.54 mmol) was added. The reaction mixture was heated under reflux for a further 1 d and cooled to room temperature. After removal of the solvent, the yellow residue was dissolved in CH$_2$Cl$_2$ (150 mL), washed with H$_2$O (3 × 100 mL), and dried (MgSO$_4$). Concentration in vacuo gave compound **21** (0.51 g, 97 %) as a yellow foam. ^{1}H NMR (CD$_3$COCD$_3$, 500 MHz): $\delta = 1.21$ (t, $J = 7.6$ Hz, 3H), 1.31 (s, 18H), 2.45 (s, 3H), 2.62 (q, $J = 7.6$ Hz, 2H), 3.08 (t, $J = 6.4$ Hz, 2H), 3.38 (t, $J = 5.8$ Hz, 2H), 3.78 (t, $J = 6.4$ Hz, 2H), 3.82 – 3.84 (m, 2H), 3.86 – 3.88 (m, 2H), 3.93 – 3.95 (m, 2H), 4.01 (t, $J = 5.8$ Hz, 2H), 4.05 – 4.07 (m, 2H), 4.10 – 4.13 (m, 4H), 4.29 – 4.31 (m, 2H), 4.36 – 4.38 (m, 2H), 6.77 and 6.78 (AB q, $J = 2.1$ Hz, 2H), 6.84 (d, $J = 8.8$ Hz, 2H), 6.95 (d, $J = 8.0$ Hz, 1H), 7.01 (d, $J = 8.0$ Hz, 1H), 7.08 – 7.16 (m, 10H), 7.32 (d, $J = 8.5$ Hz, 4H), 7.38 (t, $J = 8.0$ Hz, 1H), 7.43 (t, $J = 8.0$ Hz, 1H), 7.83 (d, $J = 8.0$ Hz, 1H), 7.88 ppm (d, $J = 8.0$ Hz, 1H); IR (KBr): $\tilde{\nu} = 2154$ cm^{-1} (S–C≡N); MS (FAB): m/z (%): 1226 (100) $[M]^+$; elemental analysis calcd (%) for C$_{67}$H$_{74}$N$_2$O$_6$S$_7$ (1227.8): C 65.54, H 6.08, N 2.28; found: C 65.49, H 6.02, N 2.13.

Dumbbell 23: Compound **21** (0.25 g, 0.20 mmol) and the chloride **22** (0.19 g, 0.24 mmol) were dissolved in anhydrous THF/EtOH (2:1 v/v, 50 mL), after which powdered NaBH$_4$ (0.077 g, 2.04 mmol) was added in one portion. The reaction mixture was stirred for 1 d at room temperature, whereupon it was poured into ice containing saturated aqueous NH$_4$Cl solution (50 mL) and extracted with CH$_2$Cl$_2$ (3 × 50 mL). The combined organic extracts were washed with H$_2$O (2 × 50 mL) and dried (MgSO$_4$). Concentration in vacuo gave a yellow oil, which was purified by column chromatography (SiO$_2$, CH$_2$Cl$_2$/EtOAc 3:2). The yellow band ($R_f = 0.4$) was collected, and the solvent evaporated affording a yellow oil, which was repeatedly dissolved in CH$_2$Cl$_2$ (3 × 20 mL) and concentrated to give compound **23** (0.35 g, 90 %) as a yellow foam. ^{1}H NMR (CD$_3$COCD$_3$, 500 MHz): $\delta = 1.20$ (t, $J = 7.6$ Hz, 3H), 1.29 (s, 18H), 2.42 (s, 3H), 2.60 (q, $J = 7.6$ Hz, 2H), 2.61 (t, $J = 6.5$ Hz, 2H), 3.04 (t, $J = 6.4$ Hz, 2H), 3.29 (s, 9H), 3.48 – 3.50 (m, 6H), 3.62 – 3.65 (m, 6H), 3.73 – 3.81 (m, 14H), 3.82 – 3.85 (m, 2H), 3.88 – 3.91 (m, 2H), 3.93 – 3.95 (m, 2H), 4.07 – 4.13 (m, 10H),

4.22–4.25 (m, 2H), 4.31–4.33 (m, 2H), 4.87 (s, 2H), 4.96 (s, 4H), 6.73–6.75 (m, 4H), 6.80 (d, $J = 8.4$ Hz, 2H), 6.81 (d, $J = 8.9$ Hz, 2H), 6.89 (d, $J = 8.1$ Hz, 1H), 6.93 (d, $J = 8.3$ Hz, 4H), 6.99 (d, $J = 8.1$ Hz, 1H), 7.05–7.13 (m, 10H), 7.28–7.32 (m, 7H), 7.35 (d, $J = 9.0$ Hz, 4H), 7.39 (t, $J = 8.1$ Hz, 1H), 7.79 (d, $J = 8.1$ Hz, 1H), 7.87 ppm (d, $J = 8.1$ Hz, 1H); MS (FAB): m/z (%): 1965 (100) $[M]^+$, 1756 (20), 1546 (22), 1202 (24); elemental analysis calcd (%) for $C_{109}H_{129}NO_{18}S_7$ (1965.7); C 66.60, H 6.61, N 0.71; found: C 66.67, H 6.54, N 0.61.

Fast two-station [2]rotaxane 3·4PF_6

Method A: A solution of **23** (0.35 g, 0.18 mmol), **8·2PF_6** (0.38 g, 0.54 mmol), and **9** (0.14 g, 0.53 mmol) in anhydrous DMF (10 mL) was stirred for 10 d at room temperature (after approximately 1 d the color changed to dark green and a white precipitate was formed). The dark green suspension was directly subjected to column chromatography (SiO_2), and unreacted **23** was eluted with Me_2CO, whereupon the eluent was changed to Me_2CO/NH_4PF_6 (1.0 g NH_4PF_6 in 100 mL Me_2CO) and the brown band containing **3·4PF_6** was collected. Most of the solvent was removed under vacuum ($T < 30\,°C$) followed by addition of H_2O (50 mL). The resulting precipitate was collected by filtration, washed with Et_2O (20 mL) and dried, affording **3·4PF_6** (0.084 g, 15%) as a brown solid. M.p. 220 °C (decomp).

Method B: A solution of **23** (0.40 g, 0.20 mmol), **8·2PF_6** (0.43 g, 0.61 mmol), and **9** (0.16 g, 0.61 mmol) in anhydrous DMF (12 mL) was transferred to a teflon tube and subjected to 10 kbar pressure at room temperature for 3 d. The dark green solution was directly subjected to column chromatography (SiO_2), and unreacted **23** was eluted with Me_2CO, whereupon the eluent was changed to Me_2CO/NH_4PF_6 (1.0 g NH_4PF_6 in 100 mL Me_2CO) and the brown band containing **3·4PF_6** was collected. Most of the solvent was removed in vacuo ($T < 30\,°C$) followed by addition of H_2O (200 mL). The resulting precipitate was collected by filtration, washed with H_2O (30 mL) and Et_2O (40 mL), and dried affording **2·4PF_6** (0.29 g, 47%) as a brown solid. M.p. 215 °C (decomp). The data given below are for the mixture of the two translational isomers; MS (FAB): m/z (%): 2919 (3) $[M - PF_6]^+$, 2774 (8) $[M - 2PF_6]^+$, 2629 (9) $[M - 3PF_6]^+$, 1964 (6), 1387 (11) $[M - 2PF_6]^{2+}$, 1314.5 (24) $[M - 3PF_6]^{2+}$, 1242 (12) $[M - 4PF_6]^{2+}$; UV/Vis (MeCN, 298 K): λ_{max} $(\varepsilon) = 520$ (960), 800 nm (1300 L mol⁻¹ cm⁻¹); UV/Vis (Me_2CO, 298 K): λ_{max} $(\varepsilon) = 540$ (760), 785 nm (740 L mol⁻¹ cm⁻¹); UV/Vis (Me_2SO, 298 K): $\lambda_{max}(\varepsilon) = 540$ (640), 765 nm (1310 L mol⁻¹ cm⁻¹); elemental analysis calcd (%) for $C_{145}H_{161}F_{24}N_5O_{18}P_4S_7$ (3066.2): C 56.80, H 5.29, N 2.28; found: C 56.43, H 5.20, N 2.21.

All attempts to separate the two translational isomers by employing PTLC failed on account of the fast shuttling of $CBPQT^{4+}$ between the two recognition sites in **3·4PF_6**. Instead, **3·4PF_6·RED** and **3·4PF_6·GREEN** were characterized as a consequence of the fact in CD_3COCD_3 at 245 K, **3·4PF_6** exists almost exclusively as **3·4PF_6·RED**, whereas in CD_3SOCD_3 at 400 K, it exists almost exclusively as **3·4PF_6·GREEN**.

Data for 3·4PF_6·RED: ¹H NMR (CD_3COCD_3, 500 MHz, 245 K): $\delta = 1.19$ (t, $J = 7.5$ Hz, 3H), 1.28 (s, 18H), 2.27 (s, 3H), 2.44 (d, $J = 8.0$ Hz, 1H), 2.51 (d, $J = 8.0$ Hz, 1H), 2.59 (q, $J = 7.5$ Hz, 2H), 2.87 (t, $J = 6.1$ Hz, 2H), 3.15 (unresolved t, 2H), 3.24 (s, 6H), 3.28 (s, 3H), 3.49–3.53 (m, 6H), 3.60 (t, $J = 6.1$ Hz, 2H), 3.63–3.68 (m, 6H), 3.73–3.77 (m, 2H), 3.79–3.83 (m, 8H), 4.03–4.08 (m, 10H), 4.18–4.22 (m, 2H), 4.23–4.27 (m, 4H), 4.30–4.34 (m, 2H), 4.38–4.42 (m, 2H), 4.48–4.52 (m, 2H), 4.67 (s, 2H), 4.88 (s, 4H), 5.88–6.15 (m, 10H), 6.22 (d, $J = 8.0$ Hz, 1H), 6.34 (d, $J = 8.0$ Hz, 1H), 6.75 (s, 2H), 6.78–6.86 (m, 8H), 7.07–7.18 (m, 12H), 7.21–7.26 (m, 8H), 7.33 (d, $J = 8.4$ Hz, 4H), 7.57 (d, $J = 6.0$ Hz, 2H), 7.61 (d, $J = 6.0$ Hz, 2H), 7.85 (d, $J = 6.0$ Hz, 2H), 8.14 (s, 2H), 8.22 (s, 2H), 8.26 (s, 2H), 8.27 (s, 2H), 8.65 (d, $J = 6.0$ Hz, 2H), 8.97 (d, $J = 6.0$ Hz, 2H), 9.09 (d, $J = 6.0$ Hz, 2H), 9.27 ppm (d, $J = 6.0$ Hz, 2H).

Data for 3·4PF_6·GREEN: ¹H NMR (CD_3SOCD_3, 500 MHz, 400 K) $\delta = 1.23$ (t, $J = 7.7$ Hz, 3H), 1.31 (s, 18H), 2.63 (q, $J = 7.7$ Hz, 2H), 2.67 (s, 3H), 2.71 (t, $J = 6.5$ Hz, 2H), 3.28 (t, $J = 7.1$ Hz, 2H), 3.30 (s, 9H), 3.49–3.51 (m, 6H), 3.62–3.64 (m, 6H), 3.73–3.78 (m, 10H), 3.92–3.98 (m, 6H), 4.07–4.31 (m, 16H), 4.42–4.44 (m, 2H), 4.88 (s, 2H), 5.01 (s, 4H), 5.83 and 5.89 (AB q, $J = 12.1$ Hz, 8H), 6.34 (br s, 2H), 6.76 (s, 2H), 6.83–6.99 (m, 10H), 7.06–7.12 (m, 10H), 7.18–7.34 (m, 14H), 7.89 (br s, 8H), 8.09 (br s, 8H), 9.27 ppm (br s, 8H).

Photophysical experiments: All the measurements were performed at room temperature in air-equilibrated MeCN, Me_2CO, or Me_2SO solutions. Hexafluorophosphate (PF_6^-) ions were the counterions in the case of all the

cationic compounds. UV/Vis absorption spectra were recorded with a Perkin–Elmer Lambda 40 spectrophotometer, a Cary 100 Bio spectrophotometer, a Shimadzu UV-160 instrument, or a Shimadzu UV-1601PC instrument. Uncorrected luminescence spectra were obtained with a Perkin–Elmer LS-50 spectrofluorimeter, equipped with a Hamamatsu R928 phototube. The estimated experimental errors are 2 nm on band maxima, ±5% on the molar absorption coefficients and fluorescence intensity.

Electrochemical experiments: Cyclic voltammetric (CV) and differential pulse voltammetric (DPV) experiments were carried out in argon-purged MeCN at room temperature with an Autolab 30 multipurpose instrument interfaced to a personal computer. The working electrode was a glassy carbon electrode (0.08 cm², Amel), whose surface was routinely polished with a 0.05 mm alumina–water slurry on a felt surface immediately prior to use. In all cases, the counter electrode was a Pt spiral, separated from the bulk solution with a fine glass frit, and an Ag wire was used as a quasi-reference electrode. 1,1-Dimethylferrocene ($+0.31$ V vs SCE)[58] was present as an internal standard. The concentrations of the compounds examined were of the order of 5×10^{-4} M, unless otherwise noted. The experiments were carried out in the presence of tetraethylammonium hexafluorophosphate (5×10^{-2} M) as supporting electrolyte. Cyclic voltammograms were obtained with sweep rates in the range $0.05 – 1.0$ V s⁻¹. DPV experiments were performed with a scan rate of 20 or 4 mV s⁻¹, a pulse height of 75 or 10 mV, and a duration of 40 ms. The reversibility of the observed processes was established by using the criteria of 1) separation of 60 mV between cathodic and anodic peaks, 2) the close to unity ratio of the intensities of the cathodic and anodic currents, and 3) the constancy of the peak potential on changing sweep rate in the cyclic voltammograms. The same halfwave potentials were obtained from the DPV peaks and from an average of the cathodic and anodic CV peaks, as expected for reversible processes. For irreversible processes, the potentials were estimated from the DPV peaks. The experimental errors on the potentials were estimated to be ±10 mV. For the [2]rotaxane 1^{4+} the potential values for the two oxidations associated with the MPTTF unit were obtained by deconvolution of the DPV profile by employing the equations proposed by Parry and Osteryoung.[59] The number of exchanged electrons for reversible processes involving the MPTTF unit was measured by comparing the current intensity of the CV waves and the area of the DPV peaks with those found for the two reversible and monoelectronic oxidation processes of the MPTTF model compound **25**, after correction for differences in concentrations and diffusion coefficients.[60]

Acknowledgement

[1] a) G. Schill, *Catenanes, Rotaxanes and Knots*, Academic Press, New York, **1971**; b) D. M. Walba, *Tetrahedron* **1985**, *41*, 3161–3212; c) C. O. Dietrich-Buchecker, J.-P. Sauvage, *Chem. Rev.* **1987**, *87*, 795–810; d) H. W. Gibson, H. Marand, *Adv. Mater.* **1993**, *5*, 11–21; e) D. B. Amabilino, J. F. Stoddart, *Chem. Rev.* **1995**, *95*, 2725–2828; f) R. Jäger, F. Vögtle, *Angew. Chem.* **1997**, *109*, 966–980; *Angew. Chem. Int. Ed. Engl.* **1997**, *36*, 930–944; g) G. A. Breault, C. A. Hunter, P. C. Mayers, *Tetrahedron* **1999**, *55*, 5265–5293; h) *Molecular Catenanes, Rotaxanes and Knots* (Eds.: J.-P. Sauvage, C. O. Dietrich-Buchecker), Wiley-VCH, Weinheim, **1999**; i) L. Raehm, D. G. Hamilton, J. K. M. Sanders, *Synlett* **2002**, 1743–1761.

[2] a) P.-L. Anelli, N. Spencer, J. F. Stoddart, *J. Am. Chem. Soc.* **1991**, *113*, 5131–5133; b) R. A. Bissell, E. Córdova, A. E. Kaifer, J. F. Stoddart, *Nature* **1994**, *369*, 133–137; c) A. Livoreil, C. O. Dietrich-Buchecker, J.-P. Sauvage, *J. Am. Chem. Soc.* **1994**, *116*, 9399–9400; d) P.-L. Anelli, M. Asakawa, P. R. Ashton, R. A. Bissell, G. Clavier, R. Górski, A. E. Kaifer, S. J. Langford, G. Mattersteig, S. Menzer, D. Philp, A. M. Z. Slawin, N. Spencer, J. F. Stoddart, M. S. Tolley, D. J. Williams, *Chem. Eur. J.* **1997**, *3*, 1113–1135; e) P. R. Ashton, R. Ballardini, V. Balzani, I.

Baxter, A. Credi, M. C. T. Fyfe, M. T. Gandolfi, M. Gómez-López, M.-V. Martínez-Díaz, A. Piersanti, N. Spencer, J. F. Stoddart, M. Venturi, A. J. P. White, D. J. Williams, *J. Am. Chem. Soc.* **1998**, *120*, 11932 – 11942; f) D. A. Leigh, A. Troisi, F. Zerbetto, *Angew. Chem.* **2000**, *112*, 358 – 361; *Angew. Chem. Int. Ed.* **2000**, *39*, 350 – 353; g) P. R. Ashton, R. Ballardini, V. Balzani, A. Credi, R. Dress, E. Ishow, C. J. Kleverlaan, O. Kocian, J. A. Preece, N. Spencer, J. F. Stoddart, M. Venturi, S. Wagner, *Chem. Eur. J.* **2000**, *6*, 3558 – 3574; h) A. M. Brouwer, C. Frochot, F. G. Gatti, D. A. Leigh, L. Mottier, F. Paolucei, S. Roffia, G. W. H. Wurpel, *Science* **2001**, *291*, 2124 – 2128; i) A. M. Elizarov, H.-S. Chiu, J. F. Stoddart, *J. Org. Chem.* **2002**, *67*, 9175 – 9181; j) F. G. Gatti, S. León, J. K. Y. Wong, G. Bottari, A. Altieri, M. A. F. Morales, S. J. Teat, C. Frochot, D. A. Leigh, A. M. Brouwer, F. Zerbetto, *Proc. Natl. Acad. Sci. USA* **2003**, *100*, 10 – 14.

[3] a) J. F. Stoddart, *Chem. Aust.* **1992**, *59*, 546 – 547 and 581; b) M. Gómez-López, J. A. Preece, J. F. Stoddart, *Nanotechnology* **1996**, *7*, 183 – 192; c) M. D. Ward, *Chem. Ind.* **1997**, 640 – 645; d) V. Balzani, M. Gómez-López, J. F. Stoddart, *Acc. Chem. Res.* **1998**, *31*, 405 – 414; e) J.-P. Sauvage, *Acc. Chem. Res.* **1998**, *31*, 611 – 619; f) A. Niemz, V. M. Rotello, *Acc. Chem. Res.* **1999**, *32*, 42 – 52; g) A. E. Kaifer, *Acc. Chem. Res.* **1999**, *32*, 62 – 71; h) L. Fabbrizzi, M. Licchelli, P. Pallavicini, *Acc. Chem. Res.* **1999**, *32*, 846 – 853; i) D. A. Leigh, A. Murphy, *Chem. Ind.* **1999**, 178 – 183; j) M. D. Ward, *Chem. Ind.* **2000**, 22 – 26; k) V. Balzani, A. Credi, F. M. Raymo, J. F. Stoddart, *Angew. Chem.* **2000**, *112*, 3486 – 3531; *Angew. Chem. Int. Ed.* **2000**, *39*, 3348 – 3391; l) R. Ballardini, V. Balzani, A. Credi, M. T. Gandolfi, M. Venturi, M. *Acc. Chem. Res.* **2001**, *34*, 445 – 455; m) A. Harada, *Acc. Chem. Res.* **2001**, *34*, 456 – 464; n) J.-P. Collin, C. Dietrich-Buchecker, P. Gavina, M. C. Jiménez-Molero J.-P. Sauvage, *Acc. Chem. Res.* **2001**, *34*, 477 – 487.

[4] *Struct. Bonding* **2001**, *99* (Special volume on Molecular Machines and Motors, Ed.: J.-P. Sauvage).

[5] a) V. Balzani, A. Credi, M. Venturi, *Chem. Eur. J.* **2002**, *8*, 5525 – 5532; b) V. Balzani, A. Credi, M. Venturi, *Molecular Devices and Machines — A Journey into the Nano World*, Wiley-VCH, Weinheim, **2003**.

[6] For investigations relating to a [2]catenane-based solid-state electronically-reconfigurable switch, see: a) M. Asakawa, M. Higuchi, G. Mattersteig, T. Nakamura, A. R. Pease, F. M. Raymo, T. Shimizu, J. F. Stoddart, *Adv. Mater.* **2000**, *12*, 1099 – 1102; b) C. P. Collier, G. Mattersteig, E. W. Wong, Y. Lou, K. Beverly, J. Sampaio, F. M. Raymo, J. F. Stoddart, J. R. Heath, *Science* **2000**, *289*, 1172 – 1175.

[7] For electronically-configurable molecular-based logic gates, see: a) C. P. Collier, E. W. Wong, M. Belohradsky, F. M. Raymo, J. F. Stoddart, P. J. Kuekes, R. S. Williams, J. R. Heath, *Science* **1999**, *285*, 391 – 394; b) E. W. Wong, C. P. Collier, M. Belohradsky, F. M. Raymo, J. F. Stoddart, J. R. Heath, *J. Am. Chem. Soc.* **2000**, *122*, 5831 – 5840.

[8] a) R. F. Service, *Science* **2001**, *291*, 426 – 427; b) A. R. Pease, J. O. Jeppesen, J. F. Stoddart, Y. Luo, C. P. Collier, J. R. Heath, *Acc. Chem. Res.* **2001**, *34*, 433 – 444; c) R. F. Service, *Science* **2001**, *294*, 2442 – 2443.

[9] a) J. S. Lindsey, *New J. Chem.* **1991**, *15*, 153 – 180; b) G. M. Whitesides, J. P. Mathias, C. T. Seto, *Science* **1991**, *254*, 1312 – 1319; c) D. Philp, J. F. Stoddart, *Synlett* **1991**, 445 – 458; d) D. Philp, J. F. Stoddart, *Angew. Chem.* **1996**, *108*, 1242 – 1286; *Angew. Chem. Int. Ed. Engl.* **1996**, *35*, 1154 – 1196; e) M. C. T. Fyfe, J. F. Stoddart, *Acc. Chem. Res.* **1997**, *30*, 393 – 401; f) J. Rebek, Jr., *Acc. Chem. Res.* **1999**, *32*, 278 – 286; g) G. M. Whitesides, B. Grzybowski, *Science* **2002**, *295*, 2418 – 2421.

[10] P.-L. Anelli, P. R. Ashton, R. Ballardini, V. Balzani, M. T. Gandolfi, T. T. Goodnow, A. E. Kaifer, D. Philp, M. Pietraszkiewicz, L. Prodi, M. V. Reddington, A. M. Z. Slawin, N. Spencer, C. Vicent, D. J. Williams, *J. Am. Chem. Soc.* **1992**, *114*, 193 – 218.

[11] a) A. G. Kolchinski, D. H. Busch, N. W. Alcock, *J. Chem. Soc. Chem. Commun.* **1995**, 1289 – 1291; b) P. R. Ashton, P. T. Glink, J. F. Stoddart, P. A. Tasker, A. J. P. White, D. J. Williams, *Chem. Eur. J.* **1996**, *2*, 729 – 736; c) N. Solladié, J.-C. Chambron, C. O. Dietrich-Buchecker, J.-P. Sauvage, *Angew. Chem.* **1996**, *108*, 957 – 960; *Angew. Chem. Int. Ed. Engl.* **1996**, *35*, 906 – 909; d) P. R. Ashton, R. Ballardini, V. Balzani, M. Belohradsky, M. T. Gandolfi, D. Philp, L. Prodi, F. M. Raymo, M. V. Reddington, N. Spencer, J. F. Stoddart, M. Venturi, D. V. Williams, *J. Am. Chem. Soc.* **1996**, *118*, 4931 – 4951; e) A. S. Lane, D. A. Leigh, A. Murphy, *J. Am. Chem. Soc.* **1997**, *119*, 11092 – 11093; f) A. P. Lyon, D. H. Macartney, *Inorg. Chem.* **1997**, *36*, 729 – 736; g) S. Anderson, R. T. Aplin, T. D. W. Claridge, T. Goodson III, A. C.

Maciel, G. Rumbles, J. F. Ryan, H. L. Anderson, *J. Chem. Soc. Perkin Trans. 1* **1998**, 2383 – 2398; h) A. E. Rowan, P. P. M. Aarts, K. W. M. Koutstaal, *Chem. Commun.* **1998**, 611 – 612; i) A. G. Kolchinski, N. W. Alcock, R. A. Roesner, D. H. Busch, *Chem. Commun.* **1998**, 1437 – 1438; j) S. J. Loeb, J. A. Wisner, *Chem. Commun.* **1998**, 2757 – 2758; k) G. M. Hübner, J. Gläser, C. Seel, F. Vögtle, *Angew. Chem.* **1999**, *111*, 395 – 398; *Angew. Chem. Int. Ed.* **1999**, *38*, 383 – 386; l) S. J. Rowan, S. J. Cantrill, J. F. Stoddart, *Org. Lett.* **1999**, *1*, 129 – 132; m) L. Raehm, J.-M. Kern, J.-P. Sauvage, *Chem. Eur. J.* **1999**, *5*, 3310 – 3317; n) C. Seel, F. Vögtle, *Chem. Eur. J.* **2000**, *6*, 21 – 24; o) S. J. Loeb, J. A. Wisner, *Chem. Commun.* **2000**, 845 – 846; p) K. Chichak, M. C. Walsh, N. R. Branda, *Chem. Commun.* **2000**, 847 – 848; q) J. E. H. Buston, J. R. Young, H. L. Anderson, *Chem. Commun.* **2000**, 905 – 906; r) S. J. Cantrill, D. A. Fulton, A. M. Heiss, A. R. Pease, J. F. Stoddart, A. J. P. White, D. J. Williams, *Chem. Eur. J.* **2000**, *6*, 2274 – 2287; s) S.-H. Chiu, J. F. Stoddart, *J. Am. Chem. Soc.* **2002**, *124*, 4174 – 4175.

[12] a) D. H. Busch, N. A. Stephenson, *Coord. Chem. Rev.* **1990**, *100*, 119 – 154; b) S. Anderson, H. L. Anderson, J. K. M. Sanders, *Acc. Chem. Res.* **1993**, *26*, 469 – 475; c) R. Hoss, F. Vögtle, *Angew. Chem.* **1994**, *106*, 389 – 398; *Angew. Chem. Int. Ed. Engl.* **1994**, *33*, 375 – 384; d) F. M. Raymo, J. F. Stoddart, *Pure Appl. Chem.* **1996**, *68*, 313 – 322; e) T. J. Hubin, A. G. Kolchinski, A. L. Vance, D. L. Busch, *Adv. Supramol. Chem.* **1999**, *5*, 237 – 357; f) T. J. Hubin, D. L. Busch, *Coord. Chem. Rev.* **2000**, *200 – 202*, 5 – 52; g) J. F. Stoddart. H.-R. Tseng, *Proc. Natl. Acad. Sci. USA* **2002**, *99*, 4797 – 4800.

[13] a) C. P. Collier, J. O. Jeppesen, Y. Luo, J. Perkins, E. W. Wong, J. R. Heath, J. F. Stoddart, *J. Am. Chem. Soc.* **2001**, *123*, 12632 – 12641; b) Y. Luo, C. P. Collier, J. O. Jeppesen, K. A. Nielsen, E. Delonno, G. Ho, J. Perkins, H.-R. Tseng, T. Yamamoto, J. F. Stoddart, J. R. Heath, *ChemPhysChem* **2002**, *3*, 519 – 525; d) M. Jacoby, *Chem. Eng. News* **2002**, *80 (39)*, 38 – 43.

[14] For reviews on TTF chemistry, see: a) M. Adam, K. Müllen, *Adv. Mater.* **1994**, *6*, 439 – 459; b) T. Jørgensen, T. K. Hansen, J. Becher, *Chem. Soc. Rev.* **1994**, *23*, 41 – 51; c) M. R. Bryce, *J. Mater. Chem.* **1995**, *5*, 1481 – 1496; d) J. Garin, *Adv. Heterocycl. Chem.* **1995**, *62*, 249 – 304; e) G. Schukat, E. Fanghänel, *Sulfur Rep.* **1996**, *18*, 1 – 294; f) M. R. Bryce, *J. Mater. Chem.* **2000**, *10*, 589 – 598; g) M. B. Nielsen, C. Lomholt, J. Becher, *Chem. Soc. Rev.* **2000**, *29*, 153 – 164; h) J. L. Segura, N. Martín *Angew. Chem.* **2001**, *113*, 1416 – 1455; *Angew. Chem. Int. Ed.* **2001**, *40*, 1372 – 1409.

[15] a) D. Philp, A. M. Z. Slawin, N. Spencer, J. F. Stoddart, D. J. Williams, *J. Chem. Soc. Chem. Commun.* **1991**, 1584 – 1586; b) W. Devonport, M. A. Blower, M. R. Bryce, L. M. Goldenberg, *J. Org. Chem.* **1997**, *62*, 885 – 887; c) M. B. Nielsen, J. O. Jeppesen, J. Lau, C. Lomholt, D. Damgaard, J. P. Jacobsen, J. Becher, J. F. Stoddart, *J. Org. Chem.* **2001**, *66*, 3559 – 3563.

[16] M. Asakawa, W. Dehaen, G. L'abbé, S. Menzer, J. Nouwen, F. M. Raymo, J. F. Stoddart, D. J. Williams, *J. Org. Chem.* **1996**, *61*, 9591 – 9595.

[17] A K_a value of 768M^{-1} in MeCN has been reported for the complex between 1,5-dihydroxynaphthalene and CBPQT^{4+}. See: R. Castro, K. R. Nixon, J. D. Evenseck, A. E. Kaifer, *J. Org. Chem.* **1996**, *61*, 7298 – 7303.

[18] V. Balzani, A. Credi, G. Mattersteig, O. A. Matthews, F. M. Raymo, J. F. Stoddart, M. Venturi, A. J. P. White, D. J. Williams, *J. Org. Chem.* **2000**, *65*, 1924 – 1936.

[19] Although a considerable range of catenanes and pseudorotaxanes that incorporate a TTF unit in conjunction with CBPQT^{4+} have been reported (vide infra), very few rotaxanes (see: ref. [19a,e,o,r]) employing these particular components have been described to date in the literature. For examples of catenanes, rotaxanes, and pseudorotaxanes containing TTF or TTF derivatives, see: a) P. R. Ashton, R. A. Bissell, N. Spencer, J. F. Stoddart, M. S. Tolley, *Synlett* **1992**, 923 – 926; b) T. Jørgensen, J. Becher, J.-C. Chambron, J.-P. Sauvage, *Tetrahedron Lett.* **1994**, *35*, 4339 – 4342; c) Z.-T. Li, P. C. Stein, N. Svenstrup, K. H. Lund, J. Becher, *Angew. Chem.* **1995**, *107*, 2719 – 2723; *Angew. Chem. Int. Ed. Engl.* **1995**, *34*, 2524 – 2528; d) Z.-T. Li, J. Becher, *Chem. Commun.* **1996**, 639 – 640; e) Z.-T. Li, P. C. Stein, J. Becher, D. Jensen, P. Mørk, N. Svenstrup, *Chem. Eur. J.* **1996**, *2*, 624 – 633; f) M. Asakawa, P. R. Ashton, V. Balzani, A. Credi, G. Mattersteig, O. A. Matthews, N. Montalti, N. Spencer, J. F. Stoddart, M. Venturi, *Chem. Eur. J.* **1997**, *3*, 1992 – 1996; g) Z.-T. Li, J. Becher, *Synlett* **1997**, 557 – 560; h) M. B.

Nielsen, Z.-T. Li, J. Becher, *J. Mater. Chem.* **1997**, *7*, 1175 – 1187; i) M. Asakawa, P. R. Ashton, V. Balzani, A. Credi, G. Hamers, G. Mattersteig, N. Montalti, A. N. Shipway, N. Spencer, J. F. Stoddart, M. S. Tolley, M. Venturi, A. J. P. White, D. J. Williams, *Angew. Chem.* **1998**, *110*, 357 – 361; *Angew. Chem. Int. Ed.* **1998**, *37*, 333 – 337; j) M. B. Nielsen, N. Thorup, J. Becher, *J. Chem. Soc. Perkin Trans. 1* **1998**, 1305 – 1308; k) A. Credi, M. Montalti, V. Balzani, S. J. Langford, F. M. Raymo, J. F. Stoddart, *New J. Chem.* **1998**, *22*, 1061 – 1065; l) M. Asakawa, P. R. Ashton, V. Balzani, S. E. Boyd, A. Credi, G. Mattersteig, S. Menzer, M. Montalti, F. M. Raymo, C. Ruffilli, J. F. Stoddart, M. Venturi, D. J. Williams, *Eur. J. Org. Chem.* **1999**, 985 – 994; m) J. Lau, M. B. Nielsen, N. Thorup, M. P. Cava, J. Becher, *Eur. J. Org. Chem.* **1999**, 3335 – 3341; n) V. Balzani, A. Credi, G. Mattersteig, O. A. Matthews, F. M. Raymo, J. F. Stoddart, M. Venturi, A. J. P. White, D. J. Williams, *J. Org. Chem.* **2000**, *65*, 1924 – 1936; o) D. Jensen, M. B. Nielsen, J. Lau, K. B. Jensen, R. Zubarev, E. Levillain, J. Becher, *J. Mater. Chem.* **2000**, *10*, 2249 – 2258; p) R. Ballardini, V. Balzani, A. Di Fabio, M. T. Gandolfi, J. Becher, J. Lau, M. B. Nielsen, J. F. Stoddart, *New J. Chem.* **2001**, *25*, 293 – 298; q) M. R. Bryce, G. Cooke, W. Devonport, F. M. A. Duclairoir, V. M. Rotello, *Tetrahedron Lett.* **2001**, *42*, 4223 – 4226; r) H.-R. Tseng, S. A. Vignon, J. F. Stoddart, *Angew. Chem.* **2003**, *115*, 1529 – 1533; *Angew. Chem. Int. Ed.* **2003**, *42*, 1491 – 1495.

[20] J. O. Jeppesen, J. Perkins, J. Becher, J. F. Stoddart, *Angew. Chem.* **2001**, *113*, 1256 – 1261; *Angew. Chem. Int. Ed.* **2001**, *40*, 1216 – 1221.

[21] Recently some of us developed an efficient synthesis of the parent pyrrolo[3,4-*d*]tetrathiafulvalene unit using a simple and nonclassical pyrrole synthesis, see: a) J. O. Jeppesen, K. Takimiya, F. Jensen, J. Becher, *Org. Lett.* **1999**, *1*, 1291 – 1294; b) J. O. Jeppesen, K. Takimiya, F. Jensen, T. Brimert, K. Nielsen, N. Thorup, J. Becher, *J. Org. Chem.* **2000**, *65*, 5794 – 5805.

[22] J. O. Jeppesen, J. Perkins, J. Becher, J. F. Stoddart, *Org. Lett.* **2000**, *2*, 3547 – 3550.

[23] K. B. Simonsen, N. Svenstrup, J. Lau, O. Simonsen, P. Mørk, G. J. Kristensen, J. Becher, *Synthesis* **1996**, 407 – 418.

[24] Although the preparation of **6** has been described before in the literature (see: ref. [21b]), it was synthesized by a different route and only on a very small scale.

[25] Unreacted dumbbell can be recovered and reused.

[26] It is well established that organic reactions with a negative volume of activation ($\Delta V^{\pm}$) are favored by high pressure, see: F.-G. Klärner, F. Wurche, *J. Prakt. Chem.* **2000**, *342*, 609 – 636.

[27] The FAB mass spectrum of the isolated mixture revealed only peaks with a substantially lower mass than the molecular weight of the desired dumbbell.

[28] Reductive cleavage of thiocyanate groups with $NaBH_4$ as a way of accessing thiolates has only been introduced recently into the growing field of TTF chemistry, see: a) J. O. Jeppesen, K. Takimiya, N. Thorup J. Becher, *Synthesis* **1999**, 803 – 810; b) J. O. Jeppesen, K. Takimiya, J. Becher, *Org. Lett.* **2000**, *2*, 2471 – 2473.

[29] A [2]rotaxane is a molecule composed of a ring and dumbbell-shaped component. The ring encircles the linear portion of the dumbbell-shaped component and is trapped mechanically around it by two bulky stoppers. By contrast, in a [2]pseudorotaxane, at least one of the stoppers on the dumbbell-shaped component is absent, with the consequence that dissociation into its two components can occur spontaneously, that is, it behaves like a 1:1 complex. The inclusion of TTF derivatives inside the cavity of the tetracationic cyclophane $CBPQT^{4+}$ is well documented (see: refs. [15, 18, 19]) and leads to the formation of pseudorotaxanes. Pseudorotaxanes are obtained under thermodynamic control upon mixing of their acyclic and cyclic components in solution, and the occurrence of the threading process is evidenced by the ^{1}H NMR and absorption spectra, see: a) ref. [10]; b) ref. [19f]; c) ref. [19k]; d) P. R. Ashton, R. Ballardini, V. Balzani, S. E. Boyd, A. Credi, M. T. Gandolfi, M. Gómez-López, S. Iqbal, D. Philp, J. A. Preece, L. Prodi, H. G. Ricketts, J. F. Stoddart, M. S. Tolley, M. Venturi, A. J. P. White, D. J. Williams, *Chem. Eur. J.* **1997**, *3*, 152 – 170.

[30] The synthesis of compound **27** will be reported elsewhere.

[31] a) P. R. Ashton, R. Ballardini, V. Balzani, A. Credi, M. T. Gandolfi, D. J.-F. Marquis, L. Pérez-Garcia, L. Prodi, J. F. Stoddart, M. Venturi, A. J. P. White, D. J. Williams, *J. Am. Chem. Soc.* **1995**, *117*, 11171 –

11197; b) M. Asakawa, P. R. Ashton, R. Ballardini, V. Balzani, M. Belohradsky, M. T. Gandolfi, O. Kocian, L. Prodi, F. M. Raymo, J. F. Stoddart, M. Venturi, *J. Am. Chem. Soc.* **1997**, *119*, 302 – 310; c) R. Ballardini, V. Balzani, W. Dehaen, A. E. Dell'Erba, F. M. Raymo, J. F. Stoddart, M. Venturi, *Eur. J. Org. Chem.* **2000**, 591 – 602.

[32] a) R. Ballardini, V. Balzani, A. Credi, M. T. Gandolfi, S. J. Langford, S. Menzer, L. Prodi, J. F. Stoddart, M. Venturi, D. J. Williams, *Angew. Chem.* **1996**, *108*, 1056 – 1059; *Angew. Chem. Int. Ed. Engl.* **1996**, *35*, 978 – 981; b) P. R. Ashton, R. Ballardini, V. Balzani, M. C. T. Fyfe, M. T. Gandolfi, M. V. Martínez-Díaz, M. Morosini, C. Schiavo, K. Shibata, J. F. Stoddart, A. J. P. White, D. J. Williams, *Chem. Eur. J.* **1998**, *4*, 2332 – 2341; c) P. R. Ashton, V. Balzani, J. Becher, A. Credi, M. C. T. Fyfe, G. Mattersteig, S. Menzer, M. B. Nielsen, F. M. Raymo, J. F. Stoddart, M. Venturi, D. J. Williams, *J. Am. Chem. Soc.* **1999**, *121*, 3951 – 3957.

[33] R. Ballardini, V. Balzani, J. Becher, A. Di Fabio, M. T. Gandolfi, G. Mattersteig, M. B. Nielsen, F. M. Raymo, S. J. Rowan, J. F. Stoddart, A. J. P. Williams, D. J. Williams, *J. Org. Chem.* **2000**, *65*, 4120 – 4126.

[34] J. O. Jeppesen, J. Becher, J. F. Stoddart, *Org. Lett.* **2002**, *4*, 557 – 560.

[35] See Supporting Information for further details.

[36] The ΔG° values were calculated using the relationship $\Delta G^{\circ} = -RT\ln K_a$, in which R is the gas constant and T is the absolute temperature.

[37] D. J. Leggett, *Computational Methods for Determination of Formation Constants*, Plenum, London and New York, **1985**, Chapter 1.

[38] A. Mirzoian, A. E. Kaifer, *J. Org. Chem.* **1995**, *60*, 8093 – 8095.

[39] a) R. Wolf, M. Asakawa, P. R. Ashton, M. Gómez-López, C. Hamers, S. Menzer, I. W. Parsons, N. Spencer, J. F. Stoddart, M. S. Tolley, D. J. Williams, *Angew. Chem.* **1998**, *110*, 1018 – 1022; *Angew. Chem. Int. Ed.* **1998**, *37*, 975 – 979; b) V. Balzani, A. Ceroni, A. Credi, M. Gómez-López, C. Hamers, J. F. Stoddart, R. Wolf, *New J. Chem.* **2001**, *25*, 25 – 31.

[40] The absorption spectrum of the [2]rotaxane 1^{4+} recorded in Me_2CO at 298 K, shows a broad CT absorption band centered on 810 nm ($\varepsilon = 1400\ L\,mol^{-1}\,cm^{-1}$).

[41] The absorption spectra were recorded on equilibrium mixtures of 2^{4+} and 3^{4+}. In the fast [2]rotaxane 3^{4+} equilibration occurs immediately. However, in the case of the slow [2]rotaxane 2^{4+} equilibration takes 24 h (see dynamic investigations).

[42] However, it cannot be certain as to whether the observed absorption in the 480 – 600 nm region of the spectrum arises only from this translational isomer. It is possible that it receives some contribution from folded conformations of the other translational isomer in which the DNP moiety enters into "alongside" fleeting interactions with $CBPQT^{4+}$.

[43] The word "roughly" is used because an exact integration of the two SMe resonances proved to be elusive on account of broad signals in the ^{1}H NMR spectrum and the appearance of an intense H_2O resonance ($\delta = 2.72 - 2.85$ ppm) close to the singlet resonating at $\delta = 2.70$ ppm.

[44] In the case of the [2]pseudorotaxane $18 \subset CBPQT^{4+}$, only resonances for complexed $CBPQT^{4+}$ were observed in the ^{1}H NMR spectrum, recorded on a 1:1 mixture of the semi-dumbbell compound **18** and $CBPQT^{4+}$ at low temperature (245 K), indicating that the complexation of **18** by $CBPQT^{4+}$ is very strong at this temperature.

[45] When a DNP moiety is located inside $CBPQT^{4+}$ the DNP-*H*-4/8 protons resonate at very high field ($\delta = 2.0 - 3.0$ ppm), see: a) M. Asakawa, P. R. Ashton, V. Balzani, C. L. Brown, A. Credi, O. A. Matthews, S. P. Newton, F. M. Raymo, A. N. Shipway, N. Spencer, A. Quick, J. F. Stoddart, A. J. P. White, D. J. Williams, *Chem. Eur. J.* **1999**, *5*, 860 – 875; b) ref. [29d].

[46] On account of the broad signals in the ^{1}H NMR spectrum, an exact integration of the resonances proved to be elusive and therefore the word "approximately" is used.

[47] The $\Delta G^{\pm}$ values were calculated using the relationship $\Delta G^{\pm} = -RT\ln(kh/k_B T)$, in which R is the gas constant, T is the absolute temperature, k is the rate constant, h is the Planck constant, and k_B is the Boltzmann constant.

[48] The exchange rate constants (k_{ex}) were measured using the spin saturation transfer method, see: a) B. E. Mann, *J. Magn. Reson.* **1977**, *25*, 91 – 94; b) M. Feigel, H. Kessler, D. Leibfritz, *J. Am. Chem. Soc.* **1979**, *101*, 1943 – 1950.

[49] Temperatures were calibrated using a neat MeOH sample. See: A. L. Van Geet, *Anal. Chem.* **1970**, *42*, 679–680.

[50] H.-R. Tseng, S. A. Vignon, P. C. Celestre, J. F. Stoddart, A. J. P. White, D. J. Williams, *Chem. Eur. J.* **2003**, *9*, 543–556.

[51] In the case of **2**·RED[4+], in which the ^{1}H NMR spectrum (500 MHz) was recorded at 225 K, the resonances for the DNP-*H*-4/8 protons are observed as part of a multiplet at $\delta = 2.50–2.60$ ppm, together with the resonances for the C*H*$_2$CH$_3$ protons. In the ^{1}H NMR spectrum (400 MHz) of the 1:1 mixture of **2**·RED[4+] and **2**·GREEN[4+] recorded at 298 K in CD$_3$COCD$_3$ a doublet ($J = 8$ Hz) resonating at $\delta = 2.72$ ppm is observed, which can be assigned to the resonance of one of the DNP-*H*-4/8 protons in **2**·RED[4+]. The other DNP-*H*-4/8 proton resonance is obscured by the intense H$_2$O signal, which appears at $\delta = 2.76–2.80$ ppm.

[52] K. J. Laidler, *Chemical Kinetics*, Harper Collins, New York, **1987**.

[53] The rate constant k was obtained from the slope of a plot of ln I(SMe, **2**·RED[4+]) against t, in which I(SMe, **2**·RED[4+]) denotes the integral of the SMe resonance for the red translational isomer, **2**·RED[4+] and t the time, see: ref. [52].

[54] In order to test our hypothesis that it is indeed the SMe group that poses the barrier to the shuttling of CBPQT[4+], we synthesized a derivative (i.e., **29**[4+], see Supporting Information) of the [2]rotaxane **2**[4+] in which the SMe group was replaced by the more bulky SEt group. As in **2**[4+], the [2]rotaxane **29**[4+] was isolated as a mixture of translational isomers, **29**·GREEN[4+] (in which CBPQT[4+] resides around the MPTTF unit) and **29**·RED[4+] (in which CBPQT[4+] resides around the DNP moiety). Perhaps surprisingly, the main isomer was **29**·RED[4+], and this isomer was isolated by preparative thin-layer chromatography (PTLC). After isolation of **29**·RED[4+], various attempts to observe the shuttling of CBPQT[4+] from the DNP station to the MPTTF station were made by ^{1}H NMR spectroscopy. However, no interconversion was observed, even at elevated temperatures (425 K, CD$_3$SOCD$_3$). This observation is consistent with our hypothesis that it is the SMe group in **2**[4+] which constitutes the steric barrier to the shuttling of CBPQT[4+] in the [2]rotaxane.

[55] The ratio between **2**·GREEN[4+] and **2**·RED[4+] was determined from the integrals of the signals for the pyrrole protons in **2**·GREEN[4+] and **2**·RED[4+], respectively.

[56] a) M. Asakawa, C. L. Brown, S. Menzer, F. M. Raymo, J. F. Stoddart, D. J. Williams, *J. Am. Chem. Soc.* **1997**, *119*, 2614–2627; b) K. N. Houk, S. Menzer, S. P. Newton, F. M. Raymo, J. F. Stoddart, D. J. Williams, *J. Am. Chem. Soc.* **1999**, *121*, 1479–1487; c) F. M. Raymo, M. D. Bartberger, K. N. Houk, J. F. Stoddart, *J. Am. Chem. Soc.* **2001**, *123*, 9264–9267.

[57] D. D. Perrin, W. L. F. Armarego, *Purification of Laboratory Chemicals*, Pergamon, New York, **1988**.

[58] S. F. Nelsen, L.-J. Chen, M. T. Ramm, G. T. Voy, D. R. Powell, M. A. Aceola, T. R. Seehafer, J. J. Sabelko, J. R. Pladziewicz, *J. Org. Chem.* **1996**, *61*, 1405–1412.

[59] E. P. Parry, R. A. Osteryoung, *Anal. Chem.* **1965**, *37*, 1634–1637.

[60] J. B. Flanagan, S. Margel, A. J. Bard, F. C. Anson, *J. Am. Chem. Soc.* **1978**, *100*, 4248–4253.